

CRYSTAL SKELETONS: COMBINATORICS AND AXIOMS

SARAH BRAUNER, SYLVIE CORTEEL, ZAJJ DAUGHERTY, AND ANNE SCHILLING

ABSTRACT. Crystal skeletons were introduced by Maas-Gariépy in 2023 by contracting quasi-crystal components in a crystal graph. On the representation theoretic level, crystal skeletons model the expansion of Schur functions into Gessel’s quasisymmetric functions. Motivated by questions of Schur positivity, we provide a combinatorial description of crystal skeletons, and prove many new properties, including a conjecture by Maas-Gariépy that crystal skeletons generalize dual equivalence graphs. We then present a new axiomatic approach to crystal skeletons. We give three versions of the axioms based on GL_n -branching, S_n -branching, and local axioms in analogy to the local Stembridge axioms for crystals based on novel commutation relations.

CONTENTS

1. Introduction	2
1.1. Combinatorics of the crystal skeleton	3
1.2. Axioms for crystal skeletons	5
1.3. Outline	5
Acknowledgements	5
2. Background: Crystals, quasi-crystals, and dual equivalence graphs	6
2.1. Tableaux	6
2.2. Crystals	6
2.3. Quasi-crystals	7
2.4. Dual equivalence graphs	9
3. Crystal skeletons	9
3.1. Vertices of the crystal skeleton	9
3.2. Edges of the crystal skeleton	10
4. Properties of the crystal skeleton	12
4.1. Dual equivalence graphs as subgraphs	12
4.2. Properties of Dyck pattern intervals	12
4.3. Self-similarity and branching property	13
4.4. Lusztig involution	15
4.5. Strongly-connected components	15
4.6. Descent compositions	17
4.7. Fans	21
4.8. Commutation relations	22
4.9. Sub-skeleton with shortest descent composition	26
5. Axiomatic characterization of the crystal skeleton	28
5.1. GL_n -axioms	28
5.2. Crystal skeleton as a CS-graph	29
5.3. Dual version of the axioms	30
5.4. Branching properties	30
5.5. Uniqueness of CS-graphs	32
5.6. S_n -axioms	35
5.7. Local axioms	36
6. Crystal skeleton for two row partitions	43
6.1. Vertices and edges in the two-row crystal skeleton	43
6.2. Rectangular decompositions and strongly-connected components	45
6.3. Descent compositions and fans	47
6.4. Lusztig involution	48

Key words and phrases. Crystal graphs, Lusztig involution, branching rules, dual equivalence graphs, Stembridge axioms.

1. INTRODUCTION

Crystal graphs provide combinatorial tools to study the representation theory of Lie algebras (see [9] for details). For instance, crystals are well-behaved with respect to taking tensor products and hence can be used to give combinatorial interpretations for Littlewood–Richardson coefficients. In type A , the character of an irreducible crystal $B(\lambda)$ of highest weight λ is the Schur function s_λ (see §2.2).

It is an important problem in representation theory and algebraic combinatorics to deduce the Schur function expansion of a symmetric function whose expansion in terms of Gessel’s fundamental quasisymmetric function [15] F_α is known. For example, combinatorial expressions for the quasisymmetric expansion of LLT polynomials, modified Macdonald polynomials [18], characters of higher Lie modules (or Thrall’s problem) [17] or the plethysm of two Schur functions [21] exist, yet their Schur expansions are in general still illusive. It is thus desirable to develop methods to deduce the Schur expansions from these quasisymmetric expansions. Some recent algebraic approaches include [13, 14, 16, 24]. Whereas Schur functions are characters of irreducible crystals in type A , Gessel’s fundamental quasisymmetric functions are characters of *quasi-crystals* [22, 12, 11], which are certain subcomponents of a crystal (see §2.3). We exploit this fact in this paper by providing a representation theoretic approach to this problem.

In [22], Maas-Gariépy introduced the *crystal skeleton* $\text{CS}(\lambda)$ by contracting the quasi-crystals in $B(\lambda)$ to a vertex. Since there is a unique standard tableau $T \in \text{SYT}(\lambda)$ in each quasi-crystal in $B(\lambda)$, it is natural to label the vertices of the crystal skeleton by standard tableaux. The crystal skeleton construction is the crystal analogue of Gessel’s formula [15]

$$(1.1) \quad s_\lambda = \sum_{T \in \text{SYT}(\lambda)} F_{\text{Des}(T)},$$

where $\text{Des}(T)$ is the descent composition of the standard tableau T (see §2.1). As such, crystal skeletons have the potential to serve as a powerful tool in deriving Schur expansions from quasisymmetric expansions. This is supported by Theorem 4.1, affirmatively answering a conjecture of Maas-Gariépy [22], stating that crystal skeletons generalize the *dual equivalence graphs*. Dual equivalence graphs were developed by Assaf [5, 3] and Roberts [25, 26] specifically as a paradigm for Schur positivity. See [4, 6, 7] for further applications.

A crystal, its quasi-crystal components and the corresponding crystal skeleton are shown in Figure 1.

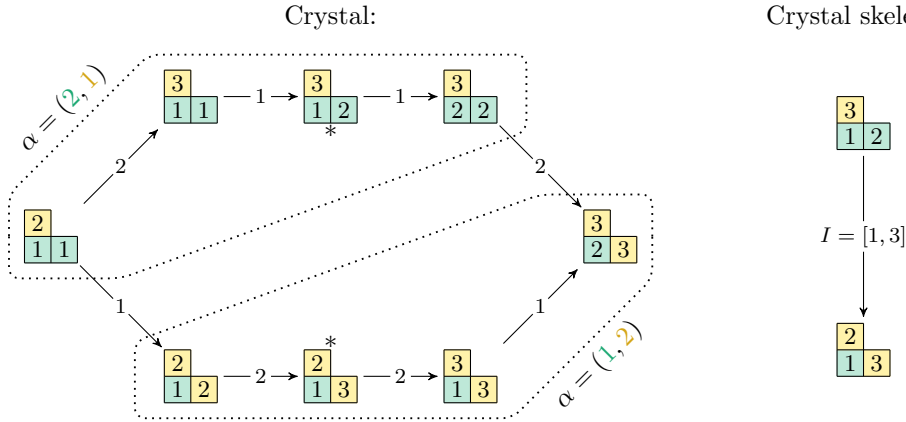


FIGURE 1. Left: Crystal $B(2,1)$ of type A_2 with two quasi-crystal components indicated with dotted lines and standard tableaux indicated by $*$. The descent composition is denoted α . Right: Corresponding crystal skeleton.

Our goal in this paper is to characterize the crystal skeleton both combinatorially and axiomatically in analogy to the local Stembridge axioms for crystals [29]. Stembridge axioms have played a crucial role in crystal theory and have facilitated proofs of Schur positivity using crystals. For example, in [23] the Schur expansion of Stanley symmetric functions was analyzed by defining a crystal structure on the combinatorial objects underlying

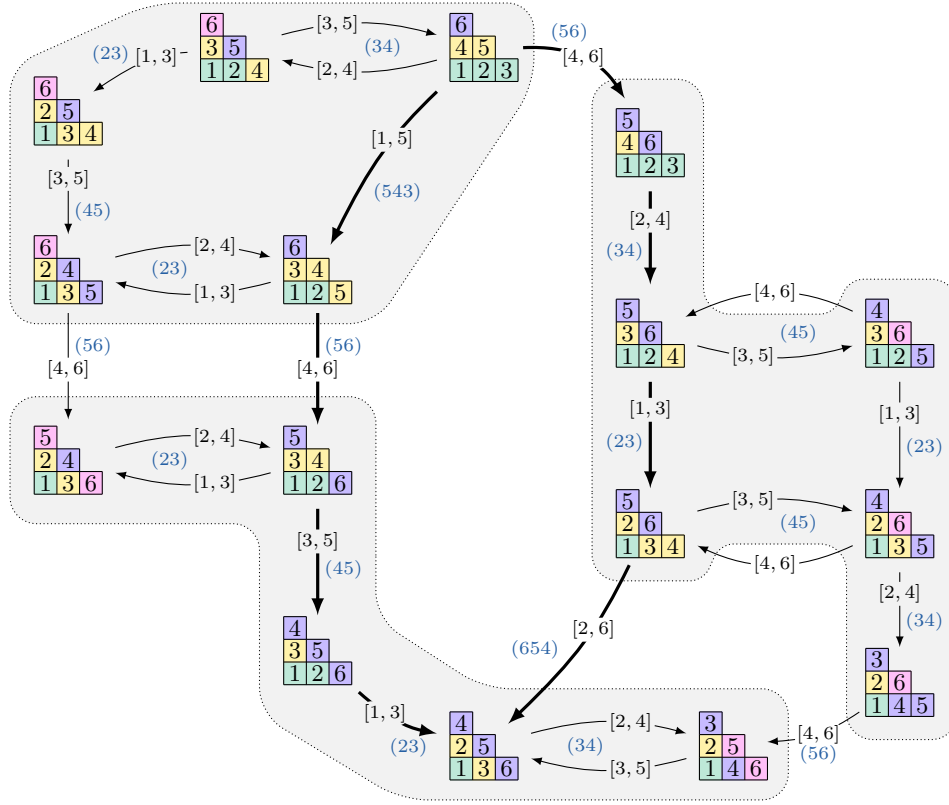


FIGURE 2. The crystal skeleton $CS(3, 2, 1)$. The edge labels in terms of intervals and cycles are defined in Sections 3.2.1 and 3.2.2. This example is further decorated by tableaux coloring to indicate the descent compositions as in Example 3.2; thick arrows to indicate the crystal $B(3, 2, 1)_3$ in Theorem 4.37; and gray components to indicate the branching in Theorem 4.11.

Stanley symmetric functions (decreasing factorizations of a permutation). The crystal structure was proved using Stembridge’s axioms. Our new axioms for crystal skeletons will have similar applications for Schur positivity in cases where the quasisymmetric expansion is known.

We summarize these characterizations below. An extended abstract with summaries of our results is available [8].

1.1. Combinatorics of the crystal skeleton. The original definition of the crystal skeleton by Maas-Gariépy comes from contracting edges of the crystal. Here, our work provides a self-contained combinatorial description of the crystal skeleton that does not reference the crystal. We highlight the combinatorial properties proved in §3 and §4 with the following example of the crystal skeleton $CS(3, 2, 1)$ in Figure 2.

1.1.1. *Vertices and edges of the crystal skeleton.* The vertices of $CS(\lambda)$ can be labeled in two ways:

- (1) by the set $SYT(\lambda)$, which is shown in Figure 2 for $SYT(3, 2, 1)$; and
- (2) by compositions α of $n = |\lambda|$, where $\alpha = \text{Des}(T)$ is the *descent composition* of the tableau $T \in SYT(\lambda)$. This is shown in Figure 2 by the coloring of the tableaux, where each color represents a part of the composition, and the composition order is given by ordering the numbers $1, \dots, n$.

We provide two natural ways to label the edges in $CS(\lambda)$:

- (1) We show in §3.2.1 that the edges of $CS(\lambda)$ can be labeled by certain odd length intervals I called *Dyck pattern intervals*. These intervals can be described in terms of Dyck paths; the interval I corresponds to a Dyck path with $|I| + 1$ steps.
- (2) In §3.2.2 we show that the edges of $CS(\lambda)$ can also be labeled by certain decreasing *cycles* $\text{cycle}(T_I)$, where I is the Dyck pattern interval and T_I is the restriction of T to the letters in I . In particular, if

there is an edge between T and T' in $\text{CS}(\lambda)$, then

$$\text{cycle}(T_I) \cdot T = T'.$$

The above marks the first explicit descriptions of the edge labels of $\text{CS}(\lambda)$, which are ambiguous in [22].

We then determine the relationship between the edge and vertex labels in $\text{CS}(\lambda)$ by describing how the descent compositions between adjacent vertices of $\text{CS}(\lambda)$ differ. See Theorem 4.26 for a complete description.

Theorem 1.1 (Theorem 4.26 summary). *Suppose there is an edge in $\text{CS}(\lambda)$ labeled by*

$$(T, \alpha = \text{Des}(T)) \xrightarrow{I} (T', \beta = \text{Des}(T')),$$

where α has ℓ parts. Then β has length $\ell - 1, \ell$ or $\ell + 1$, and there are combinatorial conditions on T and I that determine β .

1.1.2. *Subgraphs of the crystal skeleton.* We next show that $\text{CS}(\lambda)$ contains several interesting subgraphs.

First, we answer affirmatively a conjecture of Maas-Gariépy [22] by proving that crystal skeletons generalize the *dual equivalence graphs* developed by Assaf [5, 3] and Roberts [25, 26]. Write $\text{DE}(\lambda)$ for the dual equivalence graph corresponding to the partition λ .

Theorem 1.2 (Theorem 4.1). *The dual equivalence graph $\text{DE}(\lambda)$ is a subgraph of the crystal skeleton $\text{CS}(\lambda)$.*

In particular, $\text{DE}(\lambda)$ is obtained from $\text{CS}(\lambda)$ by including edges with intervals I of length 3, or equivalently, cycles of length two. For example, the graph $\text{DE}(3, 2, 1)$ can be seen in Figure 2 by considering only the edges with intervals of length 3.

Second, we show that $\text{CS}(\lambda)$ has surprising *self-similarity* properties. Let $\lambda \vdash n$ be a partition of n . Given $T \in \text{SYT}(\lambda)$ and an interval $[a, b] \subseteq [1, n]$, the skew tableau $T_{[a, b]}$ obtained by restricting T to $[a, b]$ can be straightened to a straight shaped tableau via *jeu de taquin*, which we write as $\text{jdt}(T_{[a, b]})$.

Theorem 1.3 (Theorem 4.7). *Let $T \in \text{SYT}(\lambda)$ and $[a, b] \subseteq [1, n]$ be an interval. Set $\mu = \text{shape}(\text{jdt}(T_{[a, b]}))$. Then $\text{CS}(\mu)$ is a subgraph of $\text{CS}(\lambda)$ (up to relabelling of the edges).*

As a special case of Theorem 4.7, we obtain elegant branching properties mirroring those of the symmetric group.

Theorem 1.4 (Theorem 4.11). *For $\lambda \vdash n$, denote by $\text{CS}(\lambda)_{[1, n-1]}$ the restriction of the crystal skeleton graph $\text{CS}(\lambda)$ by removing all edges labeled by I such that $n \in I$. Then we have a graph isomorphism*

$$\text{CS}(\lambda)_{[1, n-1]} \cong \bigoplus_{\lambda^-} \text{CS}(\lambda^-),$$

where the sum is over all λ^- such that λ/λ^- is a skew shape with a single box.

Theorem 4.11 thus implies that each $\text{CS}(\lambda^-)$ is a subgraph of $\text{CS}(\lambda)$. This is shown in Figure 2 by the three components in gray, obtained by removing the edges labeled by intervals containing 6. These components are isomorphic to $\text{CS}(2, 2, 1)$, $\text{CS}(3, 1, 1)$, and $\text{CS}(3, 2)$, moving from the bottom to the top, counter-clockwise. In all cases, the isomorphism sends the vertex $T \in \text{CS}(\lambda)$ to $T_{[1, n-1]}$.

The third surprising fact is that the crystal itself is a subgraph of the crystal skeleton, despite the fact that the crystal skeleton is obtained from a crystal by contracting quasi-crystal components. The length (or number of parts) of a partition λ is denoted by $\ell(\lambda)$.

Theorem 1.5 (Theorem 4.37). *The induced subgraph of the crystal skeleton $\text{CS}(\lambda)$ of vertices with descent composition of length $\ell(\lambda)$ is isomorphic to the crystal graph $B(\lambda)$ of type $A_{\ell(\lambda)-1}$.*

The crystal $B(3, 2, 1)$ of type A_2 (or equivalently $B(2, 1)$ of type A_2) is a subgraph of $\text{CS}(3, 2, 1)$ as indicated by the bold edges in Figure 2.

1.1.3. *Symmetry in the crystal skeleton.* Finally, we show that $\text{CS}(\lambda)$ satisfies similar symmetry properties to crystals. It is well-known that any crystal $B(\lambda)$ is invariant under the *Lusztig involution*, which is a map

$$\mathcal{L}: B(\lambda) \longrightarrow B(\lambda)$$

sending the highest weight of the crystal to the lowest and reversing (and relabeling) edges.

We show that this map descends to the crystal skeleton, defining a Lusztig involution \mathcal{L}_n on $\text{CS}(\lambda)$ by mapping the vertex $T \in \text{SYT}(\lambda)$ to $\mathcal{L}(T)$ and an edge

$$T \xrightarrow{I} T' \quad \text{to} \quad \mathcal{L}(T') \xrightarrow{I^c} \mathcal{L}(T),$$

where $I^{\mathcal{L}} = [n+1-b, n+1-a]$ if $I = [a, b]$.

Corollary 1.6 (Corollary 4.13). *Let $\lambda \vdash n$. The crystal skeleton $\text{CS}(\lambda)$ is invariant under the Lusztig involution \mathcal{L}_n , that is,*

$$\text{CS}(\lambda) \cong \mathcal{L}_n(\text{CS}(\lambda)).$$

1.2. Axioms for crystal skeletons. The next major focus of our work is to characterize crystal skeleton graphs with axioms, analogously to the Stembridge axioms for crystal graphs [29]. We give three different axiomatic characterizations of the crystal skeleton $\text{CS}(\lambda)$, described below.

Theorem 1.7 (Summary of §5). *There are three axiomatic descriptions that uniquely characterize crystal skeleton graphs:*

- (1) *GL_n -Axioms, found in §5.1;*
- (2) *S_n -Axioms, found in §5.6; and*
- (3) *Local Axioms, found in §5.7.*

The common thread of each of these perspectives is to prove that the combinatorial descriptions of $\text{CS}(\lambda)$ established above in §1.1 completely determine the crystal skeleton. All three axiom sets take as input a graph with vertices labeled by compositions of $n = |\lambda|$ and edges labeled by odd length intervals. In all three cases, there are several local axioms governing the behavior of the edge and vertex labels, including satisfying Theorem 1.1; see also **A0**, **A1**, and **A2**. We highlight below the differences between the axiom sets.

GL_n -Axioms. Let G be a graph with vertex set labeled by compositions of n and edges labeled by odd-length intervals of the set $[n]$. Our first axiomatic description of $\text{CS}(\lambda)$ in §5.1 requires that the input graph G satisfies a local *fan* condition (see **A3**), as well as:

- *Strong Lusztig involution (A4)* as in Corollary 1.6 on both G and the restriction of G to $G_{[1, n-1]}$, where $G_{[1, n-1]}$ is the subgraph obtained by removing edges of G whose interval label contains n :

$$\mathcal{L}_{n-1}(G_{[1, n-1]}) \cong G_{[1, n-1]}.$$

- *Top Subcrystal (A5):* G must contain a subgraph isomorphic to a crystal $B(\lambda)$ as in Theorem 1.5, obtained from the subgraph of G formed from vertices whose composition labels are of minimal length.

We call these axioms GL_n -axioms because restricting compositions by length mirrors GL_n branching rules in representation theory.

S_n -Axioms. We give our second axiomatic description of $\text{CS}(\lambda)$ in §5.6, where we require that the input graph G satisfies the same local fan condition as the GL_n -axioms (**S3**), as well as:

- *Lusztig involution (S4):* $\mathcal{L}_n(G) \cong G$ as in Corollary 1.6;
- *Branching (S5):* G must satisfy a branching recurrence analogous to Theorem 1.4;
- *Connectivity (S6):* G must satisfy certain connectivity conditions.

These axioms are called S_n -Axioms because the graphs must satisfy branching that mirrors the S_n representation theoretic branching rules.

Local Axioms. Finally, our third axiomatic description of the crystal skeleton in §5.7 most closely mirrors the Stembridge axioms for crystal graphs. This set of axioms requires that the input graph G satisfy *local commutation relations* (**L3**) (see also Theorem 4.35) similar to the Stembridge commutation rules for crystals and certain conditions on string lengths (**L4**).

1.3. Outline. In Section 2, we provide the background on crystals, quasi-crystals and dual equivalence graphs. In Section 3, we give the definition and our new combinatorial description of the crystal skeleton. In Section 4, we prove various properties of the crystal skeleton. The axioms for crystal skeletons are discussed in Section 5. We conclude in Section 6 by analyzing the crystal skeleton for two row partitions in more detail to illustrate our results.

Acknowledgements. The authors would like to thank the organizers of the conference at the Banff International Research Station entitled “Community in Algebraic and Enumerative Combinatorics” in January 2024, where this work began as a research project proposed by the last author. We would like to thank Florence Maas-Gariépy, António Malheiro, Zach Hamaker, Rosa Orellana, Franco Saliola, Mike Zabrocki, Joseph Pappé, and Mary Claire Simone for fruitful discussions.

SB was supported by the NSF MSPRF DMS-2303060. SC was partially supported by NSF grant DMS-2054482 and ANR grant ANR-19-CE48-0011. AS was partially supported by NSF grant DMS-2053350 and Simons Foundation grant MPS-TSM-00007191.

2. BACKGROUND: CRYSTALS, QUASI-CRYSTALS, AND DUAL EQUIVALENCE GRAPHS

In this section, we review some basics about tableaux, crystals, quasi-crystals and dual equivalence graphs, which will be used in this paper.

2.1. Tableaux. Let $\text{SSYT}(\lambda)_n$ be the set of *semistandard Young tableaux* of shape λ over the alphabet $[n] := \{1, 2, \dots, n\}$ and $\text{SYT}(\lambda)$ be the set of *standard Young tableaux* of shape λ .

We use French notation for partitions and tableaux, where the sizes of the rows weakly decrease from bottom to top. Work of Robinson–Schensted–Knuth defines a bijection RSK between words in the alphabet $[n]$ and pairs (P, Q) of a semistandard tableau P over $[n]$ and a standard tableau Q of the same shape. If $\text{RSK}(w) = (P, Q)$, then P is known as the *insertion tableau* and Q as the *recording tableau*. To indicate the dependence on the word w , we also write $P(w)$ and $Q(w)$ for the insertion and recording tableau of w .

There are two elementary Knuth relations for letters a, b, c

$$(2.1) \quad \begin{aligned} acb &\equiv_1 cab && \text{if } a \leq b < c, \\ bac &\equiv_2 bca && \text{if } a < b \leq c. \end{aligned}$$

Two words w and v are *Knuth equivalent*, denoted $w \equiv_K v$, if w can be transformed to v by a sequence of type 1 and 2 Knuth relations on adjacent letters. It is well-known that $P(w) = P(v)$ if and only if $w \equiv_K v$, that is, w and v are Knuth equivalent.

A semistandard tableau $b \in \text{SSYT}(\lambda)_n$ gives rise to several combinatorial objects:

- The (row) *reading word* $\text{row}(b)$ is the word obtained from b by reading rows left to right, top to bottom.
- The *weight* $\text{wt}(b)$ is the tuple $(\alpha_1, \alpha_2, \dots, \alpha_n)$ with α_j the number of letters j in b .
- The *standardization* $\text{std}(b)$ is obtained from b and $\text{wt}(b)$ by replacing the letters i in b from left to right by

$$\alpha_1 + \alpha_2 + \dots + \alpha_{i-1} + 1, \dots, \alpha_1 + \alpha_2 + \dots + \alpha_i \text{ for all } 1 \leq i \leq \ell.$$

The standardization of a word w can be defined similarly. By construction, $\text{std}(b) \in \text{SYT}(\lambda)$ and $\text{std}(w)$ is a permutation.

Example 2.1.

$$\text{Suppose } b = \begin{array}{|c|c|} \hline 4 & \\ \hline 2 & 4 \\ \hline 1 & 3 & 3 \\ \hline \end{array}. \quad \text{Then } \text{std}(b) = \begin{array}{|c|c|} \hline 5 & \\ \hline 2 & 6 \\ \hline 1 & 3 & 4 \\ \hline \end{array}$$

and $\text{row}(b) = 424133$, $\text{wt}(b) = (1, 1, 2, 2)$. Note that $\text{row}(\text{std}(b)) = 526134 = \text{std}(\text{row}(b))$.

For a standard tableau $T \in \text{SYT}(\lambda)$, the letter i is a *descent* if the letter $i+1$ is in a higher row of the tableau (in French notation). Denote the descents of T by $d_1 < d_2 < \dots < d_k$. The *descent composition* is defined as

$$(2.2) \quad \text{Des}(T) = (d_1, d_2 - d_1, \dots, d_k - d_{k-1}, n - d_k),$$

where $n = |\lambda|$.

2.2. Crystals. We briefly review the crystal of type A_{n-1} on tableaux. More details can be found in [9, Chapters 3, 8]. The *crystal* $B(\lambda)_n$ is the set $\text{SSYT}(\lambda)_n$ together with the maps

$$(2.3) \quad \begin{aligned} \text{wt}: B(\lambda)_n &\rightarrow \mathbb{Z}_{\geq 0}^n, \\ e_i, f_i: B(\lambda)_n &\rightarrow B(\lambda)_n \cup \{\emptyset\} \quad \text{for } i \in \{1, 2, \dots, n-1\}. \end{aligned}$$

A crystal is often encoded in a *crystal graph* with vertices in $\text{SSYT}(\lambda)$ and an edge $b \xrightarrow{i} b'$ if $b' = f_i(b)$.

The *crystal raising* and *crystal lowering* operators e_i and f_i are defined as follows. The operators e_i and f_i act on the subword of $w = \text{row}(b)$ containing only the letters i and $i+1$, denoted by $w^{(i)}$. Successively bracket (i.e. group) letters $i+1$ to the left of i . The subword of unbracketed letters is of the form $i^r(i+1)^s$. On this subword

$$e_i(i^r(i+1)^s) = \begin{cases} i^{r+1}(i+1)^{s-1} & \text{if } s > 0, \\ \emptyset & \text{else,} \end{cases} \quad f_i(i^r(i+1)^s) = \begin{cases} i^{r-1}(i+1)^{s+1} & \text{if } r > 0, \\ \emptyset & \text{else.} \end{cases}$$

All other letters in w remain unchanged.

Crystal operators are well-behaved with respect to Knuth equivalence (see for example [9, Theorem 8.4]) as stated in the next proposition.

Proposition 2.2. *Let $w \equiv_K v$ be two Knuth equivalent words. Then $f_i w \equiv_K f_i v$ as long as $f_i w \neq \emptyset$.*

Proposition 2.9 also follows from the observation that the crystal operator f_i under standardization acts as a cycle. To explain this, we start with a couple of definitions. This observation will be important later.

Let $b \in B(\lambda)_n$ and $1 \leq i < n$ such that $f_i(b) \neq \emptyset$. Set $w = w_1 w_2 \dots w_N = \text{row}(b)$. Let p be the position of the letter i in w on which f_i acts, which is the rightmost unbracketed letter i . Furthermore, let n_{left} (resp. n_{right}) be the number of bracketed $(i+1, i)$ pairs to the left (resp. right) of w_p in w . Note that w_p is mapped to π_p under standardization $\pi = \text{std}(w)$. We define the *cycle* of size $n_{\text{left}} + n_{\text{right}} + 1$ as

$$(2.6) \quad \text{cycle}(b, i) = (\pi_p + n_{\text{left}} + n_{\text{right}}, \pi_p + n_{\text{left}} + n_{\text{right}} - 1, \dots, \pi_p).$$

Remark 2.10. The permutation $\text{cycle}(b, i) \in S_N$ is a $(n_{\text{left}} + n_{\text{right}} + 1)$ -cycle. In particular, if $w = \text{row}(b)$ has no bracketed pair $(i+1, i)$ (or equivalently $n_{\text{left}} = n_{\text{right}} = 0$), then $\text{cycle}(b, i)$ is the identity. If w has one bracketed pair $(i+1, i)$, then $\text{cycle}(b, i)$ is a transposition.

Example 2.11. Let

$$b = \begin{array}{|c|c|} \hline 3 & \\ \hline 2 & 3 \\ \hline 1 & 2 & 2 \\ \hline \end{array} \quad \text{with} \quad f_2 b = \begin{array}{|c|c|} \hline 3 & \\ \hline 2 & 3 \\ \hline 1 & 2 & 3 \\ \hline \end{array}.$$

Then $\text{row}(b) = 323122$, $\pi = 526134$, $p = 6$, $\pi_p = 4$, $n_{\text{left}} = 2$, and $n_{\text{right}} = 0$. Hence $\text{cycle}(b, 2) = (6, 5, 4)$ written in cycle notation for permutations.

Example 2.12. Consider b and $f_3 b$ of Example 2.3. Then

$$\text{row}(b) = \begin{array}{cccccccccccccccccccc} 4 & 3 & 3 & 4 & 2 & 2 & 2 & 3 & 3 & 4 & 4 & 4 & 4 & 1 & 1 & 1 & 1 & 2 & 2 & 3 & 3 & 3 & 4 \end{array}$$

$\xleftarrow{\quad n_{\text{left}} = 2 \quad}$
 $\xrightarrow{\quad n_{\text{right}} = 3 \quad}$

$p = 9$

so that $p = 9$, $\pi_p = 13$, $n_{\text{left}} = 2$, and $n_{\text{right}} = 3$. Hence $\text{cycle}(b, 3) = (18, 17, 16, 15, 14, 13)$.

Lemma 2.13. Suppose that $f_i(b) = b'$ for $b, b' \in B(\lambda)_n$. Let

$$w = \text{row}(b), \quad w' = \text{row}(b'), \quad \pi = \text{std}(w), \quad \pi' = \text{std}(w'), \quad T = \text{std}(b), \quad T' = \text{std}(b').$$

Then

$$\text{cycle}(b, i) \cdot \pi = \pi' \quad \text{and} \quad \text{cycle}(b, i) \cdot T = T'.$$

Proof. We use the same notation as in the definition of $\text{cycle}(b, i)$. We compare the standardization π and π' . First note that all letters $1, 2, \dots, i-1$ and all letters i to the left of position p in w and w' standardize in the same way. Similarly, the letters $i+1$ to the right of position p and all letters bigger than $i+1$ in w and w' standardize in the same way. Hence π and π' agree in these letters. It remains to compare the standardization of the remaining letters:

- the element $w_p = i$ standardizes to π_p ; the element $w'_p = i+1$ standardizes to $\pi_p + n_{\text{right}} + n_{\text{left}}$ in π' ;
- the (bracketed) elements i appearing to the right of w_p are labeled $\pi_p + 1, \pi_p + 2, \dots, \pi_p + n_{\text{right}}$ in π , whereas in π' they are labeled $\pi_p, \pi_p + 1, \dots, \pi_p + n_{\text{left}} - 1$;
- the (bracketed) elements $i+1$ appearing to the left of w_p are labeled $\pi_p + n_{\text{right}} + 1, \pi_p + n_{\text{right}} + 2, \dots, \pi_p + n_{\text{right}} + n_{\text{left}}$ in π , whereas in π' they are labeled $\pi_p + n_{\text{right}}, \pi_p + n_{\text{right}} + 1, \dots, \pi_p + n_{\text{right}} + n_{\text{left}} - 1$.

Note that this difference is precisely explained by the action of $\text{cycle}(b, i)$ as defined in (2.6) on π to obtain π' .

Since $\pi = \text{row}(T)$ and $\pi' = \text{row}(T')$, it follows that also $\text{cycle}(b, i) \cdot T = T'$. \square

Example 2.14. Continuing Example 2.11, we have $w = 323122$, $w' = 323123$, $\pi = 526134$ and $\pi' = 425136$. Recall that $\text{cycle}(b, 2) = (654)$ and indeed $(654) \cdot 526134 = 425136$.

Since the standardization $\text{std}(b)$ for $b \in B(\lambda)_n$ uniquely determines the quasi-crystal component of b , Proposition 2.9 follows immediately from Lemma 2.13 since by Remark 2.10 the cycle $\text{cycle}(b, i)$ is trivial if and only if $n_{\text{left}} = n_{\text{right}} = 0$.

There are other tableaux which can index quasi-crystals. Instead of taking standard tableaux, one can index a quasi-crystal by its highest weight element.

Definition 2.15 ([1, 30]). A semistandard Young tableau T is a *quasi-Yamanouchi tableau* if when $i > 1$ appears in the tableau, some instance of i is in a higher row than some instance of $i-1$ for all i . Denote the set of all quasi-Yamanouchi tableaux of shape λ by $\text{QYT}(\lambda)$.

Lemma 2.16 ([1]). *The standardization map $\text{std}: \text{QYT}(\lambda) \rightarrow \text{SYT}(\lambda)$ is a bijection such that $\text{wt}(T) = \text{Des}(\text{std}(T))$ for $T \in \text{QYT}(\lambda)$.*

The connection between quasi-crystals and quasisymmetric functions is as follows. *Gessel's fundamental quasisymmetric function* [15] is indexed by compositions α

$$F_\alpha = \sum_{\substack{\beta \preceq \alpha \\ \text{refinement}}} M_\beta \quad \text{with} \quad M_\beta = \sum_{i_1 < i_2 < \dots < i_\ell} x_{i_1}^{\beta_1} x_{i_2}^{\beta_2} \dots x_{i_\ell}^{\beta_\ell}$$

and $\alpha \preceq \beta$ indicates that β is a refinement of α , that is, adjacent parts of β can be summed to obtain α .

The character of the quasi-crystal Q_T with $T \in \text{SYT}(\lambda)$ inside $B(\lambda)_n$ is Gessel's quasisymmetric function F_α in n variables, where $\alpha = \text{Des}(T)$. Since $B(\lambda)_n$ is the union over all Q_T with $T \in \text{SYT}(\lambda)$ (as long as T appears in $B(\lambda)_n$, which is true for n large enough), this yields Gessel's formula [15]

$$s_\lambda = \sum_{T \in \text{SYT}(\lambda)} F_{\text{Des}(T)} = \sum_{T \in \text{QYT}(\lambda)} F_{\text{wt}(T)}.$$

2.4. Dual equivalence graphs. Dual equivalence graphs were first introduced by Haiman [19]. The vertices of the *dual equivalence graph* $\text{DE}(\lambda)$ indexed by the partition λ are all standard Young tableaux $\text{SYT}(\lambda)$ of shape λ . The edges in the dual equivalence graph $\text{DE}(\lambda)$ are given by the elementary dual equivalence relations D_i ($1 < i < |\lambda| =: N$) defined on permutations as follows:

$$(2.7) \quad \begin{aligned} & \dots i \dots i + 1 \dots i - 1 \dots \xleftrightarrow{i} \dots i - 1 \dots i + 1 \dots i \dots \\ & \dots i \dots i - 1 \dots i + 1 \dots \xleftrightarrow{i} \dots i + 1 \dots i - 1 \dots i \dots \end{aligned}$$

The operator D_i is not defined for other configurations of the letters $i - 1, i, i + 1$ in the permutation. Note that descents in the permutation do not change under D_i . Hence D_i is defined on a standard Young tableau T as well using the reading word $\text{row}(T)$.

Assaf [2] proved that $D_i(T)$ on $T \in \text{SYT}(\lambda)$ can be expressed in terms of crystal operators:

$$(2.8) \quad D_i(T) = \begin{cases} f_{i-1} f_i e_{i-1} e_i(T) & \text{if } e_i(T) \neq \emptyset, \\ f_i f_{i-1} e_i e_{i-1}(T) & \text{if } e_{i-1}(T) \neq \emptyset. \end{cases}$$

Note that if $D_i(T)$ is defined, then either $e_i(T) \neq \emptyset$ or $e_{i-1}(T) \neq \emptyset$, but not both. This can be seen by inspecting (2.7).

3. CRYSTAL SKELETONS

In [22], Maas-Gariépy introduced the *crystal skeleton* by contracting the quasi-crystals in $B(\lambda)_n$ to a vertex, assuming that n is sufficiently large. Since there is a unique standard tableau $T \in \text{SYT}(\lambda)$ in each quasi-crystal in $B(\lambda)_n$, it is natural to label the vertices of the crystal skeleton by standard tableaux.

Definition 3.1. Let λ be a partition and consider the ambient crystal $B(\lambda)_n$ for $n \geq |\lambda|$.

The *crystal skeleton* $\text{CS}(\lambda)$ is an edge-labeled, directed graph whose vertices are elements in $\text{SYT}(\lambda)$. For $T, T' \in \text{SYT}(\lambda)$, there is an edge from T to T' in $\text{CS}(\lambda)$ if there exist $b \in Q_T$ and $b' \in Q_{T'}$ such that $f_i(b) = b'$ for some $1 \leq i < n$.

This definition is rather abstract. One goal of our work is to give a concrete, combinatorial description of $\text{CS}(\lambda)$ as a graph. In addition, we will give a natural way to label the edges with intervals (described below) different from the edge-labels in [22]. See Figure 1 for an example of a crystal skeleton.

3.1. Vertices of the crystal skeleton. As discussed in Definition 3.1, the vertices of $\text{CS}(\lambda)$ are labeled by standard tableaux in $\text{SYT}(\lambda)$. For our axiomatic description of crystal skeletons in Section 5, it will be important to also associate to each vertex $T \in \text{SYT}(\lambda)$ its descent composition $\text{Des}(T)$ as defined in (2.2).

Example 3.2. We color $T \in \text{SYT}(3, 2, 1)$ by its descent composition below:

$$T = \begin{array}{|c|c|} \hline 5 & \\ \hline 2 & 4 \\ \hline 1 & 3 & 6 \\ \hline \end{array}.$$

In particular, $\text{Des}(T) = (1, 2, 1, 2)$.

3.2. Edges of the crystal skeleton. The edges of the crystal skeleton are more subtle. In [22], the edge from T to T' in $\text{CS}(\lambda)$ is indexed by the minimal index j such that $f_j(b) = b'$ for $b \in Q_T$ and $b' \in Q_{T'}$. We give two alternative edge labels in $\text{CS}(\lambda)$.

3.2.1. Dyck pattern intervals. The next definition is crucial for our labeling of the edges in the crystal skeleton.

Definition 3.3. Let $I = [i, i + 2m] \subseteq [n]$ be an interval of length $2m + 1 \geq 3$.

- (1) Let $\pi \in S_n$ be a permutation and $\pi|_I$ be the subword of π restricted to the letters in I . We call I a *Dyck pattern interval* of π if

$$(3.1) \quad P(\pi|_I) = \begin{array}{|c|c|c|c|} \hline i+m+1 & i+m+2 & \cdots & i+2m \\ \hline i & i+1 & \cdots & i+m-1 & i+m \\ \hline \end{array},$$

that is, the letters in $[i, i + m]$ occur in the bottom row and the letters in $[i + m + 1, i + 2m]$ occur in the top row of $P(\pi|_I)$. We call the subword $\pi|_I$ a *Dyck pattern* of π .

- (2) Let $T \in \text{SYT}(\lambda)$ and $n = |\lambda|$. Then I is a *Dyck pattern interval* of T if it is a Dyck pattern interval of $\pi = \text{row}(T)$. Similarly, $\pi|_I$ is a *Dyck pattern* of T if it is a Dyck pattern of π .

Example 3.4. Consider T of Example 3.2, so that $\pi = \text{row}(T) = 524136$. The interval $I = [2, 4]$ is a Dyck pattern interval of T since $\pi|_{[2,4]} = 243$ and

$$P(\pi|_{[2,4]}) = \begin{array}{|c|c|} \hline 4 \\ \hline 2 & 3 \\ \hline \end{array}.$$

Example 3.5. Let $\pi = 10783142596 \in S_{10}$. Then $I = [3, 9]$ is a Dyck pattern interval of π since $\pi|_I = 7834596$ and

$$P(\pi|_I) = \begin{array}{|c|c|c|c|} \hline 7 & 8 & 9 \\ \hline 3 & 4 & 5 & 6 \\ \hline \end{array}.$$

We may think about a Dyck pattern interval $I = [i, i + 2m]$ also in terms of crystal operators. To this end, we first define the *destandardization* of $\pi|_I$ as follows. Note that the letters in $[i, i + m]$ (resp. $[i + m + 1, i + 2m]$) need to appear in increasing order in $\pi|_I$ due to the form of $P(\pi|_I)$ in Definition 3.3. Replacing the letters in $[i, i + m]$ by i and the letters in $[i + m + 1, i + 2m]$ by $i + 1$ in $\pi|_I$, we obtain a word in the letters i and $i + 1$ such that all letters $i + 1$ are bracketed with some i . Since there is one more letter i than $i + 1$, there is one unbracketed letter i . We call this word the *destandardization* of $\pi|_I$ denoted

$$(3.2) \quad \text{destd}(\pi|_I).$$

Remark 3.6. An alternate definition of a Dyck pattern interval $I = [i, i + 2m]$ of π is as follows. Suppose $m \geq 1$ and the letters in $[i, i + m]$ (resp. $[i + m + 1, i + 2m]$) appear in increasing order in $\pi|_I$. As before, let $w = \text{destd}(\pi|_I)$ be the word by replacing the letters in $[i, i + m]$ by i and the letters in $[i + m + 1, i + 2m]$ by $i + 1$. Then I is a Dyck pattern interval if

$$e_i(w) = \emptyset \quad \text{and} \quad f_i(i + 1w) = \emptyset.$$

The condition $e_i(w) = \emptyset$ ensures that all letters $i + 1$ are bracketed with some i . Viewing the letters $i + 1$ as down steps and i as up steps, the word $i + 1w$ associated to a Dyck pattern is a Dyck path. This motivates the name *Dyck pattern*.

Remark 3.7. By the RSK correspondence, the Dyck pattern $\pi|_I$ is uniquely determined by the insertion and recording tableaux $P(\pi|_I)$ and $Q(\pi|_I)$. Since $P(\pi|_I)$ is fixed by definition, a Dyck pattern is hence determined by the recording tableau, which is a standard tableau of shape $(m + 1, m)$ or equivalently a standard tableau of shape $(m + 1, m + 1)$ since the entry in cell $(m + 1, 2)$ is fixed to be $2m + 2$. It is well-known that standard tableaux of shape $(m + 1, m + 1)$ are in bijection with Dyck paths of length $2m + 2$ (see [28, pg. 243]).

Example 3.8. Consider π and I from Example 3.5. Then

$$\pi|_I = 7834596 \quad \text{and} \quad w = \text{destd}(\pi|_I) = \underbrace{44333343}_{\text{Dyck path}}.$$

Note that $e_3(w) = \emptyset$ and $f_3(4w) = \emptyset$. The Dyck path corresponding to $4w$ is



We show that the edges of $\text{CS}(\lambda)$ are labeled by Dyck pattern intervals.

Theorem 3.9. *There is a bijection between the edges in $\text{CS}(\lambda)$ and Dyck pattern intervals that occur in $\text{row}(T)$ for $T \in \text{SYT}(\lambda)$.*

Example 3.10. We describe in detail the edge below found in $\text{CS}(3, 2, 1)$ in Figure 2:

$$T = \begin{array}{|c|c|} \hline 6 \\ \hline 4 & 5 \\ \hline 1 & 2 & 3 \\ \hline \end{array} \xrightarrow{I=[1,5]} T' = \begin{array}{|c|c|} \hline 6 \\ \hline 3 & 4 \\ \hline 1 & 2 & 5 \\ \hline \end{array}.$$

In this case $\pi = \text{row}(T) = 645123$, $\pi|_{[1,5]} = 45123$, and

$$P(\pi|_I) = \begin{array}{|c|c|} \hline 4 & 5 \\ \hline 1 & 2 & 3 \\ \hline \end{array}.$$

Thus I is a Dyck pattern interval on π .

To see why there is an edge from T to T' in $\text{CS}(3, 2, 1)$, note that the word $w = 622111$ is in the same quasi-component of $B(3, 2, 1)_6$ as π , since $\text{std}(w) = \pi$. Similarly, $w' = 622112$ is in the same quasi-component as $\pi' := \text{row}(T') = 634125$ in $B(3, 2, 1)_6$, since $\text{std}(w') = \pi'$. Next, observe that in $B(3, 2, 1)_6$, we have

$$f_1(w) = f_1(622111) = 622112 = w'.$$

The idea behind Theorem 3.9 is that the Dyck pattern interval detects this edge in $B(\lambda)_n$. Note that $\text{Des}(T) = (3, 2, 1)$ and $\text{Des}(T') = (2, 3, 1)$. The way descent compositions change between edges in $\text{CS}(\lambda)$ will be described in Section 4.6.

Proof of Theorem 3.9. Suppose that $I = [i, i + 2m]$ with $m \geq 1$ is a Dyck pattern interval in $\pi = \text{row}(T)$. Replace the letters $i, i + 1, \dots, i + m$ by i and the letters $i + m + 1, i + m + 2, \dots, i + 2m$ by $i + 1$ in T to obtain a new semistandard tableau b . Note that since I is a Dyck pattern interval, the letters $i, i + 1, \dots, i + m$ (resp. $i + m + 1, i + m + 2, \dots, i + 2m$) have to appear left to right in T . Hence we have $\text{std}(b) = T$. Furthermore, since b contains one more i than $i + 1$ not all i are bracketed and hence $f_i b = b'$ exists. In addition, since I is a Dyck pattern interval, by Remark 3.6 all $i + 1$ are bracketed with an i . Hence by Proposition 2.9 since $m \geq 1$, the standard tableau $T' = \text{std}(b')$ is different from T and there is an edge from T to T' in $\text{CS}(\lambda)$. This shows that every Dyck pattern interval gives rise to an edge in $\text{CS}(\lambda)$.

Now suppose that there is an edge from T to T' in $\text{CS}(\lambda)$. This means that there exist $b \in Q_T$ and $b' \in Q_{T'}$ such that $f_i b = b'$ for some i . By the explanations in Section 2.3 before (2.6) and using the same notation, there are n_{right} bracketed pairs $(i + 1, i)$ after w_p and n_{left} bracketed pairs $(i + 1, i)$ before w_p . Restricting $\pi = \text{row}(T)$ to the interval $I = [\pi_p - n_{\text{left}}, \pi_p + n_{\text{left}} + 2n_{\text{right}}]$ yields a Dyck pattern of size $2m + 1$ with $m = n_{\text{left}} + n_{\text{right}} > 0$ by Remark 3.6. Hence every edge in $\text{CS}(\lambda)$ leaving T is associated to a Dyck pattern interval I of π . \square

3.2.2. Cycles. By Theorem 3.9, every edge leaving T in $\text{CS}(\lambda)$ is associated with a Dyck pattern interval $I = [i, i + 2m]$ with $m \geq 1$ of $\pi = \text{row}(T)$. As in the proof of Theorem 3.9, let b be the semistandard tableau obtained from T by replacing the letter $i, i + 1, \dots, i + m$ by i and the letters $i + m + 1, i + m + 2, \dots, i + 2m$ by $i + 1$. Note that $b|_I$ is $\text{destd}(\pi|_I)$. By Lemma 2.13, the edge leaving T associated to I goes to

$$(3.3) \quad T' = (m + \pi_p, m + \pi_p - 1, \dots, \pi_p) \cdot T,$$

where π_p is the letter in T (or π) which corresponds to the i in b on which f_i acts. Hence the edge from T to T' in $\text{CS}(\lambda)$ can also be labeled by a *cycle* which we shall denote by

$$\text{cycle}(\pi|_I) := (m + \pi_p, m + \pi_p - 1, \dots, \pi_p).$$

Example 3.11. Continuing Example 3.10, the semistandard tableau b associated to T is

$$b = \begin{array}{|c|c|} \hline 6 \\ \hline 2 & 2 \\ \hline 1 & 1 & 1 \\ \hline \end{array}.$$

The crystal operator f_1 acts on the rightmost 1 and hence $\pi_p = 3$. Since $|I| = 5$, we have $m = 2$, and $\text{cycle}(\pi|_I) = (5, 4, 3)$, and indeed

$$(5, 4, 3) \cdot T = T'.$$

Figure 2 shows the crystal skeleton $\text{CS}(3, 2, 1)$ with edges labeled by both Dyck pattern intervals and cycles.

As we will see later, due to self-similarity properties which respect the Dyck pattern intervals, but not the cycles, it is more natural to use the Dyck pattern intervals as edge labels.

4. PROPERTIES OF THE CRYSTAL SKELETON

In this section, we study various properties of the crystal skeleton $\text{CS}(\lambda)$.

4.1. Dual equivalence graphs as subgraphs. Recall the dual equivalence graphs of Section 2.4. The next theorem proves [22, Conjecture 5.3].

Theorem 4.1. *The dual equivalence graph $\text{DE}(\lambda)$ is a subgraph of the crystal skeleton $\text{CS}(\lambda)$ (disregarding edge labels and edge directions).*

Proof. Suppose that there is an edge labeled i in $\text{DE}(\lambda)$ between T and T' , that is, $D_i(T) = T'$. By (2.8), either $T' = f_{i-1}f_i e_{i-1}e_i(T)$ or $T' = f_i f_{i-1} e_i e_{i-1}(T)$. Suppose first that $T' = f_{i-1}f_i e_{i-1}e_i(T)$. In this case, i is to the left of $i+1$ in $\text{row}(T)$, so that

$$(4.1) \quad \begin{array}{c} \dots i \dots i+1 \dots i-1 \dots \xrightarrow{e_i} \dots i \dots i \dots i-1 \dots \xrightarrow{e_{i-1}} \dots i-1 \dots i \dots i-1 \dots \\ \xrightarrow{f_i} \dots i-1 \dots i+1 \dots i-1 \dots \xrightarrow{f_{i-1}} \dots i-1 \dots i+1 \dots i \dots \end{array}$$

or

$$(4.2) \quad \begin{array}{c} \dots i \dots i-1 \dots i+1 \dots \xrightarrow{e_i} \dots i \dots i-1 \dots i \dots \xrightarrow{e_{i-1}} \dots i \dots i-1 \dots i-1 \dots \\ \xrightarrow{f_i} \dots i+1 \dots i-1 \dots i-1 \dots \xrightarrow{f_{i-1}} \dots i+1 \dots i-1 \dots i \dots \end{array}$$

In both cases, the crystal operator e_{i-1} changes quasi-crystal components by Proposition 2.9 since there is a bracketing between i and $i-1$, whereas all other crystal operators in this sequence do not change quasi-crystal components. Hence there is an edge in $\text{CS}(\lambda)$ from T to T' .

If, on the other hand, $T' = f_i f_{i-1} e_i e_{i-1}(T)$, the letter $i-1$ must be to the left of the letter i . In this case, we start with the last elements in the sequences of (4.1) and (4.2). Reversing the arrows (changing e to f and vice versa), the dual equivalence operator D_i takes the last element to the first element. The quasi-crystal component again changes in the same arrow. Hence there is an edge in $\text{CS}(\lambda)$ from T to T' . This proves that $\text{DE}(\lambda)$ is a subgraph of $\text{CS}(\lambda)$. \square

We can characterize which edges in $\text{CS}(\lambda)$ belong to $\text{DE}(\lambda)$. Namely, they are the edges labeled by Dyck pattern intervals I of size 3, or equivalently, by transpositions when labeling by cycles.

Proposition 4.2. *Let $T \xrightarrow{I} T'$ be an edge in $\text{CS}(\lambda)$. Then there is an edge between T and T' in the dual equivalence graph $\text{DE}(\lambda)$ if and only if $|I| = 3$.*

Proof. All elementary dual equivalence relations D_i are simple transpositions on the corresponding standard tableaux T and T' . Hence in the notation of (3.3) we have $m = 1$ or equivalently $|I| = 3$.

Conversely, assume that $|I| = 3$, so that $I = [i-1, i+1]$ for some i . Since I is a Dyck pattern interval by Theorem 3.9, we must have for $\pi = \text{row}(T)$ that $\pi|_I = i-1 \ i+1 \ i$ with transposition $(i, i-1)$ or $\pi|_I = i+1 \ i-1 \ i$ with transposition $(i+1, i)$. These correspond to the dual equivalence transitions on the top and bottom (right to left) in (2.7). This proves the claim. \square

4.2. Properties of Dyck pattern intervals. We collect several properties of Dyck pattern intervals which will be useful later.

First, there is an inclusion property of Dyck pattern intervals.

Proposition 4.3. *Let $T \in \text{SYT}(\lambda)$ and suppose that $I = [i, i+2m]$ is a Dyck pattern interval of T of size $2m+1 > 3$ (or $m > 1$). Then $J = [i+1, i+2m-1]$ of size $2m-1$ is also a Dyck pattern interval of T .*

Proof. Let $\pi = \text{row}(T)$. Since I is a Dyck pattern interval, the insertion tableau $P(\pi|_I)$ is of the form (3.1) of shape $(m+1, m)$. The insertion tableau $P(\pi|_J)$ can be obtained from $P(\pi|_I)$ by removing the cells containing i and $i+2m$ and performing jeu de taquin to straighten the tableau. This yields the tableau of shape $(m, m-1)$ with the letters $i+1, i+2, \dots, i+m$ (resp. $i+m+1, i+m+2, \dots, i+2m-1$) in the bottom (resp. top) row. Hence J is a Dyck pattern interval. \square

Example 4.4. Consider the edge in Example 3.10 labeled by the Dyck pattern interval $I = [1, 5]$. As can be seen from Figure 2, there is also an edge starting at T labeled by the interval $[2, 4]$.

Second, recall from Proposition 2.2 that crystal operators respect Knuth equivalence. The same is true for edges in the crystal skeleton.

Proposition 4.5. *Suppose $\pi \equiv_K \sigma$ are two Knuth equivalent permutations. Let I be a Dyck pattern interval in π . Then I is also a Dyck pattern interval in σ . Furthermore, if*

$$\pi \xrightarrow{I} \pi' \quad \text{and} \quad \sigma \xrightarrow{I} \sigma'$$

are edges in the corresponding crystal skeletons, then $\pi' \equiv_K \sigma'$.

Proof. Since $I = [i, i+2m]$ is a Dyck pattern interval of π , $P(\pi|_I)$ is of the form (3.1). It is not hard to check from (2.1) that if $\pi \equiv_K \sigma$ then also $\pi|_I \equiv_K \sigma|_I$. Hence, $P(\sigma|_I) = P(\pi|_I)$, so that I is also a Dyck pattern interval in σ , proving the first claim.

By [9, Theorem 8.4], the crystals containing π and σ are isomorphic since $\pi \equiv_K \sigma$. Since the crystal skeleton is fully determined by the underlying crystal and its edges, the second claim follows from Proposition 2.2. \square

4.3. Self-similarity and branching property. In this section, we study self-similarity properties of the crystal skeleton. For a standard tableau $T \in \text{SYT}(\lambda)$ and an interval $[a, b]$, we define $T_{[a,b]}$ to be the skew tableau T restricted to the interval $[a, b]$. Furthermore, for a skew tableau T , let $\text{jdt}(T)$ be the jeu de taquin straightening of T .

Example 4.6.

$$\text{Let } T = \begin{array}{|c|c|c|} \hline 6 \\ \hline 4 & 5 \\ \hline 1 & 2 & 3 \\ \hline \end{array}. \quad \text{Then } T_{[2,6]} = \begin{array}{|c|c|c|} \hline 6 \\ \hline 4 & 5 \\ \hline \blacksquare & 2 & 3 \\ \hline \end{array} \quad \text{and} \quad \text{jdt}(T_{[2,6]}) = \begin{array}{|c|c|c|} \hline 6 \\ \hline 4 & 5 \\ \hline 2 & 3 \\ \hline \end{array}.$$

The self-similarity property for crystal skeletons can be stated as follows.

Theorem 4.7. *Let $T \in \text{SYT}(\lambda)$, $[a, b] \subseteq [1, |\lambda|]$ be an interval, and $\mu = \text{shape}(\text{jdt}(T_{[a,b]}))$. Then $\text{CS}(\mu)$ is a subgraph of $\text{CS}(\lambda)$ (up to relabelling of the edges). In particular, labeling the edges in the crystal skeleton by the Dyck pattern intervals, the edges in $\text{CS}(\mu)$ differ from those in $\text{CS}(\lambda)$ by a shift of $-a+1$.*

Before proving Theorem 4.7, we give an example.

Example 4.8. Recall that Figure 2 shows $\text{CS}(3, 2, 1)$. Take the subgraph of $\text{CS}(3, 2, 1)$ with the vertices

$$(4.3) \quad \begin{array}{|c|c|c|} \hline 5 \\ \hline 3 & 4 \\ \hline 1 & 2 & 6 \\ \hline \end{array}, \quad \begin{array}{|c|c|c|} \hline 4 \\ \hline 3 & 5 \\ \hline 1 & 2 & 6 \\ \hline \end{array}, \quad \begin{array}{|c|c|c|} \hline 5 \\ \hline 2 & 4 \\ \hline 1 & 3 & 6 \\ \hline \end{array}, \quad \begin{array}{|c|c|c|} \hline 4 \\ \hline 2 & 5 \\ \hline 1 & 3 & 6 \\ \hline \end{array}, \quad \begin{array}{|c|c|c|} \hline 3 \\ \hline 2 & 5 \\ \hline 1 & 4 & 6 \\ \hline \end{array}.$$

It is isomorphic to the crystal skeleton $\text{CS}(2, 2, 1)$ in Figure 3. Note that all tableaux in (4.3) restricted to the interval $[1, 5]$ have shape $(2, 2, 1)$.

Take the subgraph of Figure 2 with the vertices

$$(4.4) \quad \begin{array}{|c|c|c|} \hline 5 \\ \hline 2 & 6 \\ \hline 1 & 3 & 4 \\ \hline \end{array}, \quad \begin{array}{|c|c|c|} \hline 4 \\ \hline 3 & 6 \\ \hline 1 & 2 & 5 \\ \hline \end{array}, \quad \begin{array}{|c|c|c|} \hline 4 \\ \hline 2 & 5 \\ \hline 1 & 3 & 6 \\ \hline \end{array}, \quad \begin{array}{|c|c|c|} \hline 3 \\ \hline 2 & 6 \\ \hline 1 & 4 & 5 \\ \hline \end{array}, \quad \begin{array}{|c|c|c|} \hline 3 \\ \hline 2 & 5 \\ \hline 1 & 4 & 6 \\ \hline \end{array}.$$

It is isomorphic to the crystal skeleton $\text{CS}(3, 2)$ in Figure 3 up to shifting all intervals by -1 . Note that applying jeu de taquin to all tableaux in (4.4) restricted to the interval $[2, 6]$ yields tableaux of shape $(3, 2)$.

Proof of Theorem 4.7. The row reading word of a skew semistandard tableau P and the row reading word of $\text{jdt}(P)$ are Knuth equivalent (see for example [27]). Knuth equivalent words lie in isomorphic crystals (see for example [9, Chapter 8]).

Restricting the standard tableau $T \in \text{CS}(\lambda)$ to the subinterval $[a, b]$, we can embed T into the subcrystal generated by the crystal operators e_i, f_i for $a \leq i < b$. Shifting all letters in $T_{[a,b]}$ by $-a+1$ and operating with the crystal operators f_i, e_i for $1 \leq i \leq b-a$, $T_{[a,b]} - a+1$ sits inside a crystal isomorphic to $B(\mu)$ by the above arguments. Considering the crystal skeleton of $B(\mu)$ proves the claim. \square

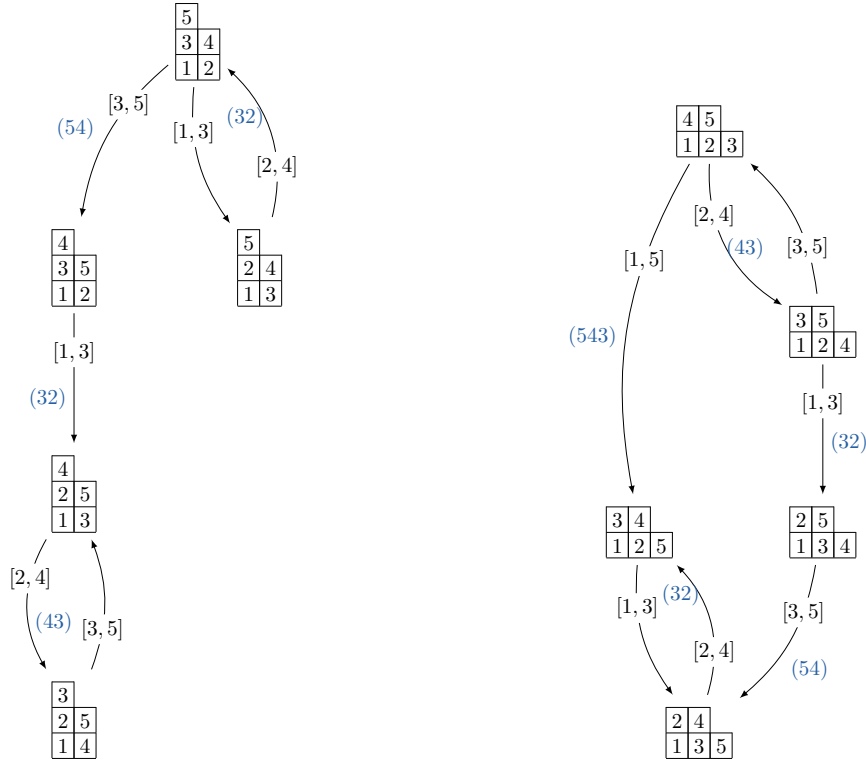


FIGURE 3. Left: The crystal skeleton $CS(2, 2, 1)$. Right: The crystal skeleton $CS(3, 2)$.

Remark 4.9. Note that Knuth relations and jeu de taquin do not preserve cycles, even before shifting the labels of the corresponding tableaux. For example

$$\begin{array}{|c|c|c|} \hline 3 & 4 & 6 \\ \hline 1 & 2 & 5 \\ \hline \end{array} \xrightarrow{(54)} \begin{array}{|c|c|c|} \hline 3 & 5 & 6 \\ \hline 1 & 2 & 4 \\ \hline \end{array}$$

is an edge in the crystal skeleton $CS(3, 3)$. However, restricting to the interval $[4, 6]$ and applying jeu de taquin we obtain the edge

$$\begin{array}{|c|} \hline 6 \\ \hline 4 \ 5 \\ \hline \end{array} \xrightarrow{(65)} \begin{array}{|c|} \hline 5 \\ \hline 4 \ 6 \\ \hline \end{array},$$

where the cycle edge label has changed from (54) to (65). If we label the edges of the crystal skeleton by the interval of the Dyck pattern instead of the cycle, then the label of the corresponding edge is $[4, 6]$ in both cases. This is one reason we will prefer Dyck pattern labeling in what follows.

One Corollary of Theorem 4.7 is that one can always find a subgraph of $CS(\lambda)$ obtained from products of intervals.

Corollary 4.10. *Let $[a_k, b_k] \subseteq [1, |\lambda|]$ be intervals for $1 \leq k \leq N$ for some $N > 0$ such that $[a_j, b_j] \cap [a_k, b_k] = \emptyset$ whenever $j \neq k$. Let $\mu_k = \text{shape}(\text{jdt}(T_{[a_k, b_k]}))$ for all $1 \leq k \leq N$. Then*

$$CS(\mu_1) \times \cdots \times CS(\mu_N)$$

is a subgraph of $CS(\lambda)$ (up to relabelling of the edges).

Proof. This follows directly from Theorem 4.7 since the intervals are not overlapping. □

We can also use Theorem 4.7 to prove the crystal skeleton has branching properties similar to the symmetric group. We first briefly review the branching properties of the symmetric group S_n . Let S^λ be the Specht module, which is the finite-dimensional, irreducible S_n -representation indexed by the partition $\lambda \vdash n$. Restricting S^λ to S_{n-1} gives the branching

$$\text{Res}_{S_{n-1}}^{S_n} S^\lambda = \bigoplus_{\lambda^-} S^{\lambda^-},$$

where the sum is over all λ^- such that λ/λ^- is a skew shape with a single box. Theorem 4.11 shows that $\text{CS}(\lambda)$ has analogous restriction properties.

Theorem 4.11. *Let $\lambda \vdash n$ be a partition of n . Denote by $\text{CS}(\lambda)_{[1, n-1]}$ the restriction of the crystal skeleton graph $\text{CS}(\lambda)$ by removing all edges labelled by I such that $n \in I$. Then we have a graph isomorphism*

$$\text{CS}(\lambda)_{[1, n-1]} \cong \bigoplus_{\lambda^-} \text{CS}(\lambda^-),$$

where the sum is over all λ^- such that λ/λ^- is a skew shape with a single box.

Proof. By Theorem 4.7, each $\text{CS}(\lambda^-)$ with λ/λ^- a skew shape with $|\lambda/\lambda^-| = 1$ is a subgraph of $\text{CS}(\lambda)_{[1, n-1]}$. Since for $T \in \text{SYT}(\lambda)$ the letter n can sit in any corner cell of λ , each vertex T in $\text{CS}(\lambda)$ corresponds to precisely one vertex in $\bigoplus_{\lambda^-} \text{CS}(\lambda^-)$. This proves the claim. \square

4.4. Lusztig involution. Recall from Section 2.2 that the crystal $B(\lambda)_n$ of type A_{n-1} enjoys a symmetry under the Schützenberger or Lusztig involution. We show below that this translates into a symmetry of the crystal skeleton as well.

If $T \in \text{CS}(\lambda)$ has descent composition $\text{Des}(T) = (\alpha_1, \dots, \alpha_\ell)$, then it follows from the definition of evacuation in Remark 2.5 that

$$\text{Des}(\text{evac}(T)) = (\alpha_\ell, \dots, \alpha_1) =: \text{rev}(\text{Des}(T)).$$

Furthermore, if there is an edge $T \xrightarrow{I} T'$ in $\text{CS}(\lambda)$, then under Lusztig involution this edge becomes $\text{evac}(T') \xrightarrow{I^c} \text{evac}(T)$, where $I^c = [n+1-b, n+1-a]$ if $I = [a, b]$.

Definition 4.12. Let $\lambda \vdash n$. We define the *Lusztig involution* on the crystal skeleton

$$\mathcal{L}_n: \text{CS}(\lambda) \rightarrow \text{CS}(\lambda),$$

by mapping the vertex $T \in \text{SYT}(\lambda)$ to $\text{evac}(T)$ and an edge $T \xrightarrow{I} T'$ to $\text{evac}(T') \xrightarrow{I^c} \text{evac}(T)$, where $I^c = [n+1-b, n+1-a]$ if $I = [a, b]$.

Corollary 4.13. *Let $\lambda \vdash n$. The crystal skeleton $\text{CS}(\lambda)$ is invariant under the Lusztig involution \mathcal{L}_n , that is,*

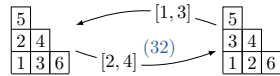
$$\text{CS}(\lambda) \cong \mathcal{L}_n(\text{CS}(\lambda)).$$

Proof. This follows directly from the fact that the crystal graph $B(\lambda)_n$ underlying $\text{CS}(\lambda)$ is invariant under the Lusztig involution. Furthermore, by Proposition 2.9 an edge f_i in the crystal gives rise to an edge in the crystal skeleton if and only if there is some $i+1$ that is bracketed with an i . Under evacuation, since a word is reversed and complemented, an $(i+1, i)$ bracketed pair will transform to an $(n+1-i, n-i)$ pair. Equivalently, whenever an edge f_i is in a quasi-crystal component, it will be mapped to another quasi-crystal component under Lusztig involution. \square

4.5. Strongly-connected components. We now turn to the strongly-connected components of the crystal skeleton.

Definition 4.14. A directed graph $G = (V, E)$ with vertex set V and edge set E is *strongly-connected* if for any two vertices $u, v \in V$ there is a sequence of directed edges e_1, e_2, \dots, e_k with $e_i = (u_{i-1}, u_i) \in E$, $u_i \in V$, $u = u_0$ and $v = u_k$.

Example 4.15. The subgraph

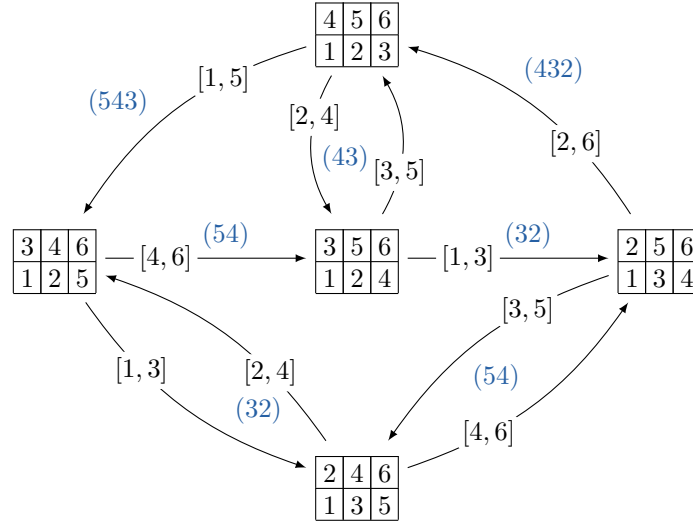


of the graph in Figure 2 forms a strongly-connected component.

We characterize the crystal skeletons that are strong-connected.

Theorem 4.16. *A crystal skeleton $\text{CS}(\lambda)$ is strongly-connected if and only if $\lambda = (w^\ell)$ is a rectangle.*

Proof. First we prove that $\text{CS}(\lambda)$ is strongly-connected if $\lambda = (w^\ell)$. Let u be the highest weight element in the crystal $B(\lambda)_n$ for $n \geq |\lambda|$. It is given by the Yamanouchi tableau with letters r in row r . Let $T_u = \text{std}(u)$, which has the letters $(r-1)w+1, (r-1)w+2, \dots, rw$ in row r . Similarly, let v be the lowest weight element in $B(\lambda)_n$. The quasi-crystal Q_{T_u} contains both u and v since $\text{std}(u) = \text{std}(v)$. For any $b \in B(\lambda)_n$, there exists a sequence j_1, j_2, \dots, j_k for some $1 \leq j_i < n$ such that $b = f_{j_1} \cdots f_{j_k} u$. Hence there exists a path from T_u to T in the crystal

FIGURE 4. The strongly-connected crystal skeleton $\text{CS}(3, 3)$.

skeleton $\text{CS}(\lambda)$, where $T = \text{std}(b)$. Conversely, for any $b \in B(\lambda)_n$, there exists a sequence j_1, j_2, \dots, j_k for some $1 \leq j_i < n$ such that $v = f_{j_1} \cdots f_{j_k} b$. Since u and v are in the same quasi-crystal component, this means that there is a path in $\text{CS}(\lambda)$ from T to T_u . This proves that $\text{CS}(\lambda)$ is strongly-connected.

Next we show that $\text{CS}(\lambda)$ is not strongly-connected if λ is not rectangular. As before, let u be the highest weight element and v be the lowest weight element in $B(\lambda)_n$. Furthermore, let $T_u = \text{std}(u)$ and $T_v = \text{std}(v)$. Since λ is not rectangular, $T_u \neq T_v$. Namely, T_u has letters $\lambda_1 + \cdots + \lambda_{r-1} + 1, \dots, \lambda_1 + \cdots + \lambda_r$ in row r and T_v has the letters $\lambda_{r+1} + \cdots + \lambda_\ell + 1, \dots, \lambda_r + \cdots + \lambda_\ell$ in row r from the top, where $\ell = \ell(\lambda)$. We now demonstrate that it is not possible to find a directed path in $\text{CS}(\lambda)$ from T_v to T_u .

Since λ is not a rectangle, λ has at least two corner cells. Let α (resp. β) be the topmost (resp. second topmost) corner cell in λ . Let a_u, b_u be the entries in cells α, β in T_u and similarly, a_v, b_v be the entries in cells α, β in T_v . We have $a_v < b_v$ and $a_u > b_u$. To find a path from T_v to T_u in $\text{CS}(\lambda)$ we can apply any crystal operator f_i , but only e_i if there is no bracketing between letters $i+1$ and i (see Proposition 2.9). In $\text{row}(T_v)$, a_v is to the left of b_v and all letters to the left of b_v are weakly smaller than b_v since $a_v < b_v$. The crystal operators f_i act on the rightmost unbracketed letter i . Hence applying f_i operators to T_v , the entry in cell α is always weakly smaller than the entry in cell β . Similarly, applying e_i only in the case when no $i+1$ is bracketed with i , the relative order of the entries in cells α and β cannot change. This proves that there is no path from T_v to T_u in $\text{CS}(\lambda)$. \square

Example 4.17. The crystal skeleton $\text{CS}(3, 2, 1)$ in Figure 2 is not strongly-connected. The crystal skeleton $\text{CS}(3, 3)$ in Figure 4 is strongly-connected.

While only crystal skeletons of rectangular length are strongly-connected, we have the following description of the strongly-connected components of $\text{CS}(\lambda)$ in general.

Theorem 4.18. *The strongly-connected components of $\text{CS}(\lambda)$ can be covered by unions of direct products*

$$\text{CS}(w_1^{\ell_1}) \times \cdots \times \text{CS}(w_N^{\ell_N})$$

of crystal skeletons of rectangular shape.

Proof. By Theorem 4.16, only crystal skeletons of rectangular shape are strongly-connected. By Corollary 4.10, whenever restricting to disjoint subintervals, by jeu de taquin the subgraphs are isomorphic to products of crystal skeletons. Hence determining the strongly-connected component containing a tableau $T \in \text{SYT}(\lambda)$, one can determine all sets of disjoint unions of intervals $I_1 \cup \cdots \cup I_k$ of $[[\lambda]]$ such that $\text{jdt}(T_{I_j})$ has rectangular shape $(w_j^{\ell_j})$ for all $1 \leq j \leq k$. One then repeats this process for all tableaux in the component isomorphic to $\text{CS}(w_1^{\ell_1}) \times \cdots \times \text{CS}(w_k^{\ell_k})$ and obtains a union of direct products of rectangular crystal skeletons. \square

More can be said about the strongly-connected components of $\text{CS}(\lambda)$ when λ has at most two parts.

Corollary 4.19. *Let λ be a partition with at most two parts. The strongly-connected components of $\text{CS}(\lambda)$ are isomorphic to direct products*

$$\text{CS}(w_1^2) \times \cdots \times \text{CS}(w_N^2)$$

of crystal skeletons of rectangular shape.

Proof. The crystal skeletons $\text{CS}(\mu)$ for μ a single column or single row are trivial. Since λ has at most two rows, $\text{shape}(\text{std}(T|_I))$ can have at most two rows. \square

A stronger version of Corollary 4.19 is stated in Corollary 6.6.

4.6. Descent compositions. We have established that the edges of a crystal skeleton are labeled by odd length intervals coming from Dyck patterns and that the vertices are labeled by compositions of n coming from $\text{Des}(T)$ for $T \in \text{SYT}(\lambda)$.

Our goal is to next describe in Theorem 4.26 the relationship between the compositions α and β in an edge in $\text{CS}(\lambda)$:

$$(v, \alpha) \xrightarrow{I} (w, \beta).$$

We first set some notation. Given a composition $\alpha \models n$, write

$$\alpha = (\alpha_1, \dots, \alpha_\ell).$$

Sometimes we will identify α with the partition $(\alpha^{(1)}, \dots, \alpha^{(\ell)})$ of $[n]$, where

$$(4.5) \quad \alpha^{(i)} = \{\alpha_1 + \cdots + \alpha_{i-1} + 1, \alpha_1 + \cdots + \alpha_{i-1} + 2, \dots, \alpha_1 + \cdots + \alpha_i\}.$$

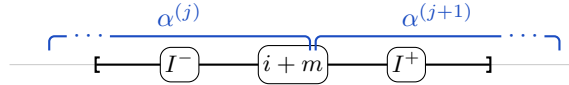
For instance, if $\alpha = (3, 2, 2)$, we will also write it as $\alpha = (123|45|67)$.

Since the edges in $\text{CS}(\lambda)$ are labeled by odd length intervals $I = [i, i + 2m]$ by Theorem 3.9, they can be written

$$I = I^- \cup \{i + m\} \cup I^+ \quad \text{where} \quad |I^-| = |I^+| > 0.$$

In other words, $I^- = [i, i + m - 1]$ and $I^+ = [i + m + 1, i + 2m]$. The decomposition of I interacts with the descent composition as follows:

Lemma 4.20. *Let $T \in \text{SYT}(\lambda)$. Suppose $\alpha = \text{Des}(T)$ and $I = [i, i + 2m] = I^- \cup \{i + m\} \cup I^+$ is a Dyck pattern interval in T . Then $I^- \cup \{i + m\} \subseteq \alpha^{(j)}$ and $I^+ \subseteq \alpha^{(j+1)}$ for some $1 \leq j < \ell$, where ℓ is the length of α :*



Proof. If I is a Dyck pattern interval on T , then (1) the elements of $I^- \cup \{i + m\}$ are in increasing order in $\pi = \text{row}(T)$, and similarly for I^+ , and (2) there is a descent at $i + m$ in $\pi|_I$, i.e. $i + m$ appears after the smallest element of I^+ in π . It follows from (1) that $I^- \cup \{i + m\} \subseteq \alpha^{(j)}$ for some j and $I^+ \subseteq \alpha^{(j')}$ for some $1 \leq j, j' \leq \ell$, and from (2) that $I^+ \not\subseteq \alpha^{(j)}$. Thus $I^+ \subseteq \alpha^{(j+1)}$, since I is a consecutive interval. \square

Example 4.21. Suppose

$$T = \begin{array}{|c|c|c|c|} \hline 5 & 6 & 7 & 8 \\ \hline 1 & 2 & 3 & 4 \\ \hline \end{array},$$

so $\alpha = (1234|5678)$. Then T contains a Dyck pattern interval on $I = [3, 5]$, where $I^- = \{3\}$, $i + m = \{4\}$ and $I^+ = \{5\}$. We see that $\{3, 4\} \subseteq \alpha^{(1)}$ and $\{5\} \subseteq \alpha^{(2)}$.

Our characterization of how descent compositions change between edges in the crystal skeleton in Theorem 4.26 will involve three cases. Recall that for an interval $[a, b] \subseteq [n]$, the restriction $T_{[a,b]}$ is the skew tableau restricted to $[a, b]$ and $\text{jdt}(T_{[a,b]})$ is the jeu de taquin straightening of $T_{[a,b]}$ with shape $\text{shape}(\text{jdt}(T_{[a,b]}))$.

Definition 4.22. Given an interval $[a, b] \subseteq [n]$ of length $2m$, the tableau $T \in \text{SYT}(\lambda)$ has a *rectangle on $[a, b]$* if

$$\text{shape}(\text{jdt}(T_{[a,b]})) = (m, m).$$

Otherwise, we say that T is *rectangle-free on $[a, b]$* .

Example 4.23. Consider T as in Example 4.21. Then T contains a rectangle on $[3, 6]$ since

$$T_{[3,6]} = \begin{array}{|c|c|c|c|} \hline 5 & 6 & & \\ \hline & & 3 & 4 \\ \hline \end{array}$$

and

$$\text{jdt}(T_{[3,6]}) = \begin{array}{|c|c|} \hline 5 & 6 \\ \hline 3 & 4 \\ \hline \end{array}.$$

We will be particularly interested in the case, where $[a, b]$ comes from a Dyck pattern interval as in Example 4.23. Recall from Section 3.2.2 that every Dyck pattern interval on $\pi = \text{row}(T)$ bijects with a cycle $\text{cycle}(\pi|_I)$ and that given $\pi|_I$, we have that $\text{destd}(\pi|_I)$ is the destandardization of $\pi|_I$ in the alphabet $\{i\}^{m+1}, \{i+1\}^m$. The presence or absence of a rectangle is closely related to the elements that appear in $\text{cycle}(\pi|_I)$.

We first prove the following preliminary lemma.

Lemma 4.24. *Given $\pi = \text{row}(T)$ for $T \in \text{SYT}(\lambda)$, let $I = [i, i + 2m]$ be a Dyck pattern interval on π . Then*

(1)

$$\text{cycle}(\pi|_I) = (i + 2m, i + 2m - 1, \dots, i + m)$$

if and only if the unbracketed i in $\text{destd}(\pi|_I)$ is the rightmost i appearing in $\text{destd}(\pi|_I)$, and

(2)

$$\text{cycle}(\pi|_I) = (i + m, i + m - 1, \dots, i)$$

if and only if the unbracketed i in $\text{destd}(\pi|_I)$ is the leftmost i in $\text{destd}(\pi|_I)$.

Proof. Suppose there is an edge from T to T' in $\text{CS}(\lambda)$ labeled by the Dyck pattern interval I . Let $\pi = \text{row}(T)$ and $\pi' = \text{row}(T')$. Recall from the discussion in Section 3.2.2 that

$$T' = (m + \pi_p, m + \pi_p - 1, \dots, \pi_p) \cdot T,$$

where π_p is the letter in T (or π) which corresponds to the i in $\text{destd}(\pi|_I)$ on which f_i acts. It follows that $\text{cycle}(\pi|_I) = (i + 2m, i + 2m - 1, \dots, i + m)$ if and only if $\pi_p = i + m$, which corresponds to f_i acting on the rightmost i in $\text{destd}(\pi|_I)$. Similarly, $\text{cycle}(\pi|_I) = (i + m, i + m - 1, \dots, i)$ if and only if $\pi_p = i$, which corresponds to f_i acting on the leftmost i in $\text{destd}(\pi|_I)$. Since f_i acts on the unique unbracketed i in $\text{destd}(\pi|_I)$, this proves the claim. \square

We will now describe when T has a rectangle coming from a Dyck pattern interval.

Lemma 4.25. *Suppose $I = [i, i + 2m]$ is a Dyck pattern interval on $T \in \text{SYT}(\lambda)$. Let $\pi = \text{row}(T)$. Then the following is true:*

(1) *T has a rectangle on $[i, i + 2m + 1]$ if and only if*

$$\pi|_{\{i+m, i+2m, i+2m+1\}} = i + 2m \quad i + 2m + 1 \quad i + m$$

and $\text{cycle}(\pi|_I) = (i + 2m, i + 2m - 1, \dots, i + m)$.

(2) *T has a rectangle on $[i - 1, i + 2m]$ if and only if*

$$\pi|_{\{i-1, i, i+1\}} = i \quad i - 1 \quad i + 1$$

and $\text{cycle}(\pi|_I) = (i + m, i + m - 1, \dots, i)$.

(3) *T cannot have a rectangle on both $[i - 1, i + 2m]$ and $[i, i + 2m + 1]$.*

Proof. Note that (3) follows immediately from (1) and (2). Since I is a Dyck pattern interval on T and T has a rectangle on both $[i - 1, i + 2m]$ and $[i, i + 2m + 1]$, then by (1) and (2) we have

$$(i + 2m, i + 2m - 1, \dots, i + m) = \text{cycle}(\pi|_I) = (i + m, i + m - 1, \dots, i),$$

which can occur only if $i + m = i$, a contradiction.

Thus it suffices to prove (1) and (2). We will prove (1); the proof of (2) is analogous and therefore omitted.

First suppose that T has a rectangle on $J := [i, i + 2m + 1]$ where $I = [i, i + 2m]$ is a Dyck pattern interval. Note that this is equivalent to the condition that

$$(4.6) \quad P(\pi|_J) = \begin{array}{|c|c|c|c|c|} \hline i+m+1 & i+m+2 & \cdots & i+2m & i+2m+1 \\ \hline i & i+1 & \cdots & i+m-1 & i+m \\ \hline \end{array}.$$

Since $i + 2m + 1$ appears in the top row, it cannot be the last letter in $\pi|_J$, and thus $i + m$ must appear to the right of $i + 2m + 1$. We must also have that $i + 2m$ appears to the left of $i + 2m + 1$, otherwise $\text{shape}(\text{jdt}(\pi|_J))$ would have three rows. Thus we have the following relative order in $\pi|_J$:

$$(4.7) \quad i + 2m \dots i + 2m + 1 \dots i + m.$$

Moreover, we must have the relative order

$$(4.8) \quad i + 2m \dots i + m - 1 \dots i + m,$$

in $\pi|_I$, since otherwise $\text{shape}(\text{jdt}(\pi|_J))$ would have first row of size larger than m . Thus we have that $i + m$ is the last letter in both $\pi|_I$ and $\pi|_J$. This implies that the unbracketed i in $\text{destd}(\pi|_I)$ is the rightmost i . By Lemma 4.24, this means $\text{cycle}(\pi|_I) = (i + 2m, \dots, i + m)$.

In the other direction, note that because I is a Dyck pattern interval,

$$P(\pi|_I) = \begin{array}{|c|c|c|c|c|} \hline i+m+1 & i+m+2 & \dots & i+2m & \\ \hline i & i+1 & \dots & i+m-1 & i+m \\ \hline \end{array}.$$

By assumption, $\pi|_J$ has the same relative order as (4.7). By Lemma 4.24, if $\text{cycle}(\pi|_I) = (i + 2m, i + 2m - 1, \dots, i + m)$, then the unbracketed i in $\text{destd}(\pi|_I)$ is its rightmost i , which implies that $\pi|_J$ has the same relative order as (4.8). It follows that $P(\pi|_J)$ has the form in (4.6), and so T has a rectangle on $J = [i, i + 2m + 1]$. \square

We will use Lemma 4.25 to characterize how descent compositions change in $\text{CS}(\lambda)$.

Theorem 4.26. *Let $T, T' \in \text{SYT}(\lambda)$ with $\text{Des}(T) = \alpha$ and $\text{Des}(T') = \beta$. Suppose there is an edge*

$$I = [i, i + 2m] = I^- \cup \{i + m\} \cup I^+$$

from T to T' in $\text{CS}(\lambda)$ with $I^- \cup \{i + m\} \subseteq \alpha^{(j)}$. Then β must be of the form

$$\beta = (\alpha^{(1)}, \dots, \alpha^{(j-2)}, \underbrace{\quad \circledast \quad}_{\text{---}}, \alpha^{(j+2)}, \dots, \alpha^{(\ell)}),$$

where \circledast is determined as follows:

(1) *If T is rectangle-free on $[i - 1, i + 2m]$ and $[i, i + 2m + 1]$, then I is a length-preserving edge, and*

$$\circledast = \left(\alpha^{(j-1)}, \alpha^{(j)} \setminus \{i + m\}, \alpha^{(j+1)} \cup \{i + m\} \right).$$

(2) *If T contains a rectangle on $[i, i + 2m + 1]$, then I is a length-increasing edge and*

$$\circledast = \left(\alpha^{(j-1)}, \alpha^{(j)} \setminus \{i + m\}, I^+ \cup \{i + m\}, \alpha^{(j+1)} \setminus I^+ \right).$$

(3) *If T contains a rectangle on $[i - 1, i + 2m]$, then $\alpha^{(j)} = I^- \cup \{i + m\}$, and I is a length-decreasing edge:*

$$\circledast = \left(\alpha^{(j-1)} \cup I^-, \alpha^{(j+1)} \cup \{i + m\} \right).$$

Proof. By Lemma 4.20, we may assume that $I^- \cup \{i + m\} \subseteq \alpha^{(j)}$ for some $1 \leq j \leq \ell$. Recall that every Dyck pattern interval defines a cycle $\text{cycle}(\pi|_I)$ such that

$$\text{cycle}(\pi|_I) \cdot T = T'.$$

Note that the elements in $\alpha^{(1)}, \dots, \alpha^{(j-2)}$ and $\alpha^{(j+2)}, \dots, \alpha^{(\ell)}$ are unchanged by applying $\text{cycle}(\pi|_I)$. Thus

$$\beta = (\alpha^{(1)}, \dots, \alpha^{(j-2)}, \underbrace{\quad \circledast \quad}_{\text{---}}, \alpha^{(j+2)}, \dots, \alpha^{(\ell)}),$$

where it remains to determine the makeup of \circledast . Furthermore, by definition of the Dyck pattern interval, in β we know that I^- is in a distinct composition part from $\{i + m\} \cup I^+$. We will go through each case in turn:

(1) Note that

$$\circledast = \left(\alpha^{(j-1)}, \alpha^{(j)} \setminus \{i + m\}, \alpha^{(j+1)} \cup \{i + m\} \right)$$

if the relative positions of $i - 1, i$ and $i + 2m, i + 2m + 1$ are preserved under $\text{cycle}(\pi|_I)$. This follows because the presence or absence of a descent between $i - 1$ and i in π will be unchanged after applying $\text{cycle}(\pi|_I)$, and similarly for a descent between $i + 2m$ and $i + 2m + 1$. Thus the only descent that is

created between T and T' is between $i + m - 1$ and $i + m$, which follows from the definition of a Dyck pattern interval.

The relative positions of $i - 1, i$ and $i + 2m, i + 2m + 1$ are preserved if $i, i + 2m \notin \text{cycle}(\pi|_I)$, since then $\text{cycle}(\pi|_I)$ fixes $i - 1, i, i + 2m$ and $i + 2m + 1$. Inspection shows it is also true when $i \in \text{cycle}(\pi|_I)$ but $i - 1$ does not appear between i and $i + 1$, as well as if $i + 2m \in \text{cycle}(\pi|_I)$ but $i + 2m + 1$ does not occur between $i + 2m$ and $i + m + 1$. By Lemma 4.25, these conditions are met precisely when T is rectangle-free on $[i - 1, i + 2m]$ and $[i, i + 2m + 1]$.

- (2) Suppose T contains a rectangle on $[i, i + 2m + 1]$. Then by Lemma 4.25,

$$\pi|_{\{i+m, i+2m, i+2m+1\}} = i \quad i + 2m \quad i + m$$

and $\text{cycle}(\pi|_I) = (i + 2m, i + 2m - 1, \dots, i + m)$. Note that since $i + 2m$ occurs before $i + 2m + 1$ in π , we have that $\{i + m, \dots, i + 2m, i + 2m + 1\} = I^+ \cup \{i + 2m + 1\} \subseteq \alpha^{(j+1)}$. Under $\text{cycle}(\pi|_I)$, $i + m + 1$ is sent to $i + 2m$, and $i + 2m + 1$ is fixed. Thus in $\text{cycle}(\pi|_I) \cdot \pi$, we have that $i + 2m$ occurs after $i + 2m + 1$, and thus these elements occur in different blocks in β . It follows that

$$\textcircled{*} = \left(\alpha^{(j-1)}, \alpha^{(j)} \setminus \{i + m\}, I^+ \cup \{i + m\}, \alpha^{(j+1)} \setminus I^+ \right).$$

Note that $i + 2m + 1 \in \alpha^{(j+1)} \setminus I^+$, so this part in β is non-empty.

- (3) Suppose T contains a rectangle on $[i - 1, i + 2m]$. Then by Lemma 4.25, we have

$$\pi|_{\{i-1, i, i+1\}} = i \quad i - 1 \quad i + 1$$

and $\text{cycle}(\pi|_I) = (i + m, i + m - 1, \dots, i)$. Since $I^- \subseteq \alpha^{(j)}$ and $i - 1$ appears to the right of i in π , we must have that $i - 1 \in \alpha^{(j-1)}$. It follows that $\alpha^{(j)} = I^- \cup \{i + m\}$. Since $\text{cycle}(\pi|_I)$ maps $i + 1$ to i , in $\text{cycle}(\pi|_I) \cdot \pi$, we have $i - 1$ occurring before i . Thus in β , the blocks $\alpha^{(j-1)}$ and $\alpha^{(j)} \setminus \{i + m\} = I^-$ merge, giving

$$\textcircled{*} = \left(\alpha^{(j-1)} \cup I^-, \alpha^{(j+1)} \cup \{i + m\} \right).$$

□

Example 4.27. Let

$$T = \begin{array}{|c|c|c|} \hline 6 & & \\ \hline 4 & 5 & \\ \hline 1 & 2 & 3 \\ \hline \end{array} \quad \text{and} \quad T' = \begin{array}{|c|c|c|} \hline 6 & & \\ \hline 3 & 5 & \\ \hline 1 & 2 & 4 \\ \hline \end{array}.$$

Then $\pi = 645123$ and $\pi' = 635124$, and there is an edge from T to T' with Dyck pattern $\pi = 423$, so that $I = [2, 4]$ with $I^- = \{2\}$ and $I^+ = \{4\}$. We have $\alpha = (123|45|6)$. Note that T contains a rectangle on $[2, 5]$. Hence I is a length-increasing edge, and $\beta = (12|34|5|6)$.

Example 4.28. Suppose

$$T = \begin{array}{|c|c|c|} \hline 2 & 5 & 6 \\ \hline 1 & 3 & 4 \\ \hline \end{array} \quad \text{and} \quad T' = \begin{array}{|c|c|c|} \hline 4 & 5 & 6 \\ \hline 1 & 2 & 3 \\ \hline \end{array}.$$

Then $\pi = 256134$ and $\pi' = 456123$, and T contains a Dyck pattern interval $I = [2, 6]$ with $I^- = \{2, 3\}$, $k = \{4\}$, and $I^+ = \{5, 6\}$. Note that T contains a rectangle on $[1, 6]$. Thus I is a length-decreasing edge, and $\beta = (123|456)$.

By Proposition 4.3 we know that if $I = [i, i + 2m]$ is a Dyck pattern interval of T , then so is $J = [i + 1, i + 2m - 1] \subsetneq I$. We show that J is always length-increasing.

Corollary 4.29. *Let $T \in \text{CS}(\lambda)$.*

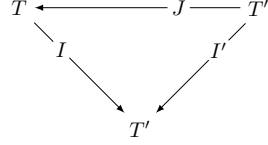
- (1) *Suppose there is an edge $I = [i, i + 2m]$ from T to T' in $\text{CS}(\lambda)$. Then the edge $J = [i + 1, i + 2m - 1]$ out of T is length-increasing.*
- (2) *Suppose there is an edge $I = [i, i + 2m]$ from T' to T in $\text{CS}(\lambda)$. Then the edge $J = [i + 1, i + 2m - 1]$ into T is length-decreasing.*

Proof. We prove part 1 as part 2 is analogous. Let $\pi = \text{row}(T)$. Since I is a Dyck pattern interval of T , we have by Definition 3.3 that $P(\pi|_I)$ is as in (3.1). Removing the letter i from $P(\pi|_I)$ and straightening, gives a tableau of shape (m, m) . Hence by Theorem 4.26, the interval J is length-increasing. □

4.7. **Fans.** We analyze the local properties of the crystal skeleton near its length increasing and decreasing edges. We call the structures that occur *fans*.

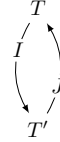
Proposition 4.30. *Suppose $T \xrightarrow{I} T'$ is a length-decreasing edge in $\text{CS}(\lambda)$ (as defined in Theorem 4.26). Then one of the two cases holds:*

(1) *We either have*



$$\text{with } |I| > 3, \quad I = [i, i + 2m], \quad J = [i - 1, i + 1], \quad I' = [i + 1, i + 2m - 1] \quad \text{or}$$

(2) *we have*



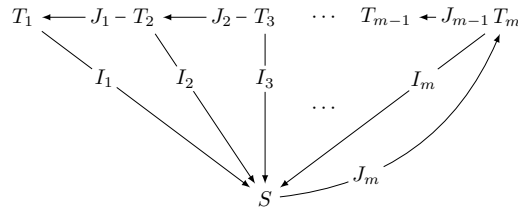
$$\text{with } |I| = |J| = 3, \quad I = [i, i + 2], \quad J = [i - 1, i + 1].$$

Proof. Since the edge labeled I is length-decreasing, by Theorem 4.26 and Lemma 4.25 the letters $i - 1, i, i + 1$ in the reading word of T appear in the order $\dots i \dots i - 1 \dots i + 1 \dots$. Hence there is an incoming arrow into T labeled $J = [i - 1, i + 1]$ from T'' which is obtained from T by the application of the cycle $(i + 1, i)$. Furthermore, T' is obtained from T by the application of the cycle $(i + m, i + m - 1, \dots, i)$.

First suppose that $|I| = 2m + 1 > 3$. In this case the letter $i + 2$ has to be to the right of the letter $i + 1$, that is, $\dots i \dots i - 1 \dots i + 1 \dots i + 2 \dots$. In T'' this reads $\dots i + 1 \dots i - 1 \dots i \dots i + 2 \dots$ and hence there is a Dyck pattern comprised of the letters in the interval $I' = [i + 1, i + 2m - 1]$. Combining Lemma 4.25 and Theorem 4.26, it follows that the new tableau is obtained by the application of the cycle $(i + m, i + m - 1, \dots, i + 1)$ on T'' . Note that this is the same as T' , proving the first claim.

Next assume that $|I| = 3$. In this case T' is obtained from T by the arrow indexed by $I = [i, i + 2]$ by the application of the cycle $(i + 1, i)$. Recall that the incoming arrow labeled $J = [i - 1, i + 1]$ also interchanges i and $i + 1$. Hence in this case $T'' = T'$, which proves the second claim. \square

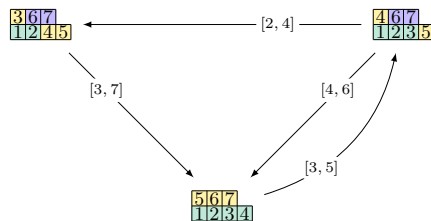
Corollary 4.31. *Suppose $T \xrightarrow{I} S$ is a length-decreasing edge in $\text{CS}(\lambda)$ (as defined in Theorem 4.26). Then all edges entering S from tableaux with longer descent compositions look as follows (with $I = I_j$ for some j):*



where

$$\begin{aligned} I_1 &= [i, i + 2m], & I_2 &= [i + 1, i + 2m - 1], & \dots, & & I_m &= [i + m - 1, i + m + 1], \\ J_1 &= [i - 1, i + 1], & J_2 &= [i, i + 2], & \dots, & & J_m &= [i + m - 2, i + m]. \end{aligned}$$

Example 4.32. In the crystal skeleton $\text{CS}(4, 3)$, we have the following local behavior:

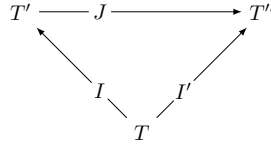


More examples in the two-row case can be found in Section 6.3.1.

There are similar descriptions when I is a length-increasing edge.

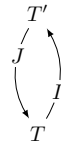
Proposition 4.33. *Suppose $T \xrightarrow{I} T'$ is a length-increasing edge in $\text{CS}(\lambda)$ (as defined in Theorem 4.26). Then one of the two cases holds:*

(1) *We either have*



with $|I| > 3$, $I = [i + 2m]$, $J = [i + 2m - 1, i + 2m + 1]$, $I' = [i + 1, i + 2m - 1]$ or

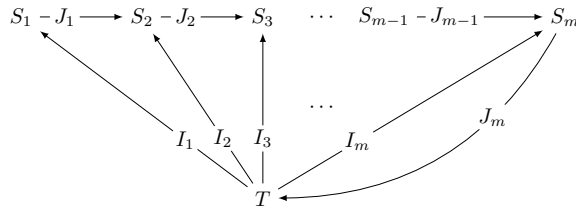
(2) *we have*



with $|I| = |J| = 3$, $I = [i, i + 2]$, $J = [i + 1, i + 3]$.

Proof. The proof is analogous to the proof of Proposition 4.30. □

Corollary 4.34. *Suppose $T \xrightarrow{I} S$ is a length-increasing edge in $\text{CS}(\lambda)$ (as defined in Theorem 4.26). Then all edges leaving T to tableaux with longer descent compositions look as follows (with $I = I_j$ for some j):*



where

$$\begin{aligned} I_1 &= [i, i + 2m], & I_2 &= [i + 1, i + 2m - 1], & \dots, & I_m &= [i + m - 1, i + m + 1], \\ J_1 &= [i + 2m - 1, i + 2m + 1], & J_2 &= [i + 2m - 2, i + 2m], & \dots, & J_m &= [i + m, i + m + 2]. \end{aligned}$$

4.8. Commutation relations. The fans of Section 4.7 are part of a larger set of local commutation relations within the crystal skeleton, which are inherited from local relations in a crystal. Stembridge [29] showed that if $f_i(b) \neq \emptyset$ and $f_j(b) \neq \emptyset$ for $b \in B(\lambda)_n$ with $1 \leq i < j < n$, then either

$$(4.9) \quad f_i f_j(b) = f_j f_i(b) \quad \text{if } \varphi_j(f_i b) = \varphi_j(b) \text{ or } \varphi_i(f_j b) = \varphi_i(b),$$

or

$$(4.10) \quad f_i f_j^2 f_i(b) = f_j f_i^2 f_j(b) \quad \text{if } \varphi_j(f_i b) = \varphi_j(b) + 1 \text{ and } \varphi_i(f_j b) = \varphi_i(b) + 1.$$

The case (4.10) can only happen when $j = i + 1$. The relation (4.9) gives rise to a *commuting square*, whereas (4.10) gives rise to a *commuting octagon*. Similar (dual) relations hold for the raising operators e_i and e_j . See [9, Chapter 4] for more details.

To set up the commutation relations in the crystal skeleton, we assume that there is a vertex $T \in \text{CS}(\lambda)$ such that

$$T \xrightarrow{I} T^I \quad \text{and} \quad T \xrightarrow{J} T^J \quad \text{with } \min I < \min J.$$

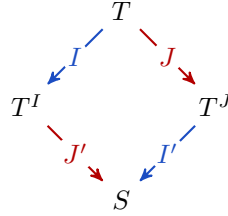
Note that if $I \neq J$, then $\min I = \min J$ is not possible by the definition of Dyck pattern intervals. Recall that I can either be length-preserving, increasing or decreasing according to Theorem 4.26; we call this the *type* of I .

In what follows, we will describe commutation relations by color coding edges; these colors refer to applications of f_i , made specific in the proof of Theorem 4.35. Edge decorations indicate the following edge types:

\dashrightarrow	length-preserving	\longrightarrow	any
\succrightarrow	length-decreasing	\longleftarrow	length-increasing
\dashrightarrow	length-preserving or decreasing	\longleftarrow	length-preserving or increasing

Theorem 4.35. *Let T be a vertex in $\text{CS}(\lambda)$ such that $T \xrightarrow{I} T^I$ and $T \xrightarrow{J} T^J$ with $I = [i, i + 2m]$ and $J = [j, j + 2\ell]$ with $i < j$. Then we have the following local commutation relations:*

Case 1. $\dashrightarrow \textcircled{I} \dashrightarrow \dashrightarrow \textcircled{J} \dashrightarrow$
If $I \cap J = \emptyset$, then we have a square



with $I' = I$ and $J' = J$, such that:

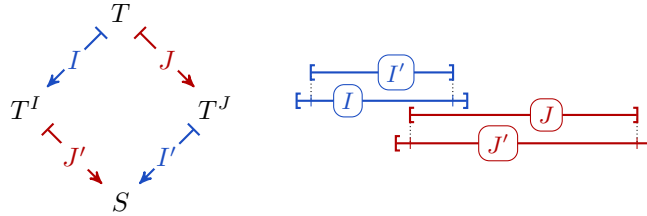
- (a) The edges labeled I and I' (resp. J and J') are of same type if
- $\max I + 1 \neq \min J$ or
 - $\max I + 1 = \min J$ and there is no edge labeled $[i, i + 2m + 2]$ into T or no edge labeled $[j - 2, j + 2\ell]$ out of S .
- (b) If $\max I + 1 = \min J$, there is an edge labeled $[i, i + 2m + 2]$ into T and an edge labeled $[j - 2, j + 2\ell]$ out of S , edge I is length-increasing, edge J' is length-decreasing, and the edges J and I' are length-preserving.

Case 2. $\dashrightarrow \textcircled{I} \dashrightarrow \dashrightarrow \textcircled{J} \dashrightarrow$

If $I \cap J \neq \emptyset$, $J \not\subseteq I$, and I is not length-increasing, consider $T^I \xrightarrow{J'} S^{J'}$ and $T^J \xrightarrow{I'} S^{I'}$. One of the following must hold:

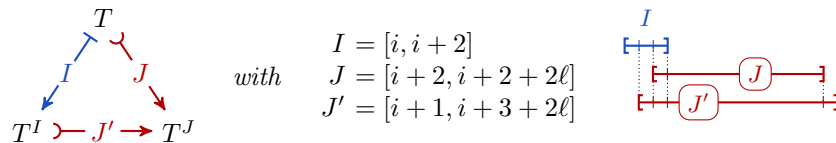
- (a) We have $J \subsetneq J'$ and one of the following cases:

- (i) If $|I| > 3$, we have a square



with $J' = [j - 1, j + 2\ell + 1]$ and $I' = [i + 1, i + 2m - 1]$, where all edges are length-preserving.

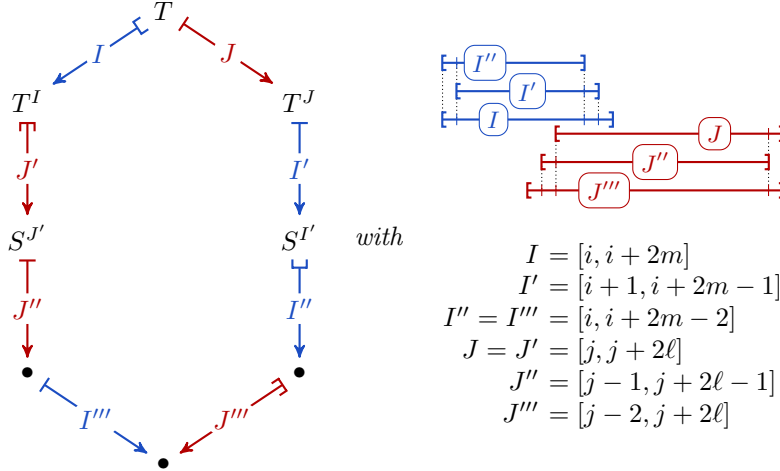
- (ii) If $|I| = 3$, we have a triangle



where I is length-preserving and J and J' are length-decreasing.

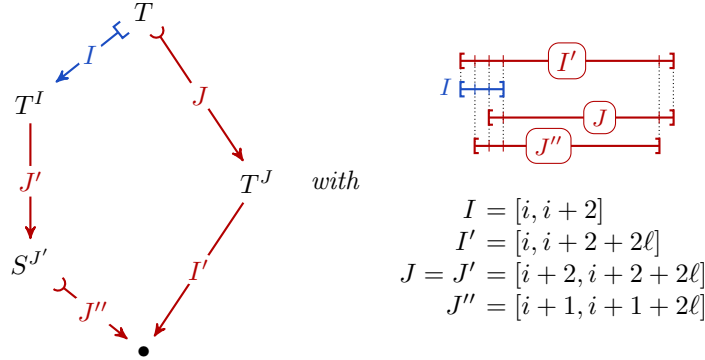
- (b) We have $J = J'$ and one of the following cases must hold:

(i) We have $I' \subsetneq I$ and an octagon



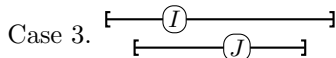
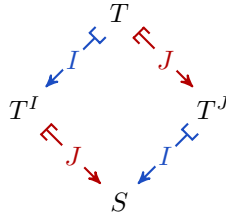
where edges I and I' are length-decreasing or preserving, edges J' and J''' are length-increasing or preserving, and all other edges are length-preserving. When J' is length-increasing, there is also an edge $[j - 1, j + 2\ell + 1]$ out of T^I and case 2(a)i applies as well.

(ii) We have $I \subsetneq I'$ with $|I| = 3$ and a pentagon



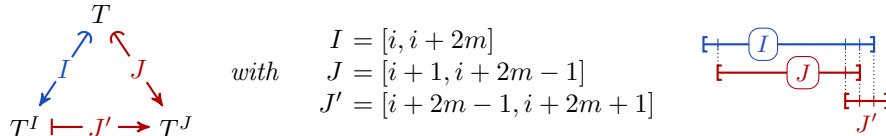
where J and J'' are length-decreasing.

(iii) We have $I' = I$ and a square with edges labeled I (resp. J) of the same type and J is not length-decreasing



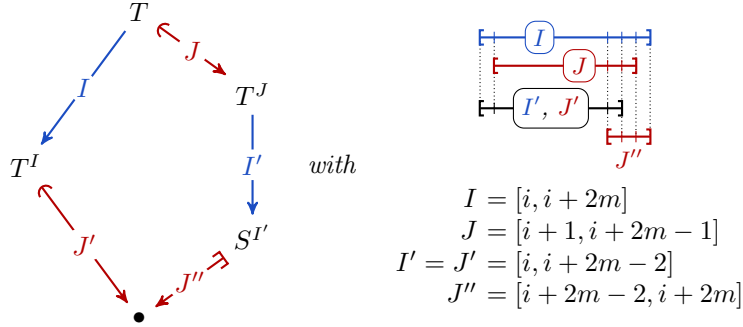
If $J \subsetneq I = [i, i + 2m]$ with $|J| = |I| - 2$, we have the following:

(a) If I is length-increasing, we have a triangle



where J is length-increasing and J' is length-preserving.

(b) We have a pentagon



where J and J' are length-increasing and J'' is not length-decreasing.

Proof. Recall from Remark 3.6 that an edge labeled by the Dyck pattern interval $I = [i, i + 2m]$ (resp. $J = [j, j + 2\ell]$) in the crystal skeleton $\text{CS}(\lambda)$ corresponds to an edge f_i (resp. f_j) in the crystal $B(\lambda)$ by destandardizing the letters in I (resp. J) to letters in $\{i, i + 1\}$ (resp. $\{j, j + 1\}$).

In the crystal $f_i f_j = f_j f_i$ if $i + 1 < j$. In this case $I \cap J = \emptyset$ with $\max I + 1 \neq \min J$ and we obtain a square as in case 1. By Theorem 4.26, the type of the edges is determined by the presence or absence of certain rectangles. These do not change when $I \cap J = \emptyset$ unless $\max I + 1 = \min J$, hence the edges I (resp. J) have the same type.

We can have $I \cap J = \emptyset$ also when $j = i + 1$. By self-similarity (see Section 4.3), we may assume without loss of generality that $I = [1, 2m + 1]$, that is $i = 1$. If I is not length-increasing, we have

$$(4.11) \quad t := \text{jdt}(\text{destd}(T_{I \cup J})) = \begin{array}{cccccccc} & & \overbrace{\quad b \quad} & & & \overbrace{\quad c \quad} & & \\ & & 3 & 3 & 3 & & & \\ & & 2 & 2 & 2 & 2 & 3 & 3 & 3 & \\ & & 1 & 1 & 1 & 1 & 1 & 2 & 2 & 2 & 2 \\ & & \underbrace{\quad m \quad} & & & \underbrace{\quad a \quad} & & & & & \end{array},$$

where $0 \leq a$, $0 \leq b \leq m$ and $0 \leq c \leq a + 1$. The boxes shaded in yellow correspond to the Dyck pattern interval I . In this setup, the edge I (resp. J) in the crystal skeleton corresponds to $f_1 t$ (resp. $f_2 t$). In the commutation relations, we have colored the edges according to the corresponding f_i :

$$\begin{array}{ccc} \xrightarrow{\text{blue } f_1} & & \xrightarrow{\text{red } f_2} \\ \text{(blue)} & & \text{(red)} \end{array}$$

Since $I \cap J = \emptyset$, we have $b + c < a$. The crystal operator f_1 acts on the rightmost 1 and f_2 acts on the rightmost 2, so that $f_1 f_2 = f_2 f_1$. Furthermore the types of the edges I (resp. J) are the same. Hence case 1 holds.

If I is length-increasing, we have

$$(4.12) \quad t := \text{jdt}(\text{destd}(T_{I \cup J})) = \begin{array}{cccccccc} & & \overbrace{\quad b \quad} & & & \overbrace{\quad c \quad} & & \\ & & 3 & 3 & 3 & & & \\ & & 2 & 2 & 2 & 2 & 2 & 3 & 3 & 3 & \\ & & 1 & 1 & 1 & 1 & 1 & 2 & 2 & 2 & 2 \\ & & \underbrace{\quad m \quad} & & & \underbrace{\quad a \quad} & & & & & \end{array},$$

where $0 \leq a$, $0 \leq b \leq m + 1$ and $0 \leq c \leq a$. Since $I \cap J = \emptyset$, we have $b + c \leq a$. When $b > 0$ or when $b + c < a$, it can be checked explicitly that the square holds and that the edges I (resp. J) have the same type. When $b = 0$ and $c = a$, we can have $\max I + 1 = \min J$. In this case, there is an incoming edge $[i, i + 2m + 2]$ into T and an outgoing edge $[j - 2, j + 2\ell]$ out of S . Again, it can be checked explicitly that case 1 holds.

Let us now assume that the conditions of case 2 hold. Again by self-similarity (see Section 4.3), we may assume without loss of generality that $I = [1, 2m + 1]$, that is $i = 1$ and that t is as in (4.11). Since $I \cap J \neq \emptyset$, we have $b + c \geq a$.

If $c = a + 1$, $b < m$, and $|I| > 3$, it can be checked explicitly using the combinatorial definitions of f_1 and f_2 that case 2(a)i holds. If $c = a + 1$, $b < m$, and $|I| = 3$, the edge $f_2 t \xrightarrow{f_1} f_1 f_2 t$ is contracted in the crystal

skeleton by Proposition 2.9 since there is no bracketed pair for the letters $\{1, 2\}$. Edge J is length-decreasing by Corollary 4.29. Hence case 2(a)ii holds.

If $c = a$, $b < m$, and $|I| > 3$, it can be checked explicitly that the octagon in case 2(b)i holds. Note that J' is length-increasing if there is a 4 next to the rightmost 3 in (4.11). This is in the same quasicrystal component as the same tableau with $c = a + 1$, so that case 2(a)i applies. If $c = a$, $b < m$, and $|I| = 3$, the octagon relation $f_1 f_2^2 f_2 t = f_2 f_1^2 f_2 t$ holds in the crystal, but the edges

$$f_2 t \xrightarrow{f_1} f_1 f_2 t, \quad f_1 f_2 t \xrightarrow{f_1} f_1^2 f_2 t, \quad \text{and} \quad f_2^2 f_1 t \xrightarrow{f_1} f_1 f_2^2 f_1 t$$

are contracted (i.e. in the same quasi-crystal) since there are no bracketed pairs in the letters $\{1, 2\}$. Edge J'' is length-decreasing by Corollary 4.29. Since $b = 0$ in this case, edge J is length-decreasing. Hence the pentagon of case 2(b)ii holds.

Finally, if $c < a$ or if $b = m$, it can be checked explicitly that case 2(b)iii holds.

Case 3a follows from Proposition 4.33. Alternatively, it can be derived from the (contracted) square relation in the crystal on the tableau

$$t := \text{jdt}(\text{destd}(T_I)) = \begin{array}{|c|c|c|c|c|} \hline 2 & 2 & 2 & 2 & 3 \\ \hline 1 & 1 & 1 & 1 & 1 \\ \hline \end{array}.$$

$\underbrace{\hspace{10em}}_m$

Case 3b can be derived from the (contracted) octagon relation in the crystal on the previous tableau with 3 replaced by 4 when I is length-increasing or on the following tableau when I is length-preserving or length-decreasing

$$t := \text{jdt}(\text{destd}(T_I)) = \begin{array}{|c|c|c|c|c|} \hline 2 & 2 & 2 & 2 & \\ \hline 1 & 1 & 1 & 1 & 1 \\ \hline \end{array}.$$

$\underbrace{\hspace{10em}}_m$

In this case all but one of the edges given by f_2 are contracted in the crystal skeleton to give a pentagon. The edge J in case 3 is length-increasing by Corollary 4.29. It can be checked explicitly that the edge J' is length-increasing. \square

Remark 4.36. We note that the commutation relations stated in Theorem 4.35 satisfy a duality. Reversing all edges and mapping edge label $I = [i, i + 2m]$ to $[n + 1 - i - 2m, n + 1 - i]$ as in the Lusztig involution, we have that:

- cases 1, 2(a)i, 2(b)i and 2(b)iii are self-dual;
- case 2(a)ii is dual to case 3a;
- case 2(b)ii is dual to case 3b.

4.9. Sub-skeleton with shortest descent composition. Let $\text{CS}(\lambda)$ be a crystal skeleton. The standardization of the highest weight element in $B(\lambda)_n$ has a descent composition with $\ell(\lambda)$ parts; note that this is the minimal length possible for compositions appearing in $\text{CS}(\lambda)$. This shows that

$$\ell(\lambda) = \min\{\text{len}(\text{Des}(T)) \mid T \in \text{CS}(\lambda)\}.$$

Let $\text{CS}(\lambda)_{\ell(\lambda)}$ be the induced subgraph of $\text{CS}(\lambda)$ consisting of the vertices $\{T \in \text{CS}(\lambda) \mid \text{len}(\text{Des}(T)) = \ell(\lambda)\}$.

Theorem 4.37. $\text{CS}(\lambda)_{\ell(\lambda)}$ is isomorphic to the crystal graph $B(\lambda)_{\ell(\lambda)}$. Under this isomorphism:

- The vertex $T \in \text{CS}(\lambda)_{\ell(\lambda)}$ is mapped to $b \in B(\lambda)_{\ell(\lambda)}$ by replacing all letters in $\alpha^{(i)}$ in T in (4.5) by i , where $\alpha = \text{Des}(T)$. Under this map, $\text{Des}(T)$ becomes $\text{wt}(b)$.
- The edge label $I = [i, i + 2m] = I^- \cup \{i + m\} \cup I^+$ with $|I^+| = |I^-|$ in $T \xrightarrow{I} T'$ in $\text{CS}(\lambda)_{\ell(\lambda)}$ becomes $b \xrightarrow{i} b'$ in $B(\lambda)_{\ell(\lambda)}$ if $I^- \cup \{k\} \subseteq \alpha^{(j)}$ and $I^+ \subseteq \alpha^{(j+1)}$.

Proof. Elements in $B(\lambda)_{\ell(\lambda)}$ are semistandard tableaux of shape λ in the alphabet $\{1, 2, \dots, \ell(\lambda)\}$. Since λ has $\ell(\lambda)$ parts, the first column of every tableau in $B(\lambda)_{\ell(\lambda)}$ is filled with the numbers $1, 2, \dots, \ell(\lambda)$. In particular, this means that for every $1 \leq i < \ell(\lambda)$, there is a bracketed $i + 1, i$ pair. Hence by Proposition 2.9 each crystal operator f_i in $B(\lambda)_{\ell(\lambda)}$ moves between quasi-crystal components and hence is associated with an arrow in $\text{CS}(\lambda)$. Furthermore, the weight $\text{wt}(b)$ for $b \in B(\lambda)_{\ell(\lambda)}$ is equal to the descent composition since the first column contains the letters $1, 2, \dots, \ell(\lambda)$ and has length $\ell(\lambda)$ in this case. In a crystal, $\text{wt}(f_i b) = \text{wt}(b) - \alpha_i$, where α_i is the i -th

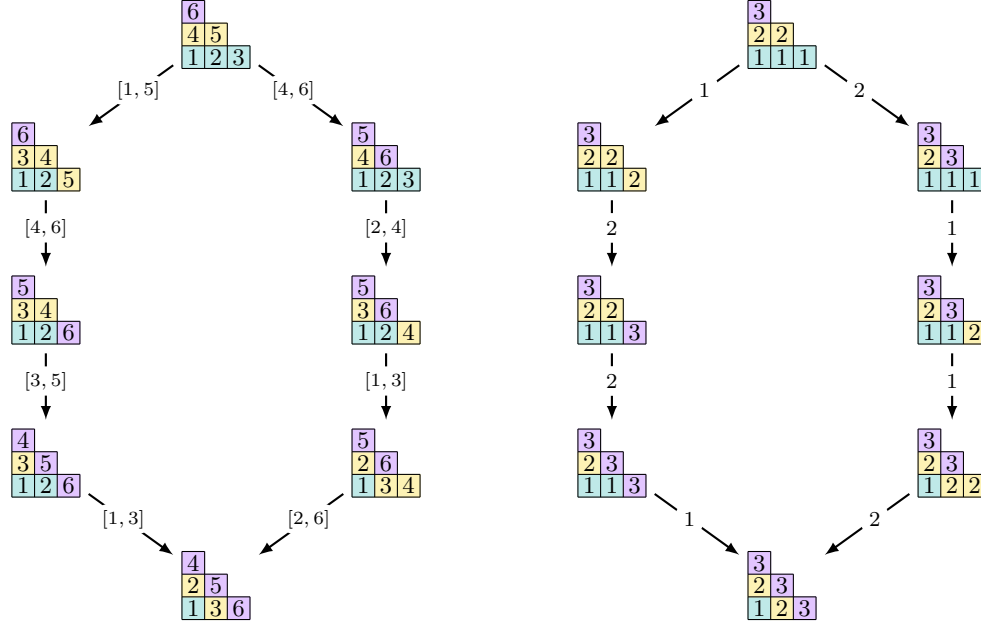


FIGURE 5. Left: Crystal skeleton subgraph $\text{CS}(3, 2, 1)_3$ of Figure 2. Right: Crystal $B(3, 2, 1)_3$ of type A_2 .

simple root with 1 in position i and -1 in position $i + 1$. These correspond to the length-preserving edges in Theorem 4.26. Hence the crystal operators f_i in $B(\lambda)_{\ell(\lambda)}$ corresponds to an edge in $\text{CS}(\lambda)_{\ell(\lambda)}$.

Conversely, suppose $T \xrightarrow{I} T'$ is an edge in $\text{CS}(\lambda)_{\ell(\lambda)}$ with $I \subseteq \alpha^{(j)} \cup \alpha^{(j+1)}$. By Corollary 4.29, I is maximal under containment among all Dyck pattern intervals J for T with $J \subseteq \alpha^{(j)} \cup \alpha^{(j+1)}$. Under the map replacing all letters in $\alpha^{(k)}$ by k , this edge becomes f_j . \square

Example 4.38. The subgraph $\text{CS}(3, 2, 1)_3$ in $\text{CS}(3, 2, 1)$ is indicated by bold edges in Figure 2. Figure 5 also shows $\text{CS}(3, 2, 1)_3$, which is isomorphic to the crystal $B(3, 2, 1)$ of type A_2 .

Recall the string lengths φ_i and ε_i in a crystal defined in (2.4). We can use Theorem 4.37 to determine string lengths on $\text{CS}(\lambda)_{\ell(\lambda)}$ as well.

Corollary 4.39. *Let $T \in \text{CS}(\lambda)_{\ell(\lambda)}$ which maps to $b \in B(\lambda)_{\ell(\lambda)}$ under the isomorphism in Theorem 4.37 and set $\alpha = \text{Des}(T)$. Suppose $T \xrightarrow{I} T'$ is an edge in $\text{CS}(\lambda)_{\ell(\lambda)}$ with $I \subseteq \alpha^{(i)} \cup \alpha^{(i+1)}$. Then*

$$\varphi_i(b) = \min I - \min \alpha^{(i)} + 1 \quad \text{and} \quad \varepsilon_i(b) = \max \alpha^{(i+1)} - \max I.$$

Proof. By self-similarity (see Section 4.3), this can be checked explicitly on a semistandard Young tableau with entries i and $i + 1$. If this tableau has m letters $i + 1$ in the second row and ℓ letters i , then $\varphi_i(b) = \ell - m = \min I - \min \alpha^{(i)} + 1$. Similarly, if the tableau has ℓ' letters $i + 1$ in the first row, then $\varepsilon_i(b) = \ell' = \max \alpha^{(i+1)} - \max I$. \square

Proposition 4.40. *Let $T \in \text{CS}(\lambda)$. Then the following is true:*

- (1) *If $\text{Des}(T) \neq \lambda$, then T has at least one incoming edge which is length-preserving or length-increasing.*
- (2) *If $\text{rev}(\text{Des}(T)) \neq \lambda$, then T has at least one outgoing edge which is length-preserving or length-decreasing.*

Proof. We prove (2) as (1) follows by applying Lusztig involution.

Assume that all outgoing edges from T are length-increasing. Then for every Dyck pattern interval $I = [i, i + 2m]$, the tableau T contains a rectangle on $[i, i + 2m + 1]$ by Theorem 4.26. In particular, this means that if $\text{Des}(T) = (\alpha_1, \dots, \alpha_\ell)$, we must have $\alpha_\ell \geq \alpha_{\ell-1} \geq \dots \geq \alpha_1$, so that $\text{rev}(\text{Des}(T))$ is a partition. Let $b \in \text{QYT}(\lambda)$ be the quasi-Yamanouchi tableau corresponding to T under the bijection in Lemma 2.16. If in the first column of b a letter $1 < j \leq \ell$ is missing, then there is a Dyck pattern interval $I = [i, i + 2m] \subseteq \alpha^{(j-1)} \cup \alpha^{(j)}$, which does not contain a rectangle $[i, i + 2m + 1]$, contradicting the fact that all Dyck pattern intervals contain such a rectangle. Hence every letter $1 \leq j \leq \ell$ appears in the first column of b , which implies that ℓ is the

number of parts of λ . Therefore $T \in \text{CS}(\lambda)_{\ell(\lambda)}$. Recall from Theorem 4.37 that $\text{CS}(\lambda)_{\ell(\lambda)}$ is isomorphic to $B(\lambda)_{\ell(\lambda)}$. Every vertex in the crystal $B(\lambda)_{\ell(\lambda)}$ has an outgoing edge except for the lowest weight vector of weight $\text{rev}(\lambda)$. Hence under the isomorphism, every vertex $T \in \text{CS}(\lambda)_{\ell(\lambda)}$ has a length-preserving outgoing edge unless $\text{Des}(T) = \text{rev}(\lambda)$. By assumption $\text{Des}(T) \neq \text{rev}(\lambda)$, proving the claim. \square

5. AXIOMATIC CHARACTERIZATION OF THE CRYSTAL SKELETON

In this section, we give an axiomatic characterization of the crystal skeleton. Graphs satisfying these axioms are called CS-graphs. We begin in Section 5.1 by stating the GL_n -version of the axioms. In Section 5.2, we show that crystal skeletons satisfy the GL_n -axioms. We state dual versions of the GL_n -axioms in Section 5.3 and show that CS-graphs satisfy S_n branching properties in Section 5.4. In Section 5.5, we show that the GL_n -axioms uniquely specify a CS-graph for each partition λ . This shows that the axioms characterize crystal skeletons. In Section 5.6, we give S_n versions of the axioms and conclude in Section 5.7 with local axioms.

5.1. GL_n -axioms. Suppose (V, E) is a finite, directed graph with vertex set V and edge set $E = \{vw \mid v, w \in V\}$. Fix $n \in \mathbb{Z}_{\geq 1}$. Let G be a vertex- and edge-labeled graph as follows:

- The vertices are labeled by compositions $\alpha = (\alpha_1, \dots, \alpha_\ell)$ of n , so that the labeled vertex set is $V_L = \{(v, \alpha) \mid v \in V\}$ with $\alpha \models n$. Sometimes we identify α with the partition $(\alpha^{(1)}, \dots, \alpha^{(\ell)})$ of $[n]$, where

$$\alpha^{(i)} = \{\alpha_1 + \dots + \alpha_{i-1} + 1, \alpha_1 + \dots + \alpha_{i-1} + 2, \dots, \alpha_1 + \dots + \alpha_i\}.$$
- The edges are labeled by (odd-length) intervals $I \subseteq [n]$, so that the labeled edge set is $E_L = \{(vw, I) \mid vw \in E\}$.

With G as above, we define the Lusztig involution on G as follows.

Definition 5.1 (Lusztig involution). The *Lusztig involution* \mathcal{L}_n on G is defined by

- relabeling the vertices by replacing (v, α) by $(v, \text{rev}(\alpha))$, and
- reversing all edge directions and changing the edge label

$$I = [a, b] \quad \text{to} \quad I^{\mathcal{L}} := [n + 1 - b, n + 1 - a].$$

Example 5.2. Suppose $n = 6$. Then \mathcal{L}_6 acts by

$$\mathcal{L}_6 : \left((v, (3, 2, 1)) \xrightarrow{[4,6]} (w, (3, 1, 2)) \right) \mapsto \left((w, (2, 1, 3)) \xrightarrow{[1,3]} (v, (1, 2, 3)) \right).$$

We will also restrict our graphs via *branched graphs* as follows.

Definition 5.3 (Branched graph). Define $G_{[1, n-1]} = (V'_L, E'_L)$, where

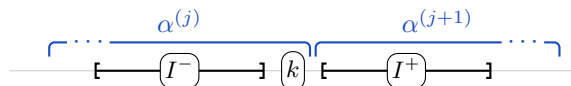
$$V'_L = \{(v, \alpha \setminus \{n\}) \mid (v, \alpha) \in V_L\} \quad \text{and} \quad E'_L = \{(vw, I) \mid (vw, I) \in E_L, I \subseteq [n-1]\}.$$

Example 5.4. In Figure 2, the graph $G_{[1,5]}$ is isomorphic to the portion of $\text{CS}(3, 2, 1)$ shaded in gray. To obtain $G_{[1,5]}$ from the gray subgraph, keep the edge labels the same and replace the vertex $\text{Des}(T)$ for $T \in \text{SYT}(3, 2, 1)$ with $\text{Des}(T_{[1,5]})$ as in Section 4.3.

We are now ready to state the axioms for crystal skeletons. Graph isomorphisms are considered to preserve vertex and edge labels.

Axiom 5.5 (Axioms for crystal skeletons). Let n be a positive integer and G be a finite, connected, vertex- and edge-labeled graph with labeled vertex set V_L and labeled edge set E_L as above. We call G a *CS-graph* if the following axioms hold:

- A0.** (*Intervals*) Suppose $(v, \alpha) \xrightarrow{I} (w, \beta)$ is an edge in G . Then the interval $I \subseteq [n]$ satisfies
- $I = I^- \cup \{k\} \cup I^+$ where $|I^-| = |I^+| > 0$,
 - $I^- \cup \{k\} \subseteq \alpha^{(j)}$ and $I^+ \subseteq \alpha^{(j+1)}$ for some $1 \leq j < \ell$, where ℓ is the length of α .



- A1.** (*Outgoing edges*) For each $(v, \alpha) \in V_L$ and each interval I satisfying **A0** exactly one of the following holds: Either
- there is exactly one outgoing edge $(v, \alpha) \xrightarrow{I} \square$ labeled by I ; or
 - there is an incoming edge $(u, \gamma) \xrightarrow{J} (v, \alpha)$ with $J \subseteq I$ and γ dominates α .

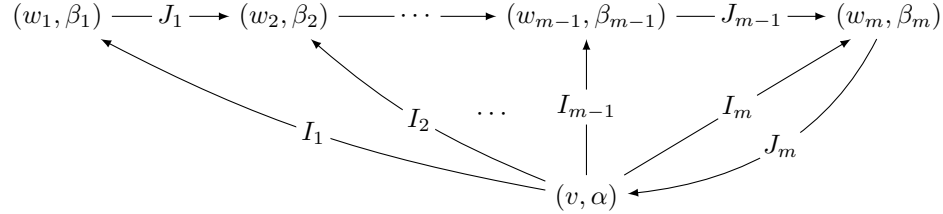
A2. (*Labels*) Let $(v, \alpha) \xrightarrow{I} (w, \beta)$ be an edge as in **A0**. Given α and I , then β must be of the form

$$\beta = (\alpha^{(1)}, \dots, \alpha^{(j-2)}, \underbrace{\quad \circledast \quad}_{\text{interval}}, \alpha^{(j+2)}, \dots, \alpha^{(\ell)}),$$

where \circledast is one of

- I.** (*length-preserving*) $\circledast = (\alpha^{(j-1)}, \alpha^{(j)} \setminus \{k\}, \alpha^{(j+1)} \cup \{k\})$;
- II.** (*length-increasing*) $\circledast = (\alpha^{(j-1)}, \alpha^{(j)} \setminus \{k\}, I^+ \cup \{k\}, \alpha^{(j+1)} \setminus I^+)$; or
- III.** (*length-decreasing*) $\circledast = (\alpha^{(j-1)} \cup I^-, \alpha^{(j+1)} \cup \{k\})$, given $\alpha^{(j)} = I^- \cup \{k\}$.

A3. (*Fans*) Suppose $(v, \alpha) \xrightarrow{I} (w, \beta)$ is an edge in G with β satisfying axiom **A2 II**. Then this edge is part of a fan



where (w, β) is one of the (w_j, β_j) and

$$I_1 = [i, i + 2m], \quad I_2 = [i + 1, i + 2m - 1], \dots, \quad I_m = [i + m - 1, i + m + 1]$$

$$J_1 = [i + 2m - 1, i + 2m + 1], \quad J_2 = [i + 2m - 2, i + 2m], \dots, \quad J_m = [i + m, i + m + 2]$$

for some i and m . The edges labeled I_1, \dots, I_m satisfy axiom **A2 II**, the edges labeled J_1, \dots, J_{m-1} satisfy axiom **A2 I** and the edge labeled J_m satisfies axiom **A2 III**.

A4. (*Strong Lusztig involution*) G and $G_{[1, n-1]}$ are invariant under Lusztig involution:

- (a) $\mathcal{L}_n(G) \cong G$;
- (b) $\mathcal{L}_{n-1}(G_{[1, n-1]}) \cong G_{[1, n-1]}$.

A5. (*Top subcrystal*) Let $s = \min\{\text{len}(\alpha) \mid (v, \alpha) \in V_L\}$ be the minimal length of all vertex labels. Let G_s be the induced subgraph of G with vertex set

$$\{(v, \alpha) \in V_L \mid \text{len}(\alpha) = s\}.$$

Then G_s is isomorphic to the crystal graph $B(\lambda)_s$ for some partition λ with $\ell(\lambda) = s$. Under this isomorphism, the vertex labels become the weights in $B(\lambda)_s$ and an edge labelled I satisfying axiom **A0** becomes f_j in $B(\lambda)_s$.

Remark 5.6. Note that the crystal $B(\lambda)_s$ appearing in axiom **A5** has a unique vertex (u, λ) with label λ . Hence G itself has a unique such vertex and so we will write G_λ for the CS-graph G containing $B(\lambda)_s$.

5.2. Crystal skeleton as a CS-graph. We first show that the crystal skeleton is indeed a CS-graph.

Theorem 5.7. *For any partition λ , the crystal skeleton $\text{CS}(\lambda)$ is a CS-graph with vertex labeling given by descent compositions and edge labeling given by Dyck pattern intervals.*

Proof. Let $G = \text{CS}(\lambda)$, with edge and vertex labelings as stated. We will show that G satisfies all of the axioms of a CS-graph. By Theorem 3.9, the edges in G are labelled by Dyck pattern intervals I , which are intervals of odd length. This implies that G satisfies axiom **A0 (a)**. Axiom **A0 (b)** follows from Lemma 4.20.

Next we show that axiom **A1** holds. Let (T, α) be a vertex in G with $T \in \text{SYT}(\lambda)$ and $\alpha = \text{Des}(T)$. Let $I = I^- \cup \{k\} \cup I^+$ be an interval satisfying Axiom **A0** such that $I^- \cup \{k\} \subseteq \alpha^{(j)}$ and $I^+ \subseteq \alpha^{(j+1)}$. There is an edge labeled I out of vertex (T, α) in $\text{CS}(\lambda)$ if and only if I is a Dyck pattern interval by Theorem 3.9.

First consider the case that there is an edge with interval I . By Theorem 4.7, G restricted to only edges labeled by intervals contained in I is isomorphic to $\text{CS}(m+1, m)$ with $m = |I^-|$ since $P(\pi|_I)$ has shape $(m+1, m)$ for $\pi = \text{row}(T)$. In $\text{CS}(m+1, m)$, the vertex (T, α) has label $(m+1, m)$. Note that $\text{CS}(m+1, m)$ has a unique vertex with label $(m+1, m)$ and this is the lexicographically largest label. Hence every incoming edge $(T', \alpha') \xrightarrow{J} (T, (m+1, m))$ in $\text{CS}(m+1, m)$ has a label α' that is smaller in dominance order than $(m+1, m)$. This remains true when embedded into the larger graph G . This confirms axiom **A1** in this case.

Next consider the case that there is no edge labeled I out of (T, α) . This means that the standard tableau T does not contain a Dyck pattern $\pi|_I$, where $\pi = \text{row}(T)$. Hence $P(\pi|_I)$ has shape μ with $\mu >_D (m+1, m)$ and $\mu_2 < m$. Furthermore, $\mu_2 > 0$ since by assumption $I^- \cup \{k\} \subseteq \alpha^{(j)}$ and $I^+ \subseteq \alpha^{(j+1)}$ so that there is at least one descent. Hence in particular, $m > 1$. In $\text{CS}(\mu)$, there is an edge labeled $[m+1, m+3]$ from the

standard tableau with descent composition $(m+2, m-1)$ to that of descent composition $(m+1, m)$. Since $(m+2, m-1) >_D (m+1, m)$, this proves axiom **A1** in this case.

Axiom **A2** holds by Theorem 4.26.

Axiom **A3** holds by Corollary 4.34.

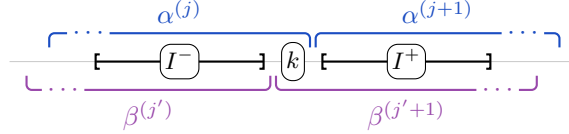
Axiom **A4 (a)** holds by Corollary 4.13.

Axiom **A4 (b)** follows from Theorem 4.11 and Corollary 4.13.

Axiom **A5** holds by Theorem 4.37. \square

5.3. Dual version of the axioms. By the Lusztig involution, the axioms **A0-A3** have dual versions:

- A0'**. (*Intervals*) Suppose $(v, \alpha) \xrightarrow{I} (w, \beta)$ is an edge in G . Then the interval $I \subseteq [n]$ satisfies
 (b') $I^- \subseteq \beta^{(j')}$ and $I^+ \cup \{k\} \subseteq \beta^{(j'+1)}$ for some $1 \leq j' < \ell'$, where ℓ' is the length of β .



- A1'**. (*Incoming edges*) For each $(w, \beta) \in V_L$ and each interval I satisfying **A0'** exactly one of the following holds: Either

(i) there is exactly one incoming edge $\square \xrightarrow{I} (w, \beta)$ labeled by I ; or

(ii) there is an outgoing edge of the form $(w, \beta) \xrightarrow{J} (u, \gamma)$ with $J \subseteq I$ and $\gamma <_D \beta$.

- A2'**. (*Labels*) Let $(v, \alpha) \xrightarrow{I} (w, \beta)$ be an edge. Given β and I , then α must be of the form

$$\alpha = (\beta^{(1)}, \dots, \beta^{(j-2)}, \square \odot \square, \beta^{(j+3)}, \dots, \beta^{(\ell')}),$$

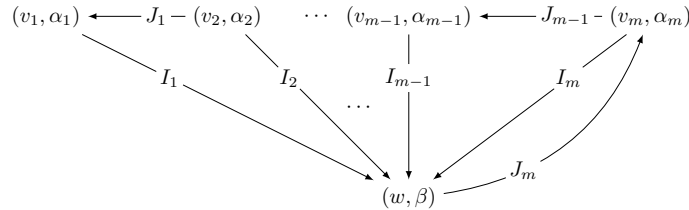
where \odot is one of

I. (*length-preserving*) $\odot = (\beta^{(j-1)}, \beta^{(j)} \cup \{k\}, \beta^{(j+1)} \setminus \{k\}, \beta^{(j+2)});$

II. (*length-increasing*) $\odot = (\beta^{(j-1)}, \beta^{(j)} \cup \{k\}, I^+ \cup \beta^{(j+2)}),$ given $\beta^{(j+1)} = I^+ \cup \{k\};$ or

III. (*length-decreasing*) $\odot = (\beta^{(j-1)} \setminus I^-, I^- \cup \{k\}, \beta^{(j)} \setminus \{k\}, \beta^{(j+1)}, \beta^{(j+2)}).$

- A3'**. (*Fans*) Suppose $(v, \alpha) \xrightarrow{I} (w, \beta)$ is an edge in G with β satisfying axiom **A2 III**. Then this edge is part of a fan



where (v, α) is one of the (v_j, α_j) and $I_1 = [i, i+2m], I_2 = [i+1, i+2m-1], \dots, I_m = [i+m-1, i+m+1], J_1 = [i-1, i+1], J_2 = [i, i+2], \dots, J_m = [i+m-2, i+m]$ for some i and m . The edges labeled I_1, \dots, I_m satisfy axiom **A2 III**, the edges labeled J_1, \dots, J_{m-1} satisfy axiom **A2 I** and the edge labeled J_m satisfies axiom **A2 II**.

5.4. Branching properties. Recall that for a CS-graph $G = (V_L, E_L)$ with labeled vertex set $V_L = \{(v, \alpha) \mid v \in V\}$ and labeled edge set $E_L = \{(vw, I) \mid v, w \in V\}$ (where labels satisfy $\alpha \models n$ and $I \subseteq [n]$ as above), we defined:

- $G_{[1, n-1]} = (V'_L, E'_L)$, with labeled vertex set $V'_L = \{(v, \alpha \setminus \{n\}) \mid (v, \alpha) \in V_L\}$, and
- labeled edge set $E'_L = \{(vw, I) \mid (vw, I) \in E_L, I \subseteq [n-1]\}$.

In addition, we define another graph:

- $G_{[2, n]} = (V''_L, E''_L)$ with labeled vertex set $V''_L = \{(v, \alpha \setminus \{1\}) \mid (v, \alpha) \in V_L\}$, and
- labeled edge set $E''_L = \{(vw, I-1) \mid (vw, I) \in E_L, I \subseteq [2, n]\}$, where $I-1$ decreases the interval bounds by 1 (e.g. $[i, j]-1 = [i-1, j-1]$).

We now study properties of these subgraphs.

Theorem 5.8. *Suppose $G := G_\lambda$ is a CS-graph. Then:*

- (1) *The graphs $G_{[1, n-1]}$ and $G_{[2, n]}$ are isomorphic.*

- (2) $G_{[1,n-1]}$ and $G_{[2,n]}$ are unions of CS-graphs.
(3) We have

$$G_{[1,n-1]} \cong \bigcup_{\substack{\lambda^- \\ |\lambda/\lambda^-|=1}} G_{\lambda^-}.$$

Proof. Recall that the Lusztig involution \mathcal{L}_n reverses all labels $\alpha = (\alpha_1, \dots, \alpha_\ell) \mapsto (\alpha_\ell, \dots, \alpha_1)$, reverses all arrows, and maps the edge label I to $\{n+1-a \mid a \in I\}$. Since G is a CS-graph, Axiom **A4** (a) holds so that $\mathcal{L}_n(G) \cong G$. Denote by ψ^n (resp. ψ^1) the map that removes all edges labelled I with $n \in I$ (resp. $1 \in I$) and set $G^n = \psi^n(G)$ and $G^1 = \psi^1(G)$. Note that $\psi^n = \mathcal{L}_n \circ \psi^1 \circ \mathcal{L}_n$ so that

$$(5.1) \quad G^n = \psi^n(G) = \mathcal{L}_n \circ \psi^1 \circ \mathcal{L}_n(G) \cong \mathcal{L}_n \circ \psi^1(G) = \mathcal{L}_n(G^1),$$

where the isomorphism applies $\mathcal{L}_n(G) \cong G$. Define the map φ^n on vertex labels $\alpha = (\alpha_1, \dots, \alpha_\ell)$ by $\alpha \mapsto (\alpha_1, \dots, \alpha_{\ell-1}, \alpha_\ell - 1)$ and φ^1 by mapping vertex labels $\alpha \mapsto (\alpha_1 - 1, \alpha_2, \dots, \alpha_\ell)$ and edge labels $I \mapsto I - 1$. Note that $G_{[1,n-1]} = \varphi^n(G^n)$ and $G_{[2,n]} = \varphi^1(G^1)$, so that using (5.1) we have

$$G_{[1,n-1]} = \varphi^n(G^n) \cong \varphi^n \mathcal{L}_n(G^1) = \mathcal{L}_{n-1} \varphi^1(G^1) = \mathcal{L}_{n-1}(G_{[2,n]}).$$

Since \mathcal{L}_{n-1} is an involution, we thus have $G_{[2,n]} \cong \mathcal{L}_{n-1}(G_{[1,n-1]}) \cong G_{[1,n-1]}$ by axiom **A4** (b). This proves (1).

Next we show that $G_{[1,n-1]}$ is a union of CS-graphs. The claim that $G_{[2,n]}$ is a union of CS-graphs then follows from (1).

Let

$$(v, \alpha) \xrightarrow{I} (w, \beta)$$

be an edge in G . This edge is also an edge in $G_{[1,n-1]}$ if $I \subseteq [1, n-1]$. Axiom **A0** is satisfied for $G_{[1,n-1]}$ since I labels an edge in G , which satisfies axiom **A0** by assumption. If (v, α) is a vertex in G , then the corresponding vertex in $G_{[1,n-1]}$ is $(v, \alpha_{[1,n-1]})$, where $\alpha_{[1,n-1]} = (\alpha_1, \alpha_2, \dots, \alpha_{\ell-1})$. Note that $\alpha' >_D \alpha$ in G implies that $\alpha'_{[1,n-1]} >_D \alpha_{[1,n-1]}$ in $G_{[1,n-1]}$. Hence axiom **A1** holds for $G_{[1,n-1]}$. If $n \notin \alpha^{(j+1)}$, then **A2** is still satisfied in $G_{[1,n-1]}$ since the conditions are local on $\alpha^{(j)}, \alpha^{(j+1)}$. Hence assume that $n \in \alpha^{(j+1)}$. If β in axiom **A2** is in case **I** or **III** in G , then it is still in these cases in $G_{[1,n-1]}$ since the presence or absence of the element n in α does not alter the form of β given in axiom **A2**. This is also true if β is in case **II**, unless $\alpha^{(j+1)} = I^+ \cup \{n\}$, in which case the edge (vw, I) becomes an edge in case **I** in $G_{[1,n-1]}$, since $\alpha^{(j+1)} \setminus \{n, I^+\} = \emptyset$. Hence axiom **A2** holds for $G_{[1,n-1]}$.

The graph G satisfies the fan axiom **A3**. If none of the intervals in the fan contain n , they will all still appear in $G_{[1,n-1]}$ and will be of the same type in axiom **A2**. Hence the fan exists in $G_{[1,n-1]}$ as desired. Note that $J_1 = [i+2m-1, i+2m+1]$ contains the largest letter among all intervals in the fan in G . Now assume that $n \in J_1$, that is, $n = i+2m+1$. In this case the edge labelled J_1 is missing in $G_{[1,n-1]}$. Furthermore, the edge

$$(v, \alpha) \xrightarrow{I_1} (w_1, \beta_1)$$

satisfies $I_1 = [n-2m+1, n-1]$ and $\beta_1 = (\alpha^{(1)}, \dots, \alpha^{(\ell-2)}, \alpha^{(\ell-1)} \setminus \{n-m\}, \{n-m, \dots, n-1\}, \{n\})$. In particular, $\alpha^{(\ell)} = I_1^+ \cup \{n\} = [n-m+1, n]$, so that the edge labelled I_1 becomes of type **I** in axiom **A2** in $G_{[1,n-1]}$. This proves that $G_{[1,n-1]}$ satisfies axiom **A3**.

By assumption G satisfies axiom **A4** (b), that is $\mathcal{L}_{n-1}(G_{[1,n-1]}) = G_{[1,n-1]}$. This is axiom **A4** (a) for $G_{[1,n-1]}$ since n is replaced by $n-1$ for $G_{[1,n-1]}$. By part (1), we have $G_{[1,n-1]} \cong G_{[2,n]}$. Acting by $\varphi^{n-1} \circ \psi^{n-1}$ on $G_{[1,n-1]}$ yields $G_{[1,n-2]}$. Acting by $\varphi^{n-1} \circ \psi^{n-1}$ on $G_{[2,n]}$ yields

$$\varphi^{n-1} \psi^{n-1} G_{[2,n]} = \varphi^{n-1} \psi^{n-1} \varphi^1 \psi^1 G = \varphi^1 \psi^1 \varphi^n \psi^n G = \varphi^1 \psi^1 G_{[1,n-1]} = G_{[2,n-1]}.$$

Hence $G_{[1,n-2]} \cong G_{[2,n-1]}$. By the same arguments as in the proof of part (1), this is equivalent to $\mathcal{L}_{n-2}(G_{[1,n-2]}) \cong G_{[1,n-2]}$ using $\mathcal{L}_{n-1}(G_{[1,n-1]}) = G_{[1,n-1]}$. This proves axiom **A4** (b) for $G_{[1,n-1]}$.

By assumption, G satisfies axiom **A5**, hence G_s is isomorphic to $B(\lambda)_s$ for some partition λ of length s . The vertices of $B(\lambda)_s$ can be indexed by semistandard tableaux of shape λ in the alphabet $\{1, 2, \dots, s\}$. The label of $t \in B(\lambda)_s$ in G is its weight $\text{wt}(t)$. Transitioning from G to $G_{[1,n-1]}$ corresponds to removing the rightmost letter s in t since under standardization this letter corresponds to n in the standard tableau. This results in a tableau t^- of shape λ^- , where λ/λ^- is the box of the corner cell containing the rightmost s .

First consider the case that the length of λ^- is still s . Then the crystal $B(\lambda^-)_s$ compared to $B(\lambda)_s$ restricted to the vertices with a letter s in λ/λ^- has potentially more edges f_{s-1} (since the s in λ/λ^- is potentially bracketed with an $s-1$). Since G satisfies axiom **A1**, there is an edge in G corresponding to such an extra edge

f_{s-1} in $B(\lambda^-)_s$ compared to $B(\lambda)_s$, however it is of type **II** in axiom **A2** and not of type **I**. It has $\alpha_{s+1} = 1$. Hence $(G_{[1,n-1]})_s$ contains $B(\lambda^-)_s$ and the connected component of $G_{[1,n-1]}$ containing $B(\lambda^-)_s$ restricted to labels of length s is isomorphic to it. This shows that this component of $G_{[1,n-1]}$ satisfies axiom **A5**.

Next consider the case that the length of λ^- is $s-1$. In this case $\lambda_s = 1$. The vertices of the crystal $B(\lambda^-)_{s-1}$ are the tableaux in $B(\lambda)_s$ with only one letter s in row s . Since $B(\lambda^-)_{s-1}$ only has arrows labelled $1, 2, \dots, s-2$, these are all contained in $B(\lambda)_s$ on the vertices in $B(\lambda^-)_{s-1}$. The connected component of $G_{[1,n-1]}$ containing $B(\lambda^-)_{s-1}$ restricted to labels of length $s-1$ is isomorphic to it. This shows that this component of $G_{[1,n-1]}$ satisfies axiom **A5**.

Part (3) follows from (2) and the fact that the crystal $B(\lambda)_s$ in G breaks into crystals $B(\lambda^-)_s$ or $B(\lambda^-)_{s-1}$, where $|\lambda/\lambda^-| = 1$, when passing from G to $G_{[1,n-1]}$. \square

Remark 5.9. Note that under the assumption that Lusztig involution holds on G_λ (axiom **A4** (a)), the proof of Theorem 5.8 (1) shows that Theorem 5.8 (1) is equivalent to axiom **A4** (b). Hence Axiom **A4** (b) can be replaced by

A4.(b) The graphs $G_{[1,n-1]}$ and $G_{[2,n]}$ are isomorphic.

5.5. Uniqueness of CS-graphs. In this section, we show that Axiom 5.5 uniquely determines CS-graphs for a given λ , and hence $G_\lambda \cong \text{CS}(\lambda)$.

We begin by considering whether a CS-graph G can be reconstructed from $G_{[1,n-1]}$. To this end, we first make some observations. As in the proof of Theorem 5.8 define the map φ on compositions by (this map is denoted by φ^n in the proof of Theorem 5.8)

$$\varphi(\alpha_1, \dots, \alpha_\ell) = (\alpha_1, \dots, \alpha_{\ell-1}, \alpha_\ell - 1).$$

We extend this to a map $\varphi: G \rightarrow G_{[1,n-1]}$ by acting on the labels of all vertices and removing all edges labelled by I which contain n . Consider an edge $(v, \alpha) \xrightarrow{I} (w, \beta)$ in G with $n \notin I$ and consider its image under φ :

$$(5.2) \quad \begin{array}{ccc} (v, \alpha) & \xrightarrow{I} & (w, \beta) & \text{in } G \\ \varphi \downarrow & & \downarrow \varphi & \\ (v, \alpha_{[1,n-1]}) & \xrightarrow{I} & (w, \beta_{[1,n-1]}) & \text{in } G_{[1,n-1]} \end{array}$$

where $\alpha_{[1,n-1]} := \varphi(\alpha)$ and $\beta_{[1,n-1]} := \varphi(\beta)$. By Theorem 5.8 both G and $G_{[1,n-1]}$ satisfy axiom **A2**, which implies

$$(5.3) \quad \begin{aligned} \text{len}(\beta) &= \text{len}(\alpha) + d && \text{with } d \in \{0, \pm 1\}, \\ \text{len}(\beta_{[1,n-1]}) &= \text{len}(\alpha_{[1,n-1]}) + d' && \text{with } d' \in \{0, \pm 1\}. \end{aligned}$$

Note that $d = 0, 1, -1$ if the edge is of type **I**, **II**, **III** in axiom **A2**, respectively. The same is true for d' . Furthermore, by definition we have

$$(5.4) \quad \begin{aligned} \text{len}(\alpha) &= \text{len}(\alpha_{[1,n-1]}) + \delta_\alpha && \text{with } \delta_\alpha \in \{0, 1\}, \\ \text{len}(\beta) &= \text{len}(\beta_{[1,n-1]}) + \delta_\beta && \text{with } \delta_\beta \in \{0, 1\}. \end{aligned}$$

Proposition 5.10. *Let G be a CS-graph and consider edges in G and $G_{[1,n-1]}$ as in (5.2), define $d, d', \delta_\alpha, \delta_\beta$ as in (5.3) and (5.4), and set $\ell = \text{len}(\alpha_{[1,n-1]})$. Then the following is true:*

- (1) $d = d'$ except possibly when $d' = 0$, $\delta_\alpha = 0$ and $I^+ = \alpha_{[1,n-1]}^{(\ell)}$ in which case $d = 1$ is possible.
- (2) $\delta_\beta = \delta_\alpha$ except possibly when $d' = 0$, $\delta_\alpha = 0$ and $I^+ = \alpha_{[1,n-1]}^{(\ell)}$ in which case $\delta_\beta = 1$ is possible.

Remark 5.11. Proposition 5.10 can be reformulated as follows. If the edge $(v, \alpha_{[1,n-1]}) \xrightarrow{I} (w, \beta_{[1,n-1]})$ in $G_{[1,n-1]}$ is of type **I**, **II** or **III** in axiom **A2**, then the corresponding edge in G is of the same type unless possibly when (1) the edge is of type **I** in axiom **A2**, (2) $\delta_\alpha = 0$, and (3) $n-1 \in I$; when (1), (2) and (3) are satisfied, the edge can become of type **II** in G .

Proof of Proposition 5.10. We first show that (1) implies (2). Note that

$$\delta_\beta = \text{len}(\beta) - \text{len}(\beta_{[1,n-1]}) = \text{len}(\alpha) + d - \text{len}(\alpha_{[1,n-1]}) - d' = d - d' + \delta_\alpha.$$

Hence $d = d'$ implies $\delta_\beta = \delta_\alpha$. Furthermore in the exceptional case $\delta_\beta = d - d' + \delta_\alpha = 1 - 0 + 0 = 1$.

Next we prove (1). Both G and $G_{[1,n-1]}$ are CS-graphs by assumption and Theorem 5.8. Hence axiom **A2** must hold for both graphs. In particular, if $j+1 < \ell$ for the edge in $G_{[1,n-1]}$ or $j+1 = \ell$ and $I^+ \subsetneq \alpha_{[1,n-1]}^{(\ell)}$, then by the properties of the map φ , the edge must be of the same type in G . This implies $d = d'$.

Now assume that $j+1 = \ell$ and $I^+ = \alpha_{[1,n-1]}^{(\ell)}$ for the edge in $G_{[1,n-1]}$. In this case type **II** in axiom **A2** reduces to type **I**, so that $d' = 1$ is not possible. When $d' = -1$, the edge in $G_{[1,n-1]}$ is of type **III** and $\beta_{[1,n-1]} >_D \alpha_{[1,n-1]}$. Since $\text{len}(\beta_{[1,n-1]}) < \text{len}(\alpha_{[1,n-1]})$ we have that $\beta >_D \alpha$ independent of whether we β is obtained from $\beta_{[1,n-1]}$ by adding one to its last part (or $\delta_\beta = 0$) or by creating a new part of size 1 (or $\delta_\beta = 1$) and same for α . This implies that the edge in G is of type **III** since edges of type **I** and **II** satisfy $\beta <_D \alpha$. Hence $d = -1 = d'$ proving the claim.

Finally assume that $I^+ = \alpha_{[1,n-1]}^{(\ell)}$ and $d' = 0$. If $d = 0$, then $d = d'$ and the claim holds. If $d = -1$, then $\delta_\beta = \delta_\alpha - 1$, which implies that $\delta_\beta = 0$ and $\delta_\alpha = 1$. Hence $\alpha_{[1,n-1]} = (\alpha^{(1)}, \dots, \alpha^{(\ell)})$ and $\alpha = (\alpha^{(1)}, \dots, \alpha^{(\ell)}, \{n\})$. Since $d' = 0$, we have $\beta_{[1,n-1]} = (\alpha^{(1)}, \dots, \alpha^{(\ell-1)} \setminus \{k\}, \alpha^{(\ell)} \cup \{k\})$ by axiom **A2 I**. Since $\delta_\beta = 0$, we have $\beta = (\alpha^{(1)}, \dots, \alpha^{(\ell-1)} \setminus \{k\}, \alpha^{(\ell)} \cup \{k, n\})$. However, from $d = -1$ using axiom **A2 III** we obtain $\beta^{(\ell)} = \{n\} \neq \alpha^{(\ell)} \cup \{k, n\}$ from the expression for α , yielding a contradiction. Hence $d = -1$ is not possible. Finally, $d = 1$ implies that $\delta_\beta = \delta_\alpha + 1$, so that $\delta_\alpha = 0$ and $\delta_\beta = 1$, proving the claim. \square

Theorem 5.12. *Let G be a CS-graph. Then G is uniquely determined by $G_{[1,n-1]}$.*

Proof. By axiom **A5**, G contains $B(\lambda)_s$ as a subgraph. The crystal $B(\lambda)_s$ has a unique vertex of weight λ and hence G has a unique vertex (u_λ, λ) with label λ . By Theorem 5.8, $G_{[1,n-1]}$ is a union of CS-graphs G_{λ^-} , where λ/λ^- is a skew shape with one box. Each G_{λ^-} has a unique vertex $(u_{\lambda^-}, \lambda^-)$ with label λ^- . Furthermore, labeling the edges in G that correspond to edges in the crystal in $B(\lambda)_s$ by f_j if the weight changes as in axiom **A2 I**, we have

$$(5.5) \quad (u_{\lambda^-}, \tilde{\lambda}^-) = f_{s-1} f_{s-2} \cdots f_r (u_\lambda, \lambda)$$

for r the row index of λ/λ^- and $\tilde{\lambda}^- = (\lambda_1, \dots, \lambda_{s-1}, \lambda_s + 1)$. Hence $G_{[1,n-1]}$ together with the sequence of edges $f^{(r)} := f_{s-1} f_{s-2} \cdots f_r$ is connected. This means that every vertex $(v, \alpha_{[1,n-1]})$ in $G_{[1,n-1]}$ can be reached by a path

$$(5.6) \quad (u_\lambda, \lambda_{[1,n-1]}) \xrightarrow{I_1} (v^{(1)}, \alpha_{[1,n-1]}^{(1)}) \xrightarrow{I_2} \cdots \xrightarrow{I_p} (v^{(p)}, \alpha_{[1,n-1]}^{(p)}) = (v, \alpha_{[1,n-1]}),$$

where either $n \notin I_j$ or the edge labeled I_j is in $B(\lambda)_s$.

To show that G is uniquely determined by $G_{[1,n-1]}$, we need to show that:

- (1) All edges in G labeled by an interval I with $n \in I$ can be recovered.
- (2) The vertex labels in G can be recovered.

We begin by proving (2) by induction. The vertex (u_λ, λ) in G has vertex label λ and label $\varphi(\lambda) = \lambda_{[1,n-1]}$ in $G_{[1,n-1]}$. Suppose by induction that it is known for all vertices along the path in (5.6) how to lift the vertex labels $\alpha_{[1,n-1]}^{(j)}$ to $\alpha^{(j)}$ in G for $1 \leq j < p$. That is, we have the path

$$(5.7) \quad (u_\lambda, \lambda) \xrightarrow{I_1} (v^{(1)}, \alpha^{(1)}) \xrightarrow{I_2} \cdots \xrightarrow{I_{p-1}} (v^{(p-1)}, \alpha^{(p-1)})$$

in G . If the edge labeled I_p in (5.6) is in $B(\lambda)_s$, then the length of the label α in G and $\alpha_{[1,n-1]}$ are the same and hence $(v, \alpha_{[1,n-1]})$ in $G_{[1,n-1]}$ lifts to (v, α) in G . Otherwise, by Remark 5.11 the lift from $(v, \alpha_{[1,n-1]})$ in $G_{[1,n-1]}$ to (v, α) in G is determined except when the last edge in (5.6) is of type **I**, $n-1 \in I_p$, and $\delta_{\alpha^{(p-1)}} = 0$. We will deal with this exceptional case using Lusztig involution (axiom **A4 (a)**) and the fans (axiom **A3**).

By axiom **A4 (a)**, the path in (5.7) implies a path

$$(u_{\text{rev}(\lambda)}, \text{rev}(\lambda)) \xleftarrow{I_1^c} (v^{(1)}, \text{rev}(\alpha^{(1)})) \xleftarrow{I_2^c} \cdots \xleftarrow{I_{p-1}^c} (v^{(p-1)}, \text{rev}(\alpha^{(p-1)})),$$

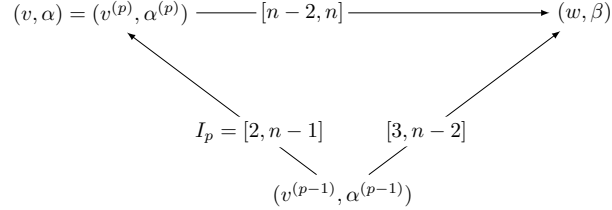
where $(u_{\text{rev}(\lambda)}, \text{rev}(\lambda))$ is the unique vertex with label $\text{rev}(\lambda)$ in G . We also know by Lusztig involution that there is an incoming edge labeled I_p^c . By Remark 5.11 the edge

$$(v^{(p)}, \text{rev}(\alpha)) \xrightarrow{I_p^c} (v^{(p-1)}, \text{rev}(\alpha^{(p-1)}))$$

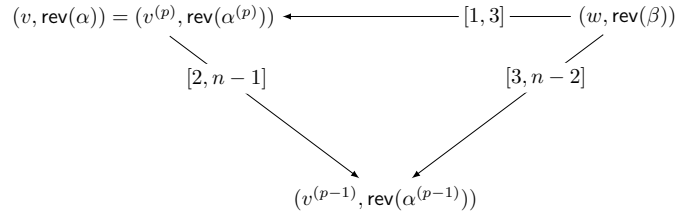
and vertex labels are determined unless $n-1 \in I_p^c$ or equivalently $2 \in I_p$.

Hence let us now assume that the edge labeled I_p in (5.6) is of type **I**, $\delta_{\alpha^{(p-1)}} = 0$, and $2, n-1 \in I_p$. This implies that either $I_p = [2, n-1]$ or $I_p = [1, n-1]$. We want to determine whether $\delta_\alpha = 0$ or 1. The case $\delta_\alpha = 1$ would require the existence of a fan by axiom **A3**. We consider the two cases separately.

Case 1: $I_p = [2, n-1]$. Since $|I_p| \geq 3$ is odd by axiom **A0**, we know that n is odd. First assume that $n \geq 7$. The case $\delta_\alpha = 1$ would require the existence of a fan by axiom **A3**, in particular

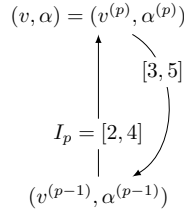


Under the Lusztig involution, this becomes

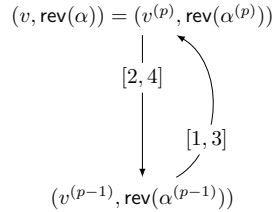


Here the edges on the right and the top and the vertex labels are determined by Remark 5.11. Hence the existence of this configuration under Lusztig involution would determine that $\delta_\alpha = 1$. If it does not exist, this requires $\delta_\alpha = 0$.

Similarly for $n = 5$, the case $\delta_\alpha = 1$ would require by axiom **A3** that

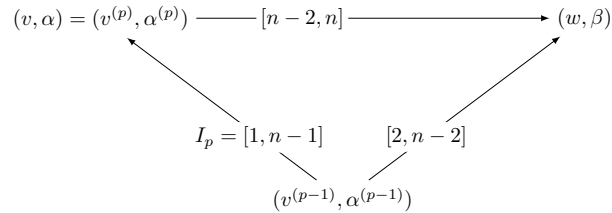


which under the Lusztig involution becomes

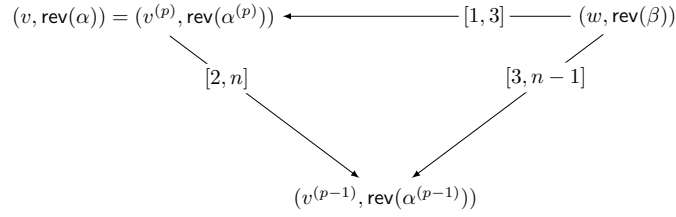


By Remark 5.11, the vertex labels are determined under the arrow labeled $[1, 3]$. Hence the existence of this configuration under Lusztig involution would determine that $\delta_\alpha = 1$. If it does not exist, this requires $\delta_\alpha = 0$.

Case 2: $I_p = [1, n-1]$. Since $|I_p| \geq 3$ is odd by axiom **A0**, we know that n is even. First assume that $n \geq 6$. The case $\delta_\alpha = 1$ would require the existence of a fan by axiom **A3**, in particular

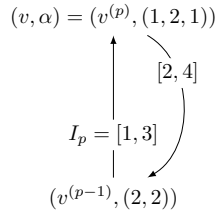


Under the Lusztig involution, this becomes



The edge labeled $[2, n-2]$ in the first picture under Remark 5.11 determines the label β in G , and the edge labeled $[1, 3]$ in the second picture under Remark 5.11 determines the label $\text{rev}(\alpha)$ and hence α in G . If these edges do not exist, then $\delta_\alpha = 0$.

For $n = 4$, by inspecting axiom A2, the case $\delta_\alpha = 1$ can only happen if $\alpha^{(p-1)} = (2, 2)$. By the fan axiom A3, $\delta_\alpha = 1$ requires



which is fixed under the Lusztig involution. By axiom A1', there has to be an incoming edge into $(v^{(p-1)}, (2, 2))$ labeled $[2, 4]$. For $\delta_\alpha = 0$, this incoming edge has to come from a vertex with label $(3, 1)$. Thus we can decide whether $\delta_\alpha = 0, 1$ depending on whether G has 3 or 2 vertices, respectively.

Hence we have recovered all vertex labels in G from $G_{[1, n-1]}$, proving (2).

Since $G_{[1, n-1]}$ together with the crystal edges is connected and since all vertex labels in G are known, the edges labeled I with $n \in I$ can be recovered using the Lusztig involution in axiom A4 (a) unless $I = [1, n]$.

The case $I = [1, n]$ can only happen if n is odd and for $(v, \alpha) \xrightarrow{I} (w, \beta)$ we have $\alpha = (\frac{n+1}{2}, \frac{n-1}{2})$. This edge has to be of type I. If it was of type III, α would have to have at least three parts. If it was of type II, by axiom A3 there would have to be an edge out of (w, β) with interval $[n-1, n+1]$, which is not possible since intervals are subsets of $[n]$. By axiom A1 (ii) there cannot be an incoming edge into (v, α) from a vertex labeled $(\frac{n+3}{2}, \frac{n-3}{2})$. Hence λ of axiom A5 is $\lambda = (\frac{n+1}{2}, \frac{n-1}{2})$ in this case, which is a unique label. This implies by axiom A4 (a) that the label $(\frac{n-1}{2}, \frac{n+1}{2})$ is also unique and hence the edge labeled $I = [1, n]$ is uniquely determined. \square

Corollary 5.13. *Suppose G_λ is a CS-graph. Then G_λ is isomorphic to the crystal skeleton $\text{CS}(\lambda)$.*

Proof. By Theorem 5.7, $\text{CS}(\lambda)$ is a CS-graph. By Theorem 5.12, G_λ is uniquely determined by $(G_\lambda)_{[1, n-1]}$. By Theorems 5.8 and 4.11, G_λ and $\text{CS}(\lambda)$ have the same branching properties. Hence we must have $G_\lambda \cong \text{CS}(\lambda)$. \square

Corollary 5.14. *Let G_λ be a CS-graph. Then G_λ has a unique vertex labelled λ and all other vertex labels α satisfy $\alpha \leq_D \lambda$. That is, λ is the unique largest label in dominance order.*

Proof. By Corollary 5.13, G_λ is isomorphic to the crystal skeleton $\text{CS}(\lambda)$. By Lemma 2.16, the descent composition associated to the vertex T in $\text{CS}(\lambda)$ is the weight α of the quasi-Yamanouchi tableau Q in the same quasi-crystal component as T . Recall that the descent compositions are precisely the labels of the vertices in G_λ by Theorem 5.7. In a crystal graph $B(\lambda)$, the weights of all vertices are smaller in dominance order than λ (see for example [9, Chapter 4.4]). Since Q is an element in the crystal graph $B(\lambda)$ underlying the crystal skeleton $\text{CS}(\lambda)$, we hence have $\alpha \leq_D \lambda$. \square

5.6. S_n -axioms. We will now state S_n analogues of the CS-graph axioms.

Axiom 5.15 (S_n -axioms for crystal skeletons). Let n be a positive integer, $\lambda \vdash n$, and G_λ be a finite, connected, vertex- and edge-labeled graph with labeled vertex set V_L and labeled edge set E_L as in Section 5.1. The S_n -axioms for G_λ require:

- S0. (*Intervals*) Same as axiom A0.
- S1. (*Outgoing edges*) Same as axiom A1.

- S2.** (*Labels*) Same as axiom **A2**.
S3. (*Fans*) Same as axiom **A3**.
S4. (*Lusztig involution*) We have $\mathcal{L}_n(G_\lambda) \cong G_\lambda$.
S5. (*Branching*) We have

$$(G_\lambda)_{[1, n-1]} \cong \bigcup_{\substack{\lambda^- \\ |\lambda/\lambda^-|=1}} G_{\lambda^-},$$

where G_{λ^-} satisfy Axiom 5.15.

- S6.** (*Connectivity*) The graph G_λ has a unique vertex (u_λ, λ) with label λ and all other labels α satisfy $\alpha \leq_D \lambda$. Denote by f_j the edge as in axiom **A2 I** and set $s = \text{len}(\lambda)$. Then for each λ^- such that $|\lambda/\lambda^-| = 1$, we have

$$(u_{\lambda^-}, \tilde{\lambda}^-) = f^{(r)}(u_\lambda, \lambda),$$

where r is the row index of λ/λ^- , $\tilde{\lambda}^- = (\lambda_1, \dots, \lambda_{s-1}, \lambda_s + 1)$, and $f^{(r)} := f_{s-1}f_{s-2} \cdots f_r$. Furthermore, $(G_\lambda)_{[1, n-1]}$ together with the sequence of edges $f^{(r)}$ is connected.

Theorem 5.16. *A graph G_λ satisfying Axiom 5.15 is a CS-graph (satisfying Axiom 5.5). Conversely, a CS-graph satisfies Axiom 5.15.*

Proof. Suppose G_λ satisfies Axiom 5.15. Axioms **S0-S3** imply axioms **A0-A3**. Axiom **S4** implies Axiom **A4(a)**. Axiom **S5** stipulates that each connected component G_{λ^-} satisfies Axiom 5.15 for $\lambda^- \vdash n-1$, and hence in particular axiom **S4** with n replaced by $n-1$. This implies axiom **A4(b)**.

We show that axiom **A5** holds by induction on n . For $n=1$, $G_{(1)}$ is a single vertex as is $B((1))_1$. Hence axiom **A5** holds. By the induction hypothesis, the connected components of $(G_\lambda)_{[1, n-1]}$ in **S5** satisfy axiom **A5**. Thus all G_{λ^-} in **S5** are CS-graphs satisfying Axiom 5.5. Analyzing the proof of Theorem 5.12, only axioms **A0-A4** and the properties in **S6** are used. This implies that G_λ is uniquely determined from the CS-graphs in $(G_\lambda)_{[1, n-1]}$ in **S5**. This proves that G_λ is a CS-graph satisfying Axiom 5.5.

For the converse, axioms **A0-A4** imply axioms **S0-S4**. Axiom **A5** implies Axiom **S6**. The unique label (u_λ, λ) is the highest weight vertex in $G_s \cong B(\lambda)_s$. Connectivity follows by the proof of Theorem 5.12. Axiom **S5** holds by Theorem 5.8. \square

5.7. Local axioms. As outlined in Section 4.8, Stembridge [29] provided a local characterization of crystal bases associated to representations of simply-laced root systems, in particular type A . Here we provide analogous local axioms (Axiom 5.19) for CS-graphs.

Let G be a finite, connected, vertex- and edge-labeled graph with labeled vertex set V_L and labeled edge set E_L as in Section 5.1. Recall that G_s with $s = \min\{\text{len}(\alpha) \mid (v, \alpha) \in V_L\}$ is the subgraph of G containing only the vertices $(v, \alpha) \in V_L$ with $\text{len}(\alpha) = s$.

To state our local axioms, we begin by defining the *crystal operators* $f_j(v, \alpha)$ and $e_i(v, \alpha)$ for $(v, \alpha) \in G_s$ and their *string lengths* $\varphi_j(v, \alpha)$ and $\varepsilon_i(v, \alpha)$ (see (2.4)). As the notation suggests, these maps will be used to prove that G_s is a crystal when Axiom 5.19 is satisfied.

Definition 5.17. Let G be a finite, connected, vertex- and edge-labeled graph with labeled vertex set V_L and labeled edge set E_L as in Section 5.1. Suppose G satisfies axioms **A0, A0', A1, A1', A2, and A2'** and the relations in Theorem 4.35 and their duals for incoming edges. Then define the following:

- (1) If there is no edge $(v, \alpha) \xrightarrow{I} (w, \beta)$ in G_s with $I \subseteq \alpha^{(j)} \cup \alpha^{(j+1)}$, then $f_j(v, \alpha) := \emptyset$, $\varphi_j(v, \alpha) := 0$, $e_j(w, \beta) := \emptyset$ and $\varepsilon_j(w, \beta) := 0$.
 - (2) Otherwise, if there is an edge $(v, \alpha) \xrightarrow{I} (w, \beta)$ in G_s with $I \subseteq \alpha^{(j)} \cup \alpha^{(j+1)}$, define
- $$(5.8) \quad f_j(v, \alpha) := (w, \beta), \quad e_j(w, \beta) = (v, \alpha),$$

and

$$(5.9) \quad \varphi_j(v, \alpha) := \min I - \min \alpha^{(j)} + 1, \quad \varepsilon_j(w, \beta) := \max \beta^{(j+1)} - \max I.$$

We first check that f_j is well-defined, and prove that whenever $(v, \alpha) \xrightarrow{I} (w, \beta)$ is in G_s , there are certain edges in G as well.

Lemma 5.18. *Let G be a graph satisfying the hypotheses in Definition 5.17, with an edge $(v, \alpha) \xrightarrow{I} (w, \beta)$ for $I = [i, i+2m]$ in G . Then*

- (1) *If I is length-preserving, $f_j(v, \alpha)$ is well-defined;*

(2) If $f_j^{k'}(v, \alpha) \in G_s$ for all $0 \leq k' \leq k$ for some $0 \leq k < \varphi_j(v, \alpha)$, then there is an edge in G

$$(5.10) \quad f_j^k(v, \alpha) \xrightarrow{I_k} f_j^{k+1}(v, \alpha)$$

with $I_k = [i - k, i - k + 2m]$. For $k = \varphi_j(v, \alpha)$ such an edge does not exist.

Analogous statements hold for $e_j(w, \beta)$.

Proof. By assumption the edge $(v, \alpha) \xrightarrow{I} (w, \beta)$ exists in G . Hence $I^- \cup \{i + m + 1\} \subseteq \alpha^{(j)}$ and $I^+ \subseteq \alpha^{(j+1)}$ for some j by axiom **A0**. Observe the following:

- (1) If I is length-preserving, we have $1 \leq j < s$. Inspecting Theorem 4.35 case 3, if $(v, \alpha) \xrightarrow{I} (w, \beta)$ in G_s , then I must be maximal among all intervals $J \subseteq \alpha^{(j)} \cup \alpha^{(j+1)}$ since if $I \subsetneq J$, then I is length-increasing and thus not an edge in G_s . Hence f_j is well-defined.
- (2) The case $\varphi_j(v, \alpha) = 0$ is vacuously true. Hence assume $\varphi_j(v, \alpha) \geq 1$. By assumption, $f_j^k(v, \alpha) \in G_s$ with $k \geq 0$. Furthermore, by assumption all edges I_0, \dots, I_{k-1} are in G_s and hence length-preserving. By axiom **A2**, this implies that the label of the vertex $f_j^k(v, \alpha)$ is $\alpha - k\epsilon_j + k\epsilon_{j+1}$, where ϵ_j is the unit vector in \mathbb{Z}^s with a 1 in position j . Note that

$$I_k^- \cup \{i - k + m + 1\} \subseteq \left(\alpha - k\epsilon_j + k\epsilon_{j+1} \right)^{(j)} \quad \text{and} \quad I_k^+ \subseteq \left(\alpha - k\epsilon_j + k\epsilon_{j+1} \right)^{(j+1)}$$

since by assumption $0 \leq k < \varphi_j(v, \alpha) = \min I - \min \alpha^{(j)} + 1 = i - \min \alpha^{(j)} + 1$. Hence by axiom **A1** either the edge in (5.10) exists and the claim holds or there is an edge $(v', \alpha') \xrightarrow{J} f_j^k(v, \alpha)$ such that $J \subsetneq I_k$ and $\alpha' \geq_D \alpha - k\epsilon_j + k\epsilon_{j+1}$. Suppose such an edge J exists. By the dual of case 3 of Theorem 4.35, this implies that J is length-decreasing which is not possible since $f_j^k(v, \alpha) \in G_s$ and hence has a label with minimal length.

Finally, if $k = \varphi_j(v, \alpha)$, we have $I_k \not\subseteq \alpha^{(j)} \cup \alpha^{(j+1)}$. Hence the edge in (5.10) does not exist. \square

We now give the set of local axioms for crystal skeletons.

Axiom 5.19 (Local axioms for crystal skeletons). Let G be a finite, connected, vertex- and edge-labeled graph with labeled vertex set V_L and labeled edge set E_L as in Section 5.1. The local axioms for G require:

L0. (*Intervals*) Same as axioms **A0** and **A0'**.

L1. (*Outgoing and incoming edges*) Same as axioms **A1** and **A1'**.

L2. (*Labels*) Same as axioms **A2** and **A2'**.

L3. (*Commutation relations*)

- (a) If there is a vertex $(v, \alpha) \in V_L$ with two distinct outgoing edges labelled I and J , respectively, then commutation relations as in Theorem 4.35 hold.
- (b) If there is a vertex $(v, \alpha) \in V_L$ with two distinct incoming edges labelled I and J , respectively, then the dual to the commutation relations as in Theorem 4.35 hold (see Remark 4.36).
- (c) For any edge $(v, \alpha) \xrightarrow{I} (w, \beta)$ with $|I| = 3$ and I length-increasing (resp. $(w, \beta) \xrightarrow{J} (v, \alpha)$ with $|J| = 3$ and J length-decreasing), we have the following subgraph with $J = \{i + 1 \mid i \in I\}$ (resp. $I = \{j - 1 \mid j \in J\}$)

$$(5.11) \quad \begin{array}{ccc} (v, \alpha) & \xrightarrow{I} & (w, \beta) \\ & \curvearrowright & \\ & & J \end{array} .$$

L4. (*Strings in G_s*)

- (a) Suppose $(v, \alpha) \xrightarrow{I} f_j(v, \alpha)$ is an edge in G_s with $I = [i, i + 2m] \subseteq \alpha^{(j)} \cup \alpha^{(j+1)}$. Then for $0 \leq k < \varphi_j(v, \alpha)$, the edge

$$f_j^k(v, \alpha) \xrightarrow{I_k} f_j^{k+1}(v, \alpha)$$

with $I_k = [i - k, i - k + 2m]$ (in G by Lemma 5.18) is length-preserving.

- (b) Suppose $e_j(v, \alpha) \xrightarrow{I} (v, \alpha)$ is an edge in G_s with $I = [i, i + 2m] \subseteq \alpha^{(j)} \cup \alpha^{(j+1)}$. Then for $0 \leq k < \varepsilon_j(v, \alpha)$, the edge

$$e_j^{k+1}(v, \alpha) \xrightarrow{J_k} e_j^k(v, \alpha)$$

with $J_k = [i + k, i + k + 2m]$ (in G by Lemma 5.18) is length-preserving.

- L5.** (*Edge types*) Let λ be a maximal label in dominance order among all vertex label. Let $(v, \alpha) \in V_L$. Then the following is true:
- (a) If $\alpha \neq \lambda$, then (v, α) has at least one incoming edge which is length-preserving or length-increasing.
 - (b) If $\text{rev}(\alpha) \neq \lambda$, then (v, α) has at least one outgoing edge which is length-preserving or length-decreasing.

We first show that Axiom 5.19 implies axiom A5.

Lemma 5.20. *Axiom 5.19 implies axiom A5 for G_s .*

Proof. We will prove that G_s is isomorphic to a crystal $B(\lambda)_s$ for some λ by showing that G_s satisfies the Stembridge axioms [29]. By [9, Theorem 4.12], this implies the isomorphism.

Suppose that $(v, \alpha) \xrightarrow{I} (w, \beta)$ and $(v', \alpha') \xrightarrow{J} (w, \beta)$ are in G_s with $J \subsetneq I$. Then J is length-decreasing by the dual of case 3 of Theorem 4.35 which holds by axiom L3. But since $(v', \alpha') \in G_s$ this is not possible. Hence the partial inverse of f_j (called e_j) is well-defined.

Next we check that the Stembridge commutation relations (4.9) and (4.10) hold. The corresponding relations for the raising operators e_i can be checked similarly. We consider a vertex (v, α) in G_s such that there are edges in G_s

$$(v, \alpha) \xrightarrow{I} f_k(v, \alpha) \quad \text{with} \quad I \subseteq \alpha^{(k)} \cup \alpha^{(k+1)} \quad \text{and} \quad (v, \alpha) \xrightarrow{J} f_\ell(v, \alpha) \quad \text{with} \quad J \subseteq \alpha^{(\ell)} \cup \alpha^{(\ell+1)}.$$

In particular, both I and J are length-preserving. By axiom L3, the commutation relations in Theorem 4.35 must hold. Inspection shows that case 3 cannot apply since this would require J to be length-increasing. Cases 2(a)ii and 2(b)ii contain length-decreasing edges, which cannot happen since G_s contains vertices with minimal length labels. Hence cases 1, 2(a)i, 2(b)i, or 2(b)iii must apply, which are squares or octagons as in the Stembridge axioms.

In cases 1, 2(a)i, and 2(b)iii, if I and J are length-preserving, then all edges in the square are length-preserving. For the octagon in case 2(b)i, length-decreasing edges cannot appear since we are in G_s . If J' is length-increasing, case 2(a)i also applies, which is a square with all length-preserving edges. Hence either case 2(b)i or case 2(a)i occurs with all edges length-preserving.

It remains to check that the conditions on the string lengths are satisfied. By Lemma 5.18 and axiom L4, we have that $\varphi_j(v, \alpha)$ in (5.9) satisfies $\varphi_j(v, \alpha) = \max\{k \in \mathbb{Z}_{\geq 0} \mid f_j^k(v, \alpha) \neq \emptyset\}$ as in (2.4). Hence to check the Stembridge axioms, it remains to check that the conditions on the string length are satisfied, namely

$$\varphi_k(f_\ell(v, \alpha)) = \varphi_k(v, \alpha) + \{0, 1\} \quad \text{and} \quad \varphi_\ell(f_k(v, \alpha)) = \varphi_\ell(v, \alpha) + \{0, 1\},$$

and

$$\varphi_k(f_\ell(v, \alpha)) = \varphi_k(v, \alpha) \quad \text{or} \quad \varphi_\ell(f_k(v, \alpha)) = \varphi_\ell(v, \alpha) \quad \text{for squares,}$$

and

$$(5.12) \quad \varphi_k(f_\ell(v, \alpha)) = \varphi_k(v, \alpha) + 1 \quad \text{and} \quad \varphi_\ell(f_k(v, \alpha)) = \varphi_\ell(v, \alpha) + 1 \quad \text{for octagons.}$$

In case 1 we have $\varphi_k(f_\ell(v, \alpha)) = \varphi_k(v, \alpha)$ and $\varphi_\ell(f_k(v, \alpha)) = \varphi_\ell(v, \alpha)$ using (5.9) since $I \cap J = \emptyset$. Hence the square applies. For case 2 we have $I \subseteq \alpha^{(k)} \cup \alpha^{(k+1)}$ and $J \subseteq \alpha^{(k+1)} \cup \alpha^{(k+2)}$, so that $\ell = k + 1$. In case 2(a)i, it can be explicitly checked using (5.9) that $\varphi_{k+1}(f_k(v, \alpha)) = \varphi_{k+1}(v, \alpha)$ and $\varphi_k(f_{k+1}(v, \alpha)) = \varphi_k(v, \alpha) + 1$. Hence the square applies. In case 2(b)iii, it can be explicitly checked that $\varphi_{k+1}(f_k(v, \alpha)) = \varphi_{k+1}(v, \alpha) + 1$ and $\varphi_k(f_{k+1}(v, \alpha)) = \varphi_k(v, \alpha)$. Hence the square applies. Finally, in case 2(b)i the relations (5.12) hold, hence the octagon applies. \square

We next prove that if a graph satisfies Axiom 5.19, then the graph must be invariant under Lusztig involution.

Lemma 5.21. *Axiom 5.19 implies axiom A4 (a).*

Proof. Since axiom A5 holds for G by Lemma 5.20, G_s is a crystal, which enjoys $\mathcal{L}_n(G_s) \cong G_s$. Let $G_{\leq \ell}$ (resp. $G_{=\ell}$) be the induced subgraph of G with all vertices (v, α) such that $\text{len}(\alpha) \leq \ell$ (resp. $\text{len}(\alpha) = \ell$). Assume by induction that $\mathcal{L}_n(G_{\leq \ell}) = G_{\leq \ell}$; the statement is true for $\ell = s$ by Lemma 5.20. We will show that $\mathcal{L}_n(G_{\leq \ell}) = G_{\leq \ell}$ implies that $\mathcal{L}_n(G_{\leq \ell+1}) = G_{\leq \ell+1}$ as well. The proof will be done in multiple steps:

Step 1. Let G^{con} be the subgraph of G consisting of $G_{\leq \ell}$ and all vertices (v, α) with $\text{len}(\alpha) = \ell + 1$ which are connected by an incoming or outgoing edge to a vertex in $G_{\leq \ell}$. We show that $\mathcal{L}_n(G^{\text{con}}) = G^{\text{con}}$.

Step 2. Suppose

$$G_{\leq \ell} \subsetneq G' \subseteq G_{\leq \ell+1}$$

is a subgraph of G such that $\mathcal{L}_n(G') = G'$. By step 1, $G' = G^{\text{con}}$ has this property. We successively extend G' by adding length-preserving edges entering or leaving the vertices $(v, \alpha) \in G_{=\ell+1} \cap G'$ in a specific order. We continue adding edges and vertices to G' until we have $G' = G_{\leq \ell+1}$. By axiom **L5**, all vertices in $G_{\leq \ell+1}$ can be reached.

Proof of Step 1. Let $(v, \alpha) \xrightarrow{I} (w, \beta)$ be a length-increasing edge in G with $\text{len}(\alpha) = \ell$. Let $(v', \text{rev}(\alpha))$ be the image of (v, α) under \mathcal{L}_n . Since $(v, \alpha) \in G_{\leq \ell}$ and $\mathcal{L}_n(G_{\leq \ell}) = G_{\leq \ell}$, we have that $(v', \text{rev}(\alpha)) \in G_{\leq \ell}$.

By axiom **A1'**, there is an edge in G

$$(5.13) \quad (w', \beta') \xrightarrow{I^{\mathcal{L}}} (v', \text{rev}(\alpha))$$

with $I^{\mathcal{L}} = [n+1-b, n+1-a]$ if $I = [a, b]$.

Since $(v', \text{rev}(\alpha)) \in G_{\leq \ell}$, by definition the segment in (5.13) is in G^{con} . Since $\mathcal{L}_n(G_{\leq \ell}) = G_{\leq \ell}$ and I is length-increasing, the vertex (w', β') cannot be in $G_{\leq \ell}$. This implies that the edge labeled $I^{\mathcal{L}}$ in (5.13) is length-decreasing and hence by axioms **A2** and **A2'** we have $\beta' = \text{rev}(\beta)$. Thus (5.13) can be rewritten as

$$(w', \text{rev}(\beta)) \xrightarrow{I^{\mathcal{L}}} (v', \text{rev}(\alpha)),$$

which is precisely the image of $(v, \alpha) \xrightarrow{I} (w, \beta)$ under \mathcal{L}_n by definition of \mathcal{L}_n .

Conversely, if $(w, \beta) \xrightarrow{I} (v, \alpha)$ is a length-decreasing edge in G with $\text{len}(\alpha) = \ell$, then by very similar arguments the image of this interval under \mathcal{L}_n is in G^{con} . Hence $\mathcal{L}_n(G^{\text{con}}) = G^{\text{con}}$.

Proof of Step 2. Suppose $G_{=\ell+1}$ contains a length-preserving edge $(v, \alpha) \xrightarrow{K} (w, \beta)$. We will show the following:

- (1) Suppose $(v, \alpha) \in G'$. Then \mathcal{L}_n maps (v, α) to $(v', \text{rev}(\alpha)) \in G'$. We prove there is an edge in G

$$(5.14) \quad (w', \beta') \xrightarrow{K^{\mathcal{L}}} (v', \text{rev}(\alpha))$$

that is length-preserving. By axioms **A2** and **A2'**, this forces $\beta' = \text{rev}(\beta)$, which shows that the image of $(v, \alpha) \xrightarrow{K} (w, \beta)$ under \mathcal{L}_n is precisely the edge in (5.14). We thus add $(v, \alpha) \xrightarrow{K} (w, \beta)$ and $(w', \text{rev}(\beta)) \xrightarrow{K^{\mathcal{L}}} (v', \text{rev}(\alpha))$ to G' .

- (2) Suppose $(w, \beta) \in G'$. Then \mathcal{L}_n sends (w, β) to $(w', \text{rev}(\beta)) \in G'$. We show there is an edge

$$(5.15) \quad (w', \text{rev}(\beta)) \xrightarrow{K^{\mathcal{L}}} (v', \alpha')$$

that is length-preserving. Again, axioms **A2** and **A2'** imply that $\alpha' = \text{rev}(\alpha)$, and so the image of $(v, \alpha) \xrightarrow{K} (w, \beta)$ under \mathcal{L}_n is precisely the segment in (5.15). We add these segments to G' as well.

We claim that all of the vertices in $G_{=\ell+1}$ can be reached by increasing/decreasing edges to $G_{\leq \ell}$ and length-preserving edges within $G_{=\ell+1}$, and thus we will eventually obtain $G' = G_{\leq \ell+1}$ through this process. Since $\mathcal{L}_n(G') = G'$ at each step, this will imply that $\mathcal{L}_n(G_{\leq \ell+1}) = G_{\leq \ell+1}$.

To see why the claim is true, note that by assumption $\ell+1 > s$, and so if $\text{len}(\alpha) = \ell+1$, then $\alpha \neq \lambda$ and $\alpha \neq \text{rev}(\lambda)$, which lie in G_s by Lemma 5.20. It follows from axiom **L5** that every vertex in $G_{=\ell+1}$ contains an incoming edge that is length-preserving or increasing. Length-preserving edges decrease labels in dominance order, hence $G_{=\ell+1}$ is acyclic. It follows that because $G_{=\ell+1}$ is finite, within each connected component of $G_{=\ell+1}$ there is a vertex (w, β) with no incoming length-preserving edges. Thus by axiom **L5**, (w, β) must have an incoming length-increasing edge from a vertex (x, γ) , which forces $(x, \gamma) \in G_{\leq \ell}$. This implies the claim.

We add the edges to G' in a specific order to be able to use the commutation relations in Theorem 4.35.

Step 2a. We prove (1) under the assumption that there exists some edge $(v, \alpha) \xrightarrow{L} (x, \gamma)$ in G which is length-decreasing. Under duality \mathcal{L}_n , this proves (2) when there is a length-increasing edge into (w, β) .

Step 2b. We prove (1) under the assumption that there exists some edge $(x, \gamma) \xrightarrow{L} (v, \alpha)$ in G which is length-increasing. Under duality \mathcal{L}_n , this proves (2) when there is a length-decreasing edge out of (w, β) .

Note that once Steps 2a and 2b are completed, G' contains all length-preserving edges into and out of any vertex $(v, \alpha) \in G^{\text{con}} \cap G_{=\ell+1}$. We proceed as follows:

Step 2c. We prove (1) when (v, α) has no edge connecting it to $G_{\leq \ell}$. By induction, we may assume that there is a length-preserving edge

$$(v, \alpha) \xrightarrow{L} (x, \gamma) \quad \text{or} \quad (v, \alpha) \xleftarrow{L} (x, \gamma)$$

such that $(x, \gamma) \in G'$, along with all its incoming and outgoing length-preserving edges. (In other words, (v, α) was added to G' in Steps 2a or 2b.) Under duality \mathcal{L}_n , this also proves (2).

Proof of Step 2a. We first prove (1) under the assumption that there is an edge $(v, \alpha) \xrightarrow{L} (x, \gamma)$ which is length-decreasing. Note that this edge and vertex (x, γ) are in G' by step 1. Since L is length-decreasing and K is length-preserving, we must have a commutation relation by the cases in Theorem 4.35. Note that by Remark 4.36 the commutation relations are dual under \mathcal{L}_n . Hence if a commutation holds at (v, α) , then the dual commutation must hold at $(v', \text{rev}(\alpha))$. We go through each of the commutation relations from Theorem 4.35 in turn.

- Suppose case 1 holds. Then since L is length-decreasing, all edges and vertices in the square are in G' by induction and hence so are their duals under \mathcal{L}_n . Furthermore, the edge labeled K out of (x, γ) in G is length-preserving as is the edge $K^{\mathcal{L}}$ out of $(x', \text{rev}(\gamma))$. This forces the edge $(w', \beta') \xrightarrow{K^{\mathcal{L}}} (v', \text{rev}(\alpha))$ to be length-preserving.
- Case 2(a)i is not applicable since all edges in that case are length-preserving.
- In case 2(a)ii, we must have $I = K$ and $J = L$ since J is length-decreasing. Since J' is length-decreasing, we have that $(w, \beta) \in G'$ and hence $(w', \beta') \xrightarrow{K^{\mathcal{L}}} (v', \text{rev}(\alpha))$ is length-preserving.
- If case 2(b)i holds, we must have $J = K$ and $I = L$ since only I can be length-decreasing. By the dual octagon, $L^{\mathcal{L}}$ is length-increasing and $K^{\mathcal{L}}$ is length-preserving as edges into $(v', \text{rev}(\alpha))$.
- In case 2(b)ii, we must have $J = L$ and $I = K$ since J is length-decreasing. In particular, I cannot be length-increasing in this case. Hence in the dual $I^{\mathcal{L}} = K^{\mathcal{L}}$ cannot be length-decreasing. If the edge $(w', \beta') \xrightarrow{K^{\mathcal{L}}} (v', \text{rev}(\alpha))$ is length-increasing, then $(w', \beta') \in G_{\leq \ell}$ and hence by induction its dual $(v, \alpha) \xrightarrow{K} (w, \beta)$ is length-decreasing, contradicting the assumption that it is length-preserving. Hence $K^{\mathcal{L}}$ is length-preserving, proving (1).
- The arguments for case 2(b)iii are analogous to those in case 1.
- Case 3 is not applicable since J is length-increasing, but neither K nor L are length-increasing.

This concludes the proof of (1) when there is a length-decreasing edge out of (v, α) .

Proof of Step 2b. Next we prove (1) under the assumption that there is an edge $(x, \gamma) \xrightarrow{L} (v, \alpha)$ which is length-increasing. Let $L = [j, j + 2m]$. We perform induction on m . If $|L| = 3$ or equivalently $m = 1$, then by (5.11), there is also an outgoing length-decreasing edge from (v, α) . Hence by step 2a, (1) holds. Therefore, we may assume that $|L| > 3$ or equivalently $m > 1$. By the fans (which are implied by the commutations in Theorem 4.35 and (5.11)), there is a length-preserving edge

$$(5.16) \quad (v, \alpha) \xrightarrow{[j+2m-1, j+2m+1]} (y, \delta),$$

which is in G' since both (v, α) and (y, δ) have incoming length-increasing edges. By case 3b starting at vertex (x, γ) with $I = L$ and $J = [j + 1, j + 2m - 1]$, the edge $J' = [j, j + 2m - 2]$ out of (v, α) is length-increasing. Hence K cannot be $[j, j + 2m - 2]$ since it is length-preserving. We will now use the commutation relations of Theorem 4.35 on the edge $(v, \alpha) \xrightarrow{K} (w, \beta)$ and the edge in (5.16) to prove (1):

- If $K \cap [j + 2m - 1, j + 2m + 1] = \emptyset$, case 1 applies. By induction on m , all length-preserving edges leaving (y, δ) are in G' . Hence under \mathcal{L}_n they are still length-preserving. Since $K \neq [j, j + 2m - 2]$, we cannot be in the case that $\max K + 1 = j + 2m - 1$. Hence by case 1, the edge $K^{\mathcal{L}}$ into $(v', \text{rev}(\alpha))$ is length-preserving, proving (1).
- The case $[j + 2m - 1, j + 2m + 1] \subseteq K$ is not possible since it would imply that the edge in (5.16) is length-increasing, a contradiction to the fact that it is length-preserving.
- If $K \cap [j + 2m - 1, j + 2m + 1] \neq \emptyset$, we are in case 2. If $I = K$ and $J = [j + 2m - 1, j + 2m + 1]$, then I cannot be length-increasing. Hence in the dual commutation, $I^{\mathcal{L}}$ cannot be length-decreasing. We also cannot have that $I^{\mathcal{L}} = K^{\mathcal{L}}$ is length-increasing since then the edge

$$(5.17) \quad (w', \beta') \xrightarrow{K^{\mathcal{L}}} (v', \text{rev}(\alpha))$$

was in G' implying that

$$(v, \alpha) \xrightarrow{K} (w, \beta)$$

is length-decreasing, contradicting the fact that this edge is length-preserving. Hence the edge in (5.17) is length-preserving, proving (1).

If $I = [j + 2m - 1, j + 2m + 1]$ and $J = K$, then case 2(a)i is not applicable since $|I| = 3$. Cases 2(a)ii and 2(b)ii are not applicable since $J = K$ is length-preserving and not length-decreasing. In case 2(b)i, $J = K$ is required to be length-preserving and hence in its dual under \mathcal{L}_n it also has to be length-preserving, proving (1). The proof in case 2(b)iii is similar to case 1.

We have now established that all length-preserving incoming and outgoing edges from $(v, \alpha) \in G_{\leq \ell+1}$ with an edge connecting to $G_{\leq \ell}$ are in G' .

Proof of Step 2c. Finally, we prove (1) when $(v, \alpha) \in G'$ has no edge connecting to $G_{\leq \ell}$. By induction, we may assume that there is an edge

$$(v, \alpha) \xrightarrow{L} (x, \gamma) \quad \text{or} \quad (v, \alpha) \xleftarrow{L} (x, \gamma)$$

such that $(x, \gamma) \in G'$ with all incoming and outgoing length-preserving edges in G' .

First assume that $(v, \alpha) \xrightarrow{L} (x, \gamma)$ as above exists. We are now going to consider the commutation relations as in Theorem 4.35 starting at vertex (v, α) with length-preserving outgoing edges K and L .

- Cases 2(a)ii and 2(b)ii are not applicable since J is length-decreasing.
- Cases 3a and 3b are not applicable since J is length-increasing.
- In case 2(a)i, all edges are length-preserving and hence also in its dual, so (1) must hold.
- In case 2(b)i, edge I cannot be length-decreasing since otherwise there is an edge connecting (v, α) to $G_{\leq \ell}$, a contradiction to our assumptions. For the same reason $I^{\mathcal{L}}$ in the dual commutation cannot be length-increasing. Hence both I and J are length-preserving and also in the dual, proving (1).
- For case 2(b)iii the edges I and I' (resp. J and J') are of the same type. In this setting $I = K$ and $J = L$ or vice versa. By induction hypothesis, the edges on one side of the square are in G' and length-preserving. Hence the edges on the other side of the square must also be length-preserving since by case 2(b)iii are of the same type. This proves (1). Case 1a can be proved in the same fashion.
- Case 1b is not applicable since in this case I is length-increasing and should be K or L . But both L and K are length-preserving.

Next we assume that $(v, \alpha) \xleftarrow{L} (x, \gamma)$ as above exists. Hence we have

$$(5.18) \quad (x, \gamma) \xrightarrow{L} (v, \alpha) \xrightarrow{K} (w, \beta),$$

where both edges are length-preserving and $(x, \gamma), (v, \alpha) \in G'$. When $K \cap L = \emptyset$, there is an edge $(x, \gamma) \xrightarrow{K} \bullet$ by axiom A1. Hence case 1 of Theorem 4.35 applies. In case 1a, all edges must be length-preserving since the edges in (5.18) are length-preserving. Since the length-preserving edges out of (x, γ) are in G' by induction, they also must be length-preserving in the dual showing that $(w', \beta') \xrightarrow{K^{\mathcal{L}}} (v', \text{rev}(\alpha))$ is length-preserving by case 1a, proving (1). In case 1b, since the edges in (5.18) are length-preserving we must have $K = I$. Since the edge $(x, \gamma) \xrightarrow{L} (v, \alpha)$ is in G' , it must be length-preserving in the dual forcing the dual of the edge labelled K in (5.18) to be length-preserving, proving (1). The case $L \subseteq K$ is not possible since $\gamma \geq_D \alpha$ and hence by axiom A1 the edge K in (5.18) could not exist. If $K \subseteq L$, K in (5.18) would be length-increasing by axiom A1', contradicting that K is length-preserving.

Hence we may now assume that $K \cap L \neq \emptyset$, $K \not\subseteq L$ and $L \not\subseteq K$. First assume that $\min L < \min K$. By axiom A1, there is an outgoing edge from (x, γ) labeled $K = [k, k + 2b]$ or $[k + 1, k + 2b - 1]$. By axiom A1 this would not happen if there was an incoming edge $(y, \delta) \xrightarrow{M} (x, \gamma)$ with $M \subseteq K$ and $\delta \geq_D \gamma$. But then (v, α) would have such an incoming edge contradicting the fact the edge $(v, \alpha) \xrightarrow{K} (w, \beta)$ exists. We are now in case 2 of Theorem 4.35 with $I = L$, $J = K$ or $J = [k + 1, k + 2b - 1]$, and $J' = K$.

- If case 2(a)i holds, all edges are length-preserving and hence also in the dual, proving (1).
- Case 2(a)ii is not applicable since J' is length-decreasing, contradicting our assumption that all edges in (5.18) are length-preserving.

- Suppose case **2(b)i** applies. Then $J' = K = [k, k + 2b]$ is length-preserving or length-increasing. Hence its dual can be length-decreasing or length-preserving. In the latter case (1) holds and we are done. If it is length-decreasing, then the dual of case **2(b)i** stipulates that the dual of case **2(a)i** also holds. This would imply an edge $[k - 1, k + 2b + 1]$ leaving (v, α) . But then by the fans, the edge $(v, \alpha) \xrightarrow{K} (w, \beta)$ is length-increasing, contradicting our assumptions that it is length-preserving.
- If case **2(b)ii** holds, then edge J'' is length-decreasing implying that (w, β) is attached to $G_{\leq \ell}$ by an edge. In this case, $(w, \beta) \in G'$ by a previous case, proving (1).
- In case **2(b)iii**, the edges labeled $J = J' = K$ have the same type and are length-preserving in this case. Since the edge labeled K out of (x, γ) is in G' , it must be length-preserving under \mathcal{L}_n , proving (1) using case **2(b)iii** for the dual.

It remains to consider the case $\min L > \min K$. By the previous case, all length-preserving edges M out of (v, α) with $\min L < \min M$ are in G' . Since by assumption there is no edge connecting (v, α) to $G_{\leq \ell}$, it follows that also all length-increasing edges M out of (v, α) with $\min L < \min M$ are in G' . Note that $\min L < \min M$ implies that $M \cap K = \emptyset$. Unless $\ell = s$, such an edge M must exist. By case **1**, we have a commuting square originating at (v, α) with the outgoing edges M and K . Since we are either in case **1a** or **1b**, the types of the edges are determined and hence also under \mathcal{L}_n , proving (1). \square

Next, we show that if a graph G satisfies Axiom **5.19**, then so does each component of $G_{[1, n-1]}$.

Lemma 5.22. *Suppose G satisfies Axiom **5.19**. Then each connected component of $G_{[1, n-1]}$ does as well.*

Proof. It is not hard to see that axioms **L0-L2** and axiom **L4** still hold for $G_{[1, n-1]}$.

Regarding axiom **L3**, the commutation relations in Theorem **4.35** still hold as long as all intervals appearing in the relations do not contain n . Assuming that I and J do not contain n , then no interval in cases **1**, **2(b)i**, **2(b)ii**, **2(b)iii**, **3b** contains n .

In case **2(a)i**, the interval $J' = [j - 1, j + 2\ell + 1]$ contains n if $j + 2\ell + 1 = n$. By axiom **L1**, the vertex from which J' originates also has an outgoing edge labeled $J = [j, j + 2\ell] \subseteq J'$. Hence in the absence of J' (when n is removed) case **2(b)i** holds which implies an octagon relation. Similarly, in case **2(a)ii** we have $n \in J' = [i + 1, i + 3 + 2\ell]$ if $n = i + 3 + 2\ell$. By axiom **L1**, the vertex from which J' originates also has an outgoing edge labeled $J = [i + 2, i + 2 + 2\ell]$. Hence in the absence of J' (when n is removed) case **2(b)ii** holds which implies a pentagon relation. Furthermore, in case **3a** we have $n \in J' = [i + 2m - 1, i + 2m + 1]$ if $n = i + 2m + 1$. Removing n changes I from length-increasing to length-preserving. But then case **3b** still applies. Finally for **(5.11)** if $n \in J$, then I in $G_{[1, n-1]}$ is no longer length-increasing, so the loop does not need to exist any longer.

We next show $G_{[1, n-1]}$ satisfies axiom **L5**. The partition λ in axiom **L5** is the same as the weight of the crystal $B(\lambda)_s$ in axiom **A5**, which we showed must hold by Lemma **5.20**. Suppose $\text{rev}(\alpha) \neq \lambda$. By axiom **L5**, there exists a length-preserving (resp. length-decreasing) edge $(v, \alpha) \xrightarrow{L} (w, \beta)$ in G .

- If $n \notin L$, this edge is still length-preserving (resp. length-decreasing) in $G_{[1, n-1]}$.
- If $L = [i, n]$ with $|L| > 3$, there is a length-increasing edge $(v, \alpha) \xrightarrow{J} (x, \gamma)$ with $J = [i + 1, n - 1]$ in G . This turns into a length-preserving edge in $G_{[1, n-1]}$ since the above forces $\gamma = (\gamma_1, \gamma_2, \dots, \gamma_{\ell-1}, 1)$.
- If $L = [n - 2, n]$ is length-decreasing, by **(5.11)** in axiom **L3** there exists a length-increasing edge

$$(w, \beta) \xrightarrow{[n-3, n-1]} (v, \alpha)$$

in G . Furthermore, $\alpha = (\alpha_1, \dots, \alpha_{\ell-2}, 2, 1)$ and $\beta = (\alpha_1, \dots, \alpha_{\ell-2} + 1, 2)$. If $\text{rev}(\beta) \neq \lambda$, by axiom **L5** in G there must be an edge $(w, \beta) \xrightarrow{K} (x, \gamma)$ which is not length-increasing. Employing the commutation relations of Theorem **4.35** with $I = K$ and $J = [n - 3, n - 1]$, only case **1** or **2(b)iii** can apply since J is length-increasing. In these cases, $I' = I = K$ out of (v, α) is not length-increasing and does not contain n . Hence it is still length-preserving or length-decreasing in $G_{[1, n-1]}$. If $\text{rev}(\beta) = \lambda$, we have $\beta = (1^k, 2^{\ell-1-k})$ and $\alpha = (1^k, 2^{\ell-3-k}, 1, 2, 1)$. If $\ell - 3 - k > 0$, (v, α) has an outgoing length-preserving edge $[n - 5, n - 3]$, which remains length-preserving in $G_{[1, n-1]}$. If $\ell - 3 - k = 0$, the label $(\alpha_1, \dots, \alpha_{\ell-1}) = (1^{k+1}, 2)$ in $G_{[1, n-1]}$ is minimal in its component.

- The last case to consider is when $L = [n - 2, n]$ is length-preserving in G . Note that in this case $\alpha = (\alpha_1, \dots, \alpha_{\ell-1}, 1)$. If this edge is the only length-preserving/decreasing edge out of (v, α) , the label $(\alpha_1, \dots, \alpha_{\ell-1})$ is minimal in its connected component.

This proves axiom **L5**(b) in $G_{[1,n-1]}$. Axiom **L5**(a) in $G_{[1,n-1]}$ follows similarly. \square

Recall that a CS-graph is a graph satisfying Axiom 5.5. We are finally ready to prove that the local axioms characterize CS-graphs as well.

Theorem 5.23. *A graph G satisfying Axiom 5.19 is a CS-graph. Conversely, a CS-graph satisfies Axiom 5.19.*

Proof. Suppose G satisfies Axiom 5.19. Axioms **L0-L2** imply axioms **A0-A2**. Axiom **A3** follows from the iteration of case 3a in Theorem 4.35 together with (5.11). Axiom **A5** follows from Lemma 5.20. Axiom **A4** (a) follows from Lemma 5.21. It remains to prove axiom **A4** (b).

We proceed by induction on n . For $n = 1, 2$, both Axiom 5.5 and Axiom 5.19 imply that G is a single vertex since no odd length intervals $I \subseteq [n]$ with $|I| \geq 3$ exist. Assume by induction hypothesis that Axiom 5.19 implies Axiom 5.5 for graphs with index $n - 1$ or smaller.

By Lemma 5.22, if G satisfies Axiom 5.19, then the connected components of $G_{[1,n-1]}$ satisfies Axiom 5.19. Thus, the connected components of $G_{[1,n-1]}$ satisfy Axiom 5.5 by induction. In particular, axiom **A4** (a) for $G_{[1,n-1]}$ states that

$$\mathcal{L}_{n-1}(G_{[1,n-1]}) \cong G_{[1,n-1]},$$

which is precisely axiom **A4** (b) for G .

We conclude by proving that a CS-graph satisfies Axiom 5.19. Axioms **A0-A2** together with Lusztig involution **A4** imply axioms **L0-L2**. By Corollary 5.13, a CS-graph is isomorphic to $\text{CS}(\lambda)$ for some partition λ . Axiom **L3** hence follows from Theorem 4.35, Corollaries 4.31 and 4.34, and their duals by Lusztig involution. Axiom **L4** follows from Theorem 4.37 and Corollary 4.39. Axiom **L5** follows from Proposition 4.40. \square

6. CRYSTAL SKELETON FOR TWO ROW PARTITIONS

In this section, we illustrate our general findings for crystal skeletons in the two row case, where the combinatorics is particularly elegant.

6.1. Vertices and edges in the two-row crystal skeleton. When λ has two rows, the vertices and edges of $\text{CS}(\lambda)$ can be translated into the language of paths. Recall that vertices of $\text{CS}(\lambda)$ are indexed by $\text{SYT}(\lambda)$.

Fix $\lambda = (\lambda_1, \lambda_2)$. Then standard Young tableaux of shape λ are in bijection with sequences

$$(6.1) \quad p = (p_1, \dots, p_{\lambda_1 + \lambda_2}) \in \{1, -1\}^{\lambda_1 + \lambda_2} \quad \text{satisfying} \quad h_k(p) := \sum_{i=1}^k p_i \leq 0,$$

for all $1 \leq k \leq \lambda_1 + \lambda_2$. A tableau $T \in \text{SYT}(\lambda)$ (and thus a vertex in $\text{CS}(\lambda)$) corresponds to the sequence

$$p_i = \begin{cases} -1 & \text{if } i \text{ appears in the first row of } T, \\ 1 & \text{if } i \text{ appears in the second row of } T. \end{cases}$$

We associate p to the path from $(0, 0)$ to $(\lambda_1 + \lambda_2, -\lambda_1 + \lambda_2)$, where at step i the path proceeds in the direction $(1, p_i)$. See Example 6.1 below. We call $h_k = h_k(p)$ in (6.1) the *height* of path p at the end of step k and set $h_0 = 0$.

It will be useful at times to think of a path as an arrangement of boxes, piled into the corner formed by the row-reading path (λ_1 downward steps, followed by λ_2 upward steps), where boxes never get piled above height 0; this is illustrated in Example 6.1. To recover a path from an arrangement of boxes, trace the upper face of the arrangement.

Given a tableau T , denote the corresponding path by p^T ; conversely denote the tableau associated to a path p by T_p . The word $\text{row}(p) := \text{row}(T_p)$ is obtained from p by reading (left to right) the locations of the upward steps (i such that $p_i = 1$), followed by the locations of the downward steps. As a result, descents in $\text{row}(p)$ occur precisely at (internal) local minima (where a down-step is followed by an up-step).

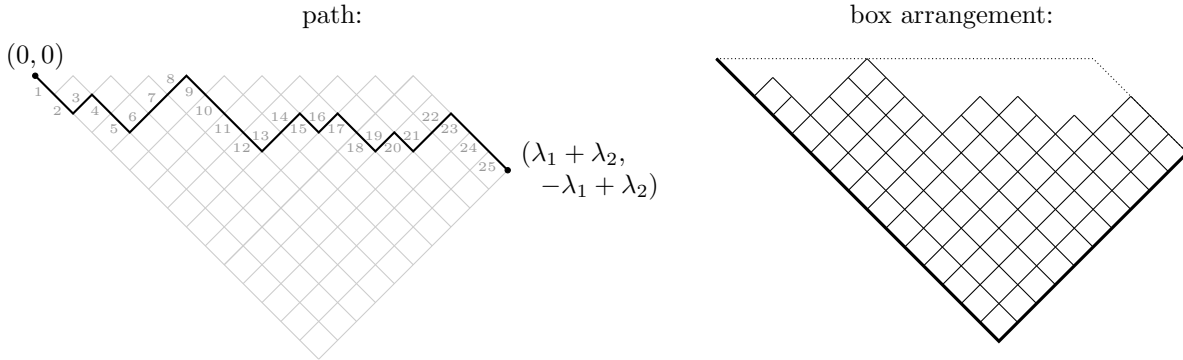
Example 6.1. Consider $\lambda = (15, 10)$. The tableau

$$T = \begin{array}{|c|c|c|c|c|c|c|c|c|c|c|c|c|c|c|} \hline 3 & 6 & 7 & 8 & 13 & 14 & 16 & 19 & 21 & 22 & & & & & & \\ \hline 1 & 2 & 4 & 5 & 9 & 10 & 11 & 12 & 15 & 17 & 18 & 20 & 23 & 24 & 25 & \\ \hline \end{array}$$

corresponds to the sequence

$$p = p^T = (-1, -1, 1, -1, -1, 1, 1, 1, -1, -1, -1, -1, 1, 1, -1, 1, -1, -1, 1, -1, 1, 1, -1, -1, -1)$$

drawn as



Reading the positions of the up-steps in p , followed by the positions of the down-steps, recovers

$$\text{row}(p) = 3\ 6\ 7\ 8\ 13\ 14\ 16\ 19\ 21\ 22\ 1\ 2\ 4\ 5\ 9\ 10\ 11\ 12\ 15\ 17\ 18\ 20\ 23\ 24\ 25 = \text{row}(T).$$

The (right) descents of $\text{row}(p)$ occur exactly at the 6 internal local minima of p .

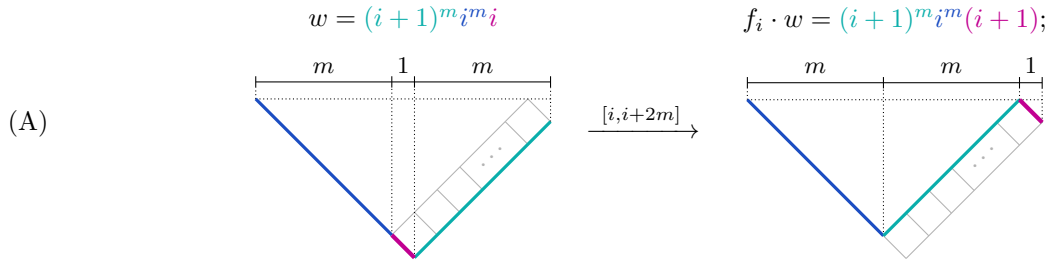
As before, if $I = [i, i + 2m]$ is a Dyck pattern interval in $\pi = \text{row}(p)$, we write

$$I \cdot p := \text{cycle}(\pi|_I)p,$$

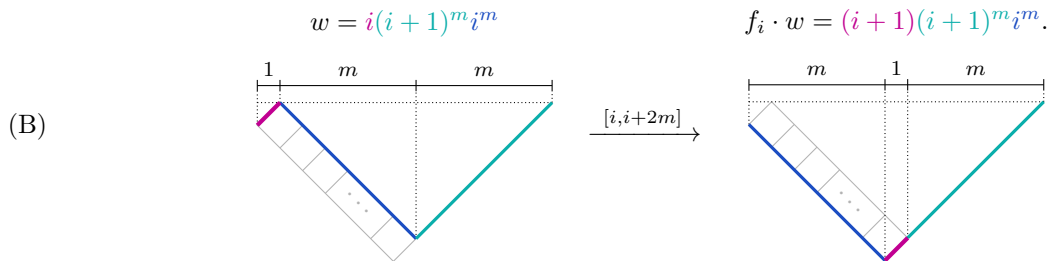
where $\text{cycle}(\pi|_I)$ acts on p according to its action on T_p as in Section 3.2.2.

Recall that descents in $\pi = \text{row}(p)$ correspond to local minima in p . It follows that if $I = [i, i + 2m]$ is a Dyck pattern interval such that $\text{row}(p|_I)$ destandardizes to a word in i and $i + 1$, then the path $p|_I$ has exactly one (internal) local minima; the possible local paths are shown below in Lemma 6.2. We can thus succinctly describe the paths $p|_I$ that appear in $\text{CS}(\lambda)$, as well as the corresponding adjacent vertex.

Lemma 6.2. *Suppose $\lambda = (\lambda_1, \lambda_2)$ has two rows. There is an edge $p \xrightarrow{I} p'$ in $\text{CS}(\lambda)$ if and only if p and p' agree on any $j \notin I$, and on I we have the following local behavior, where $w = \text{destd}(\text{row}(p)|_I)$ is the destandardization of the subword of $\text{row}(p)$ over the interval I :*



or



We will refer to the case in (A) as a type (A) edge, and the case in (B) as a type (B) edge. As depicted above, in the box-arrangement model, we can think of an edge of type (A) as adding a right strip of boxes, and an edge of type (B) as removing a left strip of boxes.

6.2. Rectangular decompositions and strongly-connected components. Throughout this paper, we have seen the importance of intervals $I = [a, b]$ where jeu de taquin takes $T|_I$ to a rectangular shape. For two-row partitions, the rectangles can only have one or two rows. In particular, we have the following cases:

- *One row:* $\text{jdt}(T|_I)$ forms a single row precisely when $\text{row}(T)|_I$ has no descents. In terms of the path, this means p^T has no local minima over I , that is, $p^T|_I = (1)^\ell(-1)^m$.
- *Two rows:* $\text{jdt}(T|_I)$ forms a two-row rectangle (m, m) precisely when $p^T|_I$ is a *Dyck subpath*, meaning that $p^T|_I$ starts and ends at the same height and never exceeds that height:

$$h_{a-1} = h_b \quad \text{and} \quad h_i \leq h_{a-1} \text{ for all } i \in [a, b]$$

(so that $b = a + 2m - 1$).

We can then decompose any lattice path $p \in \text{CS}(\lambda_1, \lambda_2)$ uniquely into a sequence of maximal rectangles as

$$(6.2) \quad p = (-1)^{n_0} D_1 (-1)^{n_1} D_2 (-1)^{n_2} \cdots D_\ell (-1)^{n_\ell},$$

where $n_1, \dots, n_{\ell-1} \geq 1$,
 $n_0 + n_1 + \cdots + n_\ell = \lambda_1 - \lambda_2$, and
 D_k is a Dyck subpath from height $-(n_0 + \cdots + n_{k-1})$.

We call (6.2) the (maximal) *rectangular decomposition* of p (or of T_p). One can also check that

$$|D_1| + \cdots + |D_\ell| = 2\lambda_2.$$

Note that the $(-1)^{n_k}$ in (6.2) correspond to downsteps in p . Define the *rectangular composition* $\text{rcomp}(p)$ to be the set composition of $\{1, \dots, n\}$ corresponding to the intervals spanning the rectangles in (6.2), so that

$$(6.3) \quad \text{rcomp}(p) = (\alpha^{(0)}, \beta^{(1)}, \alpha^{(1)}, \dots, \beta^{(\ell)}, \alpha^{(\ell)}),$$

where

$$\alpha^{(k)} = \left[1 + \sum_{r=0}^{k-1} (n_r + |D_r|), n_k + \sum_{r=0}^{k-1} (n_r + |D_r|) \right], \quad \text{i.e. the interval covering the terms } (-1)^{n_k}, \text{ and}$$

$$\beta^{(k)} = \left[1 + n_k + \sum_{r=0}^{k-1} (n_r + |D_r|), |D_k| + n_k + \sum_{r=0}^{k-1} (n_r + |D_r|) \right], \quad \text{i.e. the interval covering the terms in } D_k.$$

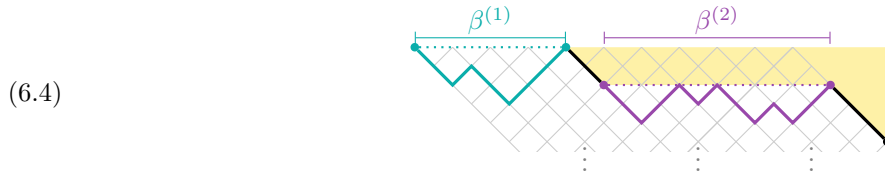
The only terms that can be the empty set are $\alpha^{(0)}$ and $\alpha^{(\ell)}$, which occur when $n_0 = 0$ or $n_\ell = 0$, respectively. Note that $\text{rcomp}(p)$ is not the same composition as the descent composition $\text{Des}(T_p)$; see Section 6.3 for a discussion on descent compositions obtained from a path p .

Example 6.3. Continuing Example 6.1, the rectangular decomposition of p from (6.2) is

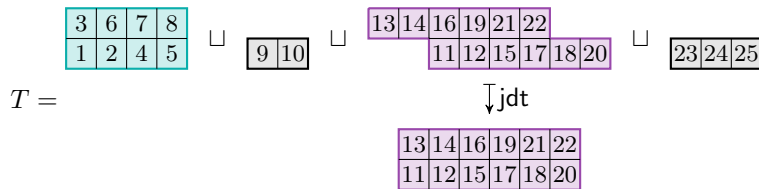
$$p = (-1)^0 D_1 (-1)^2 D_2 (-1)^3 \quad \text{with} \quad \text{rcomp}(p) = (\emptyset, [1, 8], [9, 10], [11, 22], [23, 25]),$$

$\alpha^{(0)} \quad \beta^{(1)} \quad \alpha^{(1)} \quad \beta^{(2)} \quad \alpha^{(2)}$

as illustrated below:



Compare this decomposition to that of T into the maximal rectangles:



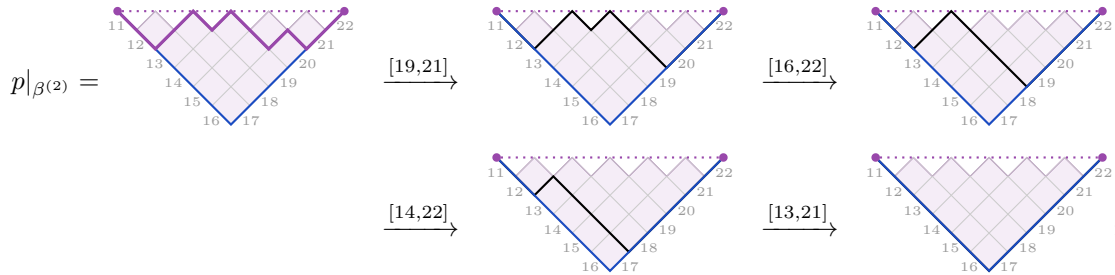
In particular, $\beta^{(1)}$ and $\beta^{(2)}$ correspond to the teal and purple rectangles, respectively. The gray rectangles with a single row correspond to the black downsteps $(-1)^2$ (i.e. $\alpha^{(1)}$) and $(-1)^3$ (i.e. $\alpha^{(2)}$) in (6.4) above.

As depicted in (6.4), one can think visually of the terms in p that appear in $(-1)^{n_k}$ in (6.2) as *eastern-exposed* down-steps, or equivalently, those exposed to a light shined horizontally from the right.

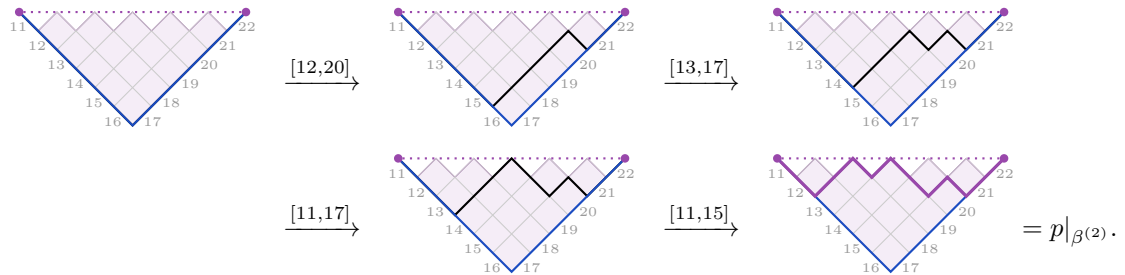
Returning to the results of Section 4.5 on strongly-connected components, we can now interpret Theorem 4.16 and Corollary 4.19 in the two-row case to say that if $p, q \in \text{CS}(\lambda_1, \lambda_2)$ have the same rectangular composition, then they are in the same strongly-connected component.

In particular, given a rectangular decomposition of p as in (6.2), one can systematically apply a sequence of type (B) edges that will take p to the path that replaces any D_i with the *trivial Dyck path* $(-1)^{m_i}(1)^{m_i}$ over the same interval, where $m_i = |D_i|$. One natural choice of sequence corresponds to removing one strip of boxes below the path at a time, moving right-to-left (see Example 6.4). A similar natural sequence of type (A) edges will walk us back to p , adding one full strip of boxes at a time left-to-right.

Example 6.4. Picking up from Example 6.3, one sequence of (B) edges from $p|_{\beta(2)}$ to the path that replaces D_2 by $(-1)^6(1)^6$ is



and one sequence of (A) edges moving back to p is



In the two-row case, we can in fact characterize the strongly-connected components of $\text{CS}(\lambda)$: the rectangular compositions *exactly* index the strongly-connected components. In order to prove the characterization (Corollary 6.6), we first prove Lemma 6.5 below.

Lemma 6.5. *Let $I = [i, i + 2m]$ be a Dyck pattern interval in $p \in \text{CS}(\lambda_1, \lambda_2)$. If I is of type (B), then $\text{rcomp}(I \cdot p) = \text{rcomp}(p)$. If I is of type (A), then $\text{rcomp}(I \cdot p) \geq_D \text{rcomp}(p)$.*

Proof. Let $I = [i, i + 2m]$ be a Dyck pattern interval in p , and consider

$$\text{rcomp}(p) = \left(\alpha^{(0)}, \beta^{(1)}, \alpha^{(1)}, \dots, \beta^{(\ell)}, \alpha^{(\ell)} \right)$$

as in (6.3).

If I is of type (B), then since the height of both p and $I \cdot p$ at the left endpoint is less than that of the right endpoint, we know $I \subseteq \beta^{(k)}$ for some k . Hence $\text{rcomp}(p) = \text{rcomp}(I \cdot p)$.

On the other hand, if I is of type (A), then $[i + 1, i + 2m] \subseteq \beta^{(k)}$ for some k , but we may have $i \in \beta^{(k)}$ or $i \in \alpha^{(k-1)}$. If $i \in \beta^{(k)}$, then $\text{rcomp}(p) = \text{rcomp}(I \cdot p)$. Otherwise, there are four cases:

- If $\beta^{(k)} = I \setminus \{i\}$, then D_k is precisely the Dyck path in I . Under the type (A) edge, this Dyck path moves one step to the left. Otherwise, $\beta^{(k)} \supseteq I \setminus \{i\}$, in which the initial trivial path moves one step to the left of D_k . For example, compare the effect of $[1, 5]$ in Example 6.7 to that of $[10, 14]$ in Example 6.3.
- If $n_{k-1} = 1$, then the portion of D_k that moves left will merge with D_{k-1} . Otherwise, if $n_{k-1} > 1$, then there is room for that trivial Dyck path to move left without merging.

In any of these four cases, $\text{rcomp}(p) <_D \text{rcomp}(I \cdot p)$. □

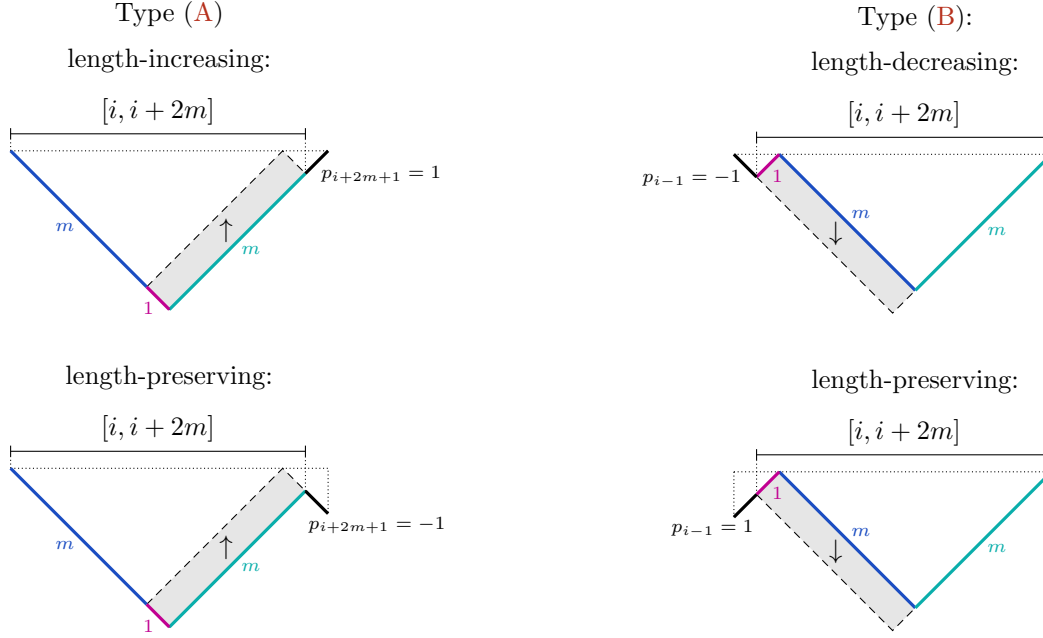


FIGURE 6. The effect of each type of edge $p \xrightarrow{[i, i+2m]} p'$ on a path's descent composition obtained from combining Theorem 4.26 and (6.5).

One consequence of Lemma 6.5 is that if an edge $p \xrightarrow{I} p'$ changes the rectangular composition of a path, there is no sequence of edges from p' to p .

Corollary 6.6. *Two paths (i.e. vertices) $p, q \in \text{CS}(\lambda_1, \lambda_2)$ are in the same strongly-connected component of $\text{CS}(\lambda_1, \lambda_2)$ if and only if $\text{rcomp}(p) = \text{rcomp}(q)$. Hence, the strongly-connected components of $\text{CS}(\lambda_1, \lambda_2)$ are indexed by rectangular compositions.*

6.3. Descent compositions and fans. Suppose the local minima of a path p occur at positions m_1, m_2, \dots, m_h ; that is, $(p_{m_i}, p_{m_i+1}) = (-1, 1)$ for $1 \leq i \leq h$. Then for $n = \lambda_1 + \lambda_2$ we have

$$\text{Des}(T_p) = (m_1, m_2 - m_1, \dots, m_h - m_{h-1}, n - m_h).$$

Recall the behavior of descent compositions of adjacent vertices in $\text{CS}(\lambda)$ described in Theorem 4.26. We can specialize the conditions in Theorem 4.26 to the case that λ has two rows, and translate them into conditions on paths. This is done below in (6.5), where the edge labeled $I = [i, i+2m]$ is either of type (A) or (B).

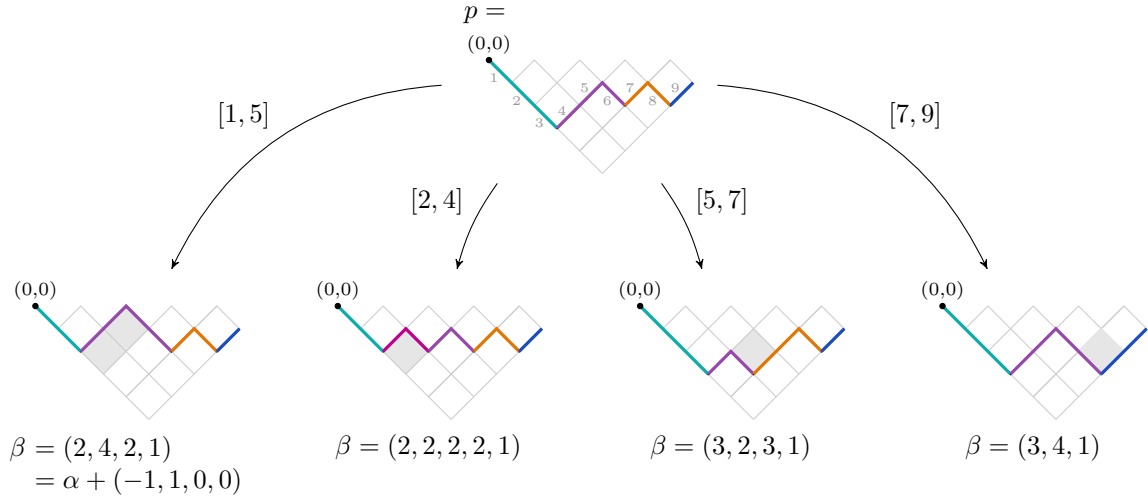
	$I = [i, i+2m]$	$\{i-1\} \sqcup I$	$I \sqcup \{i+2m+1\}$
(6.5)	Type (A)	always rectangle-free	rectangle if $p_{i+2m+1} = -1$ rectangle-free if $p_{i+2m+1} = 1$
	Type (B)	rectangle if $p_{i-1} = -1$ rectangle-free if $p_{i-1} = 1$	always rectangle-free

The effect of each case on the associated descent compositions is then given in Figure 6.

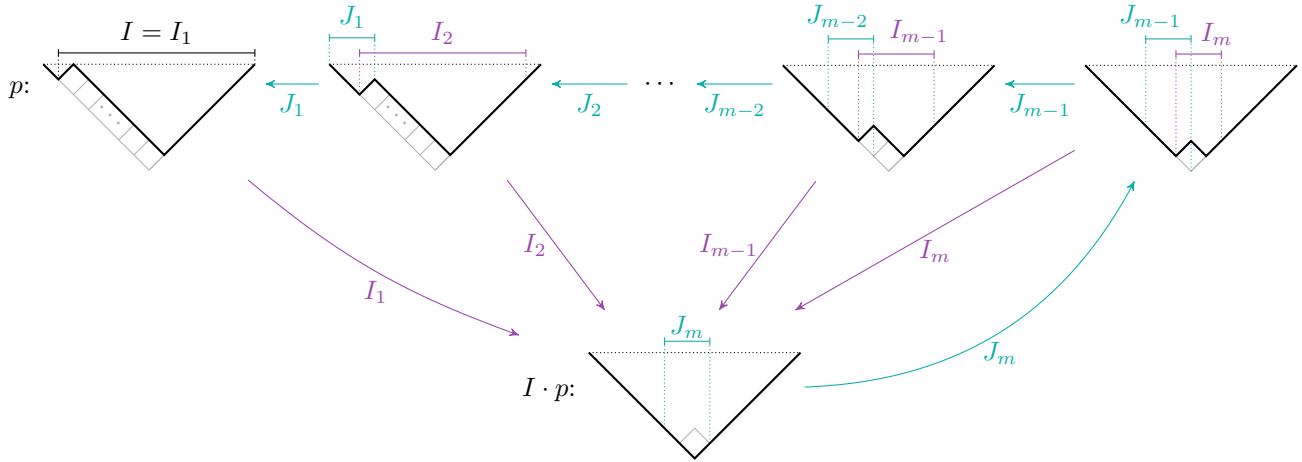
Example 6.7. The path p below has

$$\text{row}(p) = 457912368, \quad \text{and descent composition } \alpha = (3, 3, 2, 1).$$

The four Dyck patterns moving out from p are two type (A) edges, one length-preserving and one length increasing; and two type (B) edges, one length-preserving and one length-decreasing.



6.3.1. *Fans.* The path model in the two row case also allows us to be more concrete about the fans introduced in Section 4.7. Recall that a fan occurs in $\text{CS}(\lambda)$ whenever there is a length-decreasing edge $I = [i, i + 2m]$. In the language of paths, this means that there is a sequence length-preserving type (A) edges moving from $I \cdot p$ to p , adding one box at a time. In particular, if $[i - 2, i + 2m + 1]$ is not a rectangle in $I \cdot p$, then the local fan looks as follows.



Similarly, if I is a type (A) length-increasing edge, then there is an incoming fan consisting of a sequence of length-preserving (B) edges, *removing* one box at a time. The following section will reveal concretely the dual relationships of these fans via Lusztig involution.

6.4. **Lusztig involution.** Recall the technique for computing Lusztig involution on any crystal skeleton $\text{CS}(\lambda)$ discussed in Remark 2.5. This map has a nice specialization to paths, summarized below in Lemma 6.9.

Given a tableau T with $\text{row}(T) = \pi = \pi_1 \pi_2 \dots \pi_n$, the word $\pi^\# = (n + 1 - \pi_n) \dots (n + 1 - \pi_1)$ is the reading word of the tableau $T^\#$ obtained by rotating T 180° and taking the *complement* of the fillings (i.e. replacing each filling i with $n + 1 - i$).

Performing jeu de taquin on $T^\#$ gives the same tableau as the RSK insertion tableau for $\pi^\#$:

$$\text{evac}(T) = \text{jdt}(T^\#) = P(\pi^\#).$$

If one follows the maximal rectangular decomposition of T (in the sense of (6.2) and the end of Example 6.1) through the rotation-complement transformation, then jeu de taquin can be performed efficiently by first resolving the rectangles individually.

Example 6.8. Returning to Example 6.1, the rotation and complement of T is

$$\begin{aligned}
 T^\# &= \begin{array}{|c|c|c|c|c|c|c|c|c|c|c|c|c|c|c|c|c|c|} \hline 1 & 2 & 3 & 6 & 8 & 9 & 11 & 14 & 15 & 16 & 17 & 21 & 22 & 24 & 25 \\ \hline & & & & & 4 & 5 & 7 & 10 & 12 & 13 & 18 & 19 & 20 & 23 \\ \hline \end{array} \\
 &= \begin{array}{|c|c|c|} \hline 1 & 2 & 3 \\ \hline \end{array} \sqcup \begin{array}{|c|c|c|c|c|c|c|} \hline 6 & 8 & 9 & 11 & 14 & 15 \\ \hline 4 & 5 & 7 & 10 & 12 & 13 \\ \hline \end{array} \sqcup \begin{array}{|c|c|} \hline 16 & 17 \\ \hline \end{array} \sqcup \begin{array}{|c|c|c|c|} \hline 21 & 22 & 24 & 25 \\ \hline 18 & 19 & 20 & 23 \\ \hline \end{array} \\
 &\quad \downarrow \text{jdt} \quad \downarrow \text{jdt} \quad \downarrow \text{jdt} \quad \downarrow \text{jdt} \\
 &= \begin{array}{|c|c|c|} \hline 1 & 2 & 3 \\ \hline \end{array} \sqcup \begin{array}{|c|c|c|c|c|c|c|} \hline 6 & 8 & 9 & 11 & 14 & 15 \\ \hline 4 & 5 & 7 & 10 & 12 & 13 \\ \hline \end{array} \sqcup \begin{array}{|c|c|} \hline 16 & 17 \\ \hline \end{array} \sqcup \begin{array}{|c|c|c|c|} \hline 21 & 22 & 24 & 25 \\ \hline 18 & 19 & 20 & 23 \\ \hline \end{array}
 \end{aligned}$$

(compare to the end of Example 6.1). Then

$$\begin{aligned}
 \text{evac}(T) &= \text{jdt}(T^\#) = \text{jdt} \left(\begin{array}{|c|c|c|c|c|c|c|c|c|c|c|c|c|c|c|c|c|c|} \hline & & & 6 & 8 & 9 & 11 & 14 & 15 & & 21 & 22 & 24 & 25 \\ \hline 1 & 2 & 3 & 4 & 5 & 7 & 10 & 12 & 13 & 16 & 17 & 18 & 19 & 20 & 23 \\ \hline \end{array} \right) \\
 &= \begin{array}{|c|c|c|c|c|c|c|c|c|c|c|c|c|c|c|c|c|c|} \hline 6 & 8 & 9 & 11 & 14 & 15 & 21 & 22 & 24 & 25 \\ \hline 1 & 2 & 3 & 4 & 5 & 7 & 10 & 12 & 13 & 16 & 17 & 18 & 19 & 20 & 23 \\ \hline \end{array}.
 \end{aligned}$$

Lemma 6.9. Suppose $\lambda = (\lambda_1, \lambda_2)$. Let p be a vertex in $\text{CS}(\lambda)$, and denote its rectangular decomposition and the associated set composition as

$$p = (-1)^{n_0} D_1 (-1)^{n_1} D_2 (-1)^{n_2} \dots D_\ell (-1)^{n_\ell} \quad \text{and} \quad \text{rcomp}(p) = (\alpha^{(0)}, \beta^{(1)}, \alpha^{(1)}, \dots, \beta^{(\ell)}, \alpha^{(\ell)}).$$

Then the following are equivalent methods to compute $\text{evac}(p)$.

- (1) Rectangular decomposition. Let $D_k^\#$ be the horizontal reflection of D_k obtained from negating each term in the corresponding subsequence and reversing its order. Then

$$\text{evac}(p) = (-1)^{n_\ell} D_\ell^\# \dots (-1)^{n_2} D_2^\# (-1)^{n_1} D_1^\# (-1)^{n_0}.$$

- (2) Sequence. For $i = 1, \dots, n$, the i th term in $\text{evac}(p)$ is

$$\text{evac}(p)_i = \epsilon p_{n+1-i}, \quad \text{where} \quad \epsilon = \begin{cases} -1 & \text{if } n+1-i \in \beta^{(k)} \text{ for some } k, \\ 1 & \text{if } n+1-i \in \alpha^{(k)} \text{ for some } k. \end{cases}$$

- (3) Graph of the path. Horizontally reflect the path p and place the new left endpoint at $(0,0)$. Then shine a light from the left and reflect each up-step that is exposed to light. The result is a graph of the path $\text{evac}(p)$.

Proof. Rotation of T_p is the same as swapping the sign of each term of the sequence corresponding to p , and taking the complement is the same as reversing the order of the resulting sequence. Equivalently, $p^\#$ is the path obtained by horizontally reflecting p and placing the left-endpoint at $(0,0)$. In terms of the rectangular decomposition above, this means

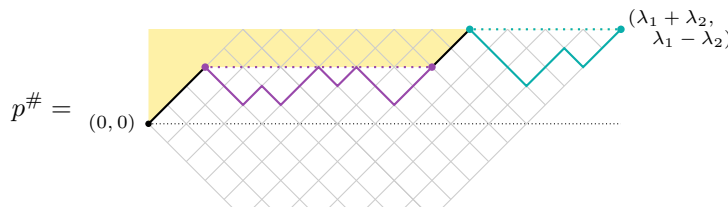
$$p^\# = 1^{n_\ell} D_\ell^\# \dots 1^{n_2} D_2^\# 1^{n_1} D_1^\# 1^{n_0}.$$

Just as $T^\#$ may be a filling of a skew-shape rather than a partition, the path $p^\#$ may now exceed height 0. But since the boxes that changed rows from $T_p^\#$ to $\text{jdt}(T_p^\#)$ were precisely those that started in 1-row rectangles in the maximal rectangular decomposition of T_p , the only steps that will change sign from $p^\#$ to $\text{jdt}(p^\#)$ are those that corresponded to the eastern-exposed down-steps in p . Specifically,

$$\text{evac}(p) = \text{jdt}(p^\#) = (-1)^{n_\ell} D_\ell^\# \dots (-1)^{n_2} D_2^\# (-1)^{n_1} D_1^\# (-1)^{n_0}.$$

Tracking the resulting sequence will give (2). □

Example 6.10. The path corresponding to the tableau T in Examples 6.1 and 6.8 reverses to



so that

$$\text{evac}(p) = \text{jdt}(p^\#) =$$

One strength of this method of computing $\text{evac}(p)$ is how it interfaces locally with the behavior of Dyck patterns. Recall from Definition 4.12 that every edge $T \xrightarrow{I} T'$ in $\text{CS}(\lambda)$ has a corresponding edge $\mathcal{L}(T') \xrightarrow{I^c} \mathcal{L}(T)$, where if $I = [a, b]$, then $I^c = [n+1-b, n+1-a]$.

Proposition 6.11. *Let $\lambda = (\lambda_1, \lambda_2)$ and let $p \xrightarrow{I} p'$ be an edge in $\text{CS}(\lambda)$ with $I = [i, i+2m]$. As in (6.3), write*

$$\text{rcomp}(p) = (\alpha^{(0)}, \beta^{(1)}, \alpha^{(1)}, \dots, \beta^{(\ell)}, \alpha^{(\ell)}).$$

1. *If $I \subseteq \beta^{(k)}$ for some k , then*

$$p \xrightarrow{I} p' \text{ is of type (A)}$$

if and only if

$$\mathcal{L}(p') \xrightarrow{I^c} \mathcal{L}(p) \text{ is of type (B)}.$$

2. *Otherwise, $[i+1, i+m] \subseteq \beta^{(k)}$ for some k but $i \in \alpha^{(k-1)}$, in which case both*

$$p \xrightarrow{I} p' \quad \text{and} \quad \mathcal{L}(p') \xrightarrow{I^c} \mathcal{L}(p)$$

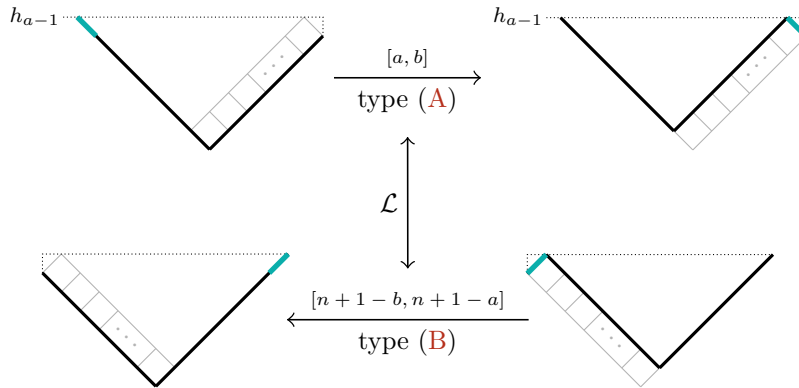
are of type (A).

Proof. This is a direct consequence of Lemmas 6.2 and 6.9, and Lemma 6.5. For edges of both type (A) or (B), the subpath over the interval $[i+1, i+2m]$ is the trivial Dyck path, and hence must be contained in some $\beta^{(k)}$. Thus

$$\text{evac}(p)_{n+1-j} = -p_j \quad \text{for each } j \in [i+1, i+2m],$$

i.e. $\text{evac}(p)$ over $[n+1-(i+1), n+1-(i+2m)]$ is a horizontal reflection of p over $[i+1, i+2m]$.

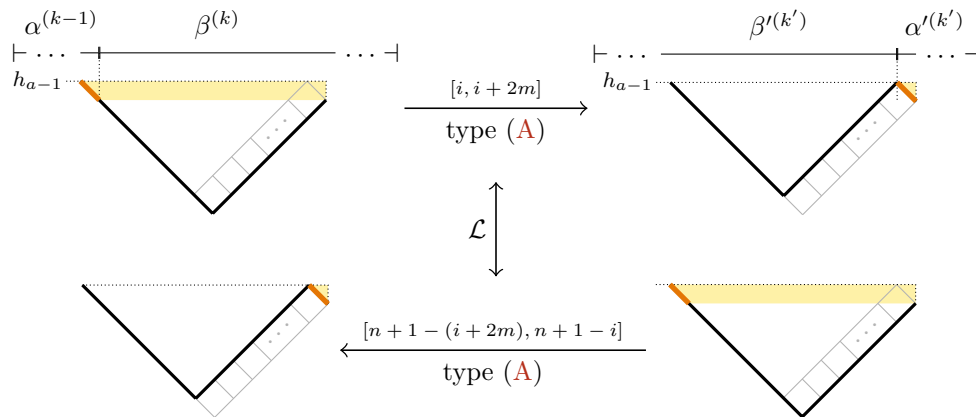
If $i \in \beta^{(k)}$ as well, then the same equality holds for $j = i$, in which case $\mathcal{L}(p)$ and $\mathcal{L}(p')$ are locally just horizontal reflections of p and p' , respectively:



On the other hand, suppose $i \notin \beta^{(k)}$. Then by Lemma 6.5, i is an eastern-exposed down-step of p ($i \in \alpha^{(k-1)}$) and $i+2m$ is an eastern-exposed down-step in $I \cdot p$, so that

$$\text{evac}(p)_{n+1-i} = p_i = -1 \quad \text{and} \quad \text{evac}(p')_{n+1-(i+2m)} = p'_{i+2m} = -1.$$

Then we see the following:



□

REFERENCES

- [1] Sami Assaf and Dominic Searles. Schubert polynomials, slide polynomials, Stanley symmetric functions and quasi-Yamanouchi pipe dreams. *Adv. Math.*, 306:89–122, 2017.
- [2] Sami H. Assaf. A combinatorial realization of Schur-Weyl duality via crystal graphs and dual equivalence graphs. In *20th Annual International Conference on Formal Power Series and Algebraic Combinatorics (FPSAC 2008)*, Discrete Math. Theor. Comput. Sci. Proc., AJ, pages 141–152. Assoc. Discrete Math. Theor. Comput. Sci., Nancy, 2008.
- [3] Sami H. Assaf. Dual equivalence graphs I: A new paradigm for Schur positivity. *Forum Math. Sigma*, 3:Paper No. e12, 33, 2015.
- [4] Sami H. Assaf and Sara C. Billey. Affine dual equivalence and k -Schur functions. *J. Comb.*, 3(3):343–399, 2012.
- [5] Sami Hayes Assaf. *Dual equivalence graphs, ribbon tableaux and Macdonald polynomials*. ProQuest LLC, Ann Arbor, MI, 2007. Thesis (Ph.D.)—University of California, Berkeley.
- [6] Jonah Blasiak. What makes a D_0 graph Schur positive? *J. Algebraic Combin.*, 44(3):677–727, 2016.
- [7] Jonah Blasiak and Sergey Fomin. Noncommutative Schur functions, switchboards, and Schur positivity. *Selecta Math. (N.S.)*, 23(1):727–766, 2017.
- [8] Sarah Brauner, Sylvie Corteel, Zaij Daugherty, and Anne Schilling. Crystal skeletons and their axioms. Séminaire Lotharingien de Combinatoire, to appear, 2025.
- [9] Daniel Bump and Anne Schilling. *Crystal bases*. World Scientific Publishing Co. Pte. Ltd., Hackensack, NJ, 2017. Representations and combinatorics.
- [10] Lynne M. Butler. Subgroup lattices and symmetric functions. *Mem. Amer. Math. Soc.*, 112(539):vi+160, 1994.
- [11] A. J. Cain, A. Malheiro, F. Rodrigues, and I. Rodrigues. A local characterization of quasi-crystal graphs. preprint, [arXiv:2309.14898](https://arxiv.org/abs/2309.14898), 2023.
- [12] A. J. Cain, A. Malheiro, F. Rodrigues, and I. Rodrigues. Structure of quasi-crystal graphs and applications to the combinatorics of quasi-symmetric functions. preprint, [arXiv:2309.14887](https://arxiv.org/abs/2309.14887), 2023.
- [13] Eric Egge, Nicholas A. Loehr, and Gregory S. Warrington. From quasisymmetric expansions to Schur expansions via a modified inverse Kostka matrix. *European J. Combin.*, 31(8):2014–2027, 2010.
- [14] Adriano Garsia and Jeff Remmel. A note on passing from a quasi-symmetric function expansion to a Schur function expansion of a symmetric function. preprint, [arXiv:1802.09686](https://arxiv.org/abs/1802.09686), 2018.
- [15] Ira M. Gessel. Multipartite P -partitions and inner products of skew Schur functions. In *Combinatorics and algebra (Boulder, Colo., 1983)*, volume 34 of *Contemp. Math.*, pages 289–317. Amer. Math. Soc., Providence, RI, 1984.
- [16] Ira M. Gessel. On the Schur function expansion of a symmetric quasi-symmetric function. *Electron. J. Combin.*, 26(4):Paper No. 4.50, 5, 2019.
- [17] Ira M. Gessel and Christophe Reutenauer. Counting permutations with given cycle structure and descent set. *J. Combin. Theory Ser. A*, 64(2):189–215, 1993.
- [18] J. Haglund, M. Haiman, and N. Loehr. A combinatorial formula for Macdonald polynomials. *J. Amer. Math. Soc.*, 18(3):735–761, 2005.
- [19] Mark D. Haiman. Dual equivalence with applications, including a conjecture of Proctor. *Discrete Math.*, 99(1-3):79–113, 1992.
- [20] Cristian Lenart. On the combinatorics of crystal graphs. I. Lusztig’s involution. *Adv. Math.*, 211(1):204–243, 2007.
- [21] Nicholas A. Loehr and Gregory S. Warrington. Quasisymmetric expansions of Schur-function plethysms. *Proc. Amer. Math. Soc.*, 140(4):1159–1171, 2012.
- [22] Florence Maas-Gariépy. Quasicrystal structure of fundamental quasisymmetric functions, and skeleton of crystals. preprint, [arXiv:2302.07694](https://arxiv.org/abs/2302.07694), 2023.
- [23] Jennifer Morse and Anne Schilling. Crystal approach to affine Schubert calculus. *Int. Math. Res. Not. IMRN*, (8):2239–2294, 2016.

- [24] Rosa Orellana, Franco Saliola, Anne Schilling, and Mike Zabrocki. From quasi-symmetric to Schur expansions with applications to symmetric chain decompositions and plethysm. *Electron. J. Combin.*, 31(4):Paper No. 4.12 [4.23 on table of contents], 29, 2024.
- [25] Austin Roberts. *Dual Equivalence Graphs and their Applications*. ProQuest LLC, Ann Arbor, MI, 2014. Thesis (Ph.D.)–University of Washington.
- [26] Austin Roberts. Dual equivalence graphs revisited and the explicit Schur expansion of a family of LLT polynomials. *J. Algebraic Combin.*, 39(2):389–428, 2014.
- [27] Richard P. Stanley. *Enumerative combinatorics. Vol. 2*, volume 62 of *Cambridge Studies in Advanced Mathematics*. Cambridge University Press, Cambridge, 1999. With a foreword by Gian-Carlo Rota and appendix 1 by Sergey Fomin.
- [28] Richard P. Stanley. *Enumerative combinatorics. Vol. 2*, volume 208 of *Cambridge Studies in Advanced Mathematics*. Cambridge University Press, Cambridge, second edition, [2024] ©2024. With an appendix by Sergey Fomin.
- [29] John R. Stembridge. A local characterization of simply-laced crystals. *Trans. Amer. Math. Soc.*, 355(12):4807–4823, 2003.
- [30] George Wang. A cornucopia of quasi-Yamanouchi tableaux. *Electron. J. Combin.*, 26(1):Paper No. 1.10, 21, 2019.

(S. Brauner) DIVISION OF APPLIED MATHEMATICS, BROWN UNIVERSITY, PROVIDENCE, RI, USA

Email address: sarahbrauner@gmail.com

URL: <https://www.sarahbrauner.com/>

(S. Corteel) DEPARTMENT OF MATHEMATICS, UNIVERSITY OF CALIFORNIA, BERKELEY, CA, USA AND CNRS, IMJ-PRG, SORBONNE UNIVERSITÉ, FRANCE

Email address: corteel@berkeley.edu

(Z. Daugherty) DEPARTMENT OF MATHEMATICS AND STATISTICS, REED COLLEGE, 3203 SE WOODSTOCK BLVD, PORTLAND, OR 97202-8199, USA

Email address: zdaugherty@reed.edu

URL: <https://people.reed.edu/~zdaugherty/>

(A. Schilling) DEPARTMENT OF MATHEMATICS, UNIVERSITY OF CALIFORNIA, ONE SHIELDS AVENUE, DAVIS, CA 95616-8633, U.S.A.

Email address: anne@math.ucdavis.edu

URL: <http://www.math.ucdavis.edu/~anne>